Iron Acquisition via SLUSH Peptides in *Staphylococcus lugdunensis* and Microbial Interactions with *Pseudomonas aeruginosa* and *Staphylococcus aureus*: A Computational and Experimental Analysis

Dissertation

der Mathematisch-Naturwissenschaftlichen Fakultät
der Eberhard Karls Universität Tübingen
zur Erlangung des Grades eines
Doktors der Naturwissenschaften
(Dr. rer. nat.)

vorgelegt von
M.Sc. Sharmila Sekar
aus Chennai, India

Tübingen
2025

Gedruckt mit Genehmigung der Mathematisch-Naturwissenschaftlichen Fakultät der Eberhard Karls Universität Tübingen.

Tag der mündlichen Qualifikation:	21.07.2025
Dekan:	Prof. Dr. Thilo Stehle
1. Berichterstatter/-in:	Prof. Dr. Simon Heilbronner
2. Berichterstatter/-in:	Prof. Dr. Andreas Peschel

TABLE OF CONTENTS

Abstract

During infection, bacterial pathogens face significant challenges due to host-imposed nutritional immunity, particularly iron limitation. *Staphylococcus lugdunensis*, a known opportunistic pathogen, has evolved to overcome this restriction by utilizing host-derived heme as an iron source, facilitated by the SLUSH locus. This locus encodes SLUSH peptides that exhibit hemolytic activity, enabling the pathogen to lyse erythrocytes and release heme. Our study reveals that the SLUSH peptides play a critical role in iron acquisition and contribute significantly to *S. lugdunensis* virulence, particularly under iron-restricted conditions. We show that the SLUSH peptides are essential for erythrocyte-dependent growth of *S. lugdunens*is in vitro, confirming their role in heme acquisition. Additionally, Agr (accessory gene regulator), a key regulator of PSM expression in *Staphylococcus aureus*, also regulates the SLUSH locus in *S. lugdunensis*, underscoring its importance in overcoming host defenses.

In the context of cystic fibrosis (CF), *Pseudomonas aeruginosa* and *S. aureus* frequently co-colonize the lungs, leading to complex metabolic interactions. Genome-scale metabolic models (GEMs) are widely used to predict microbial interactions, but their accuracy is often limited in complex environments when transcriptional data are excluded. In this study, we integrated transcriptomic data to refine GEMs for *P. aeruginosa* and *S. aureus* under cystic fibrosis (CF)-like conditions. While co-culturing these species revealed significant metabolic changes, particularly in amino acid biosynthesis and fermentation, the refined models still failed to capture the dynamic metabolic shifts driven by interspecies competition fully. Notably, we observed downregulation of the *pvdE* gene in *P. aeruginosa*, involved in iron acquisition, suggesting that *S. aureus* modulates *P. aeruginosa* iron metabolism. These findings highlight key limitations of current GEMs, particularly their inability to account for complex interspecies interactions such as siderophore utilization and regulatory network dynamics. Overall, our study provides new insights in *S. lugdunensis* hemolytic activity and microbial interactions in CF lungs, underscoring

the need for further refinement of GEMs by incorporating regulatory and interspecies signalling mechanisms.

Zusammenfassung

Während der Infektion stehen bakterielle Krankheitserreger aufgrund der vom Wirt auferlegten Ernährungsimmunität, insbesondere der Eisenlimitierung, vor großen Herausforderungen. *Staphylococcus lugdunensis*, ein bekannter opportunistischer Erreger, hat sich so entwickelt, dass er diese Beschränkung überwindet, indem er vom Wirt stammendes Häm als Eisenquelle nutzt, was durch den SLUSH-Locus erleichtert wird. Dieser Locus kodiert für SLUSH-Peptide, die eine hämolytische Aktivität aufweisen und es dem Erreger ermöglichen, Erythrozyten zu lysieren und Häm freizusetzen. Unsere Studie zeigt, dass die SLUSH-Peptide eine entscheidende Rolle beim Eisenerwerb spielen und wesentlich zur Virulenz von *S. lugdunensis* beitragen, insbesondere unter eisenarmen Bedingungen. Wir zeigen, dass die SLUSH-Peptide für das erythrozytenabhängige Wachstum von *S. lugdunensis* in vitro wesentlich sind, was ihre Rolle beim Eisenerwerb bestätigt. Darüber hinaus reguliert Agr (accessory gene regulator), ein Schlüsselregulator der PSM-Expression in *Staphylococcus aureus*, auch den SLUSH-Locus in *S. lugdunensis,* was seine Bedeutung für die Überwindung der Wirtsabwehr unterstreicht.

Im Zusammenhang mit Mukoviszidose (CF) besiedeln *Pseudomonas aeruginosa* und *S. aureus* häufig gemeinsam die Lunge, was zu komplexen metabolischen Interaktionen führt. Stoffwechselmodelle auf Genomebene (GEMs) werden häufig zur Vorhersage mikrobieller Interaktionen verwendet, aber ihre Genauigkeit ist in komplexen Umgebungen oft begrenzt, wenn transkriptionelle Daten ausgeschlossen werden. In dieser Studie haben wir transkriptomische Daten integriert, um GEMs für *P. aeruginosa* und *S. aureus* unter zystische Fibrose (CF)-ähnlichen Bedingungen zu verfeinern. Während die Co-Kultivierung dieser Spezies signifikante metabolische Veränderungen - insbesondere in der Aminosäurebiosynthese und Fermentation - ergab, konnten die verfeinerten Modelle die dynamischen metabolischen Verschiebungen, die durch den Wettbewerb zwischen den Spezies verursacht werden, immer noch nicht vollständig erfassen. Insbesondere beobachteten wir eine

Herunterregulierung des *pvdE*-Gens in *P. aeruginosa*, das am Eisenerwerb beteiligt ist, was darauf hindeutet, dass *S. aureus* den Eisenstoffwechsel von *P.* aeruginosa moduliert. Diese Ergebnisse verdeutlichen die wesentlichen Einschränkungen der derzeitigen GEMs, insbesondere ihre Unfähigkeit, komplexe Interaktionen zwischen den Spezies, wie die Nutzung von Siderophoren und die Dynamik regulatorischer Netzwerke, zu berücksichtigen. Insgesamt bietet unsere Studie neue Einblicke in die hämolytische Aktivität von *S. lugdunensis* und die mikrobiellen Interaktionen in Mukoviszidose-Lungen und unterstreicht gleichzeitig die Notwendigkeit einer weiteren Verfeinerung von GEMs durch die Einbeziehung von regulatorischen und interspezifischen Signalmechanismen.

Abbreviations

S. aureus	*Staphylococcus aureus*
S. lugdunensis	*Staphylococcus lugdunensis*
E. coli	*Escherichia coli*
P. aeruginosa	*Pseudomonas aeruginosa*
CoPS -	Coagulase-Positive Staphylococci
CoNS	Coagulase Negative Staphylococci
MRSA	Methicillin-Resistant *S. aureus*
EPS	Extra Polymeric Substance
IE	Infective Endocarditis
eDNA	Extracellular DNA
ISD	Iron Regulated Surface Determinant
Spa	Staphylococcal Protein A
Fnbp	Fibrinogen Binding Protein
Aap	Accumulation Associated Protein
Embp	Extracellular Matrix Binding Protein
Sasg	*S. aureus* Surface Protein G
PG	Peptidglycan
ECF	Energy Coupling Factor
Fbi	Fribrinogen Binding Surface Protein
Ica	Intracellular Adhesin
vWbf	Willebrand Factor Binding Protein
SLUSH	*S. Lugdunensis* Synergistic Hemolysins
QS	Quorum Sensing
PQS	Pseudomonas Quinolone System

HQNO	4-Hydroxy-2-Heptylquinoline N-Oxide
SCVs	Small Colony Variants
CF	Cystic Fibrosis
CFTR	CF Transmembrane Conductance Regulator
ABC	ATP-BINDING CASSETTE
Lha	Lugdunensis Heme Acquisition system
Fur	Ferric Uptake Repressor
ROS	Reactive Oxygen Species
PSM	Phenol Soluble Modulins
Agr	Accessory Gene Regulator
GEMs	Genome Scale Metabolic Models
FBA	Flux-Based Analysis
Hts	Heme Transport System
Sir	Stapylococcal Iron Regulated
SA	Staphyloferrin A
SB	Staphyloferrin B
pvd	Pyoverdine
GPR	Gene Protein Reaction
ASM	Artificial Sputum Medium
TSB	Tryptic Soy Broth
LB	Luria-Bertani Broth
NTML	Nebraska Transposon Mutant Library
PCR	Polymerase Chain reaction
SOE	Spliced Overlap Extension
EDDHA	Ethylenediamine-N, N'-bis (2-hydroxyphenylacetic acid)

Chapter 1

General Introduction

1. Staphylococci

Bacteria of the genus Staphylococcus are gram-positive bacteria that can infect humans (*1*). Staphylococcal cells are sized of 0.5 – 1.5 µm in diameter and typically form grape-like clusters (*2*). Staphylococci are facultative anaerobes that can grow by fermentation or by respiration. *Staphylococcus* species are differentiated by their ability to produce coagulase, an enzyme that binds and activates prothrombin, resulting in clotting of plasma by conversion of fibrinogen to fibrin (*3*). Based on this ability, *Staphylococcus* species are classified into coagulase-positive staphylococci (CoPS) and coagulase-negative staphylococci (CoNS) (*2, 4*).

1.1 *Staphylococcus aureus*

Staphylococcus aureus (S. aureus) is a human pathogen, known for its ability to evade the immune system (*5, 6*) and cause a wide range of infections, including abscess, skin lesions, and life-threatening systemic diseases, including bacteremia and endocarditis (*6, 7*). *S. aureus* is primarily a human commensal and colonises approximately 30% of the human population in the nasal passages. This colonisation leads to an increased risk of infection in a hospital setting, where it represents a major cause of nosocomial infections (*8, 9*).

During infection, an immune reaction is initially initiated by macrophages summoning neutrophils by releasing cytokines (*10*). *S. aureus* is generally susceptible to antibiotic treatment; however, it has demonstrated a remarkable capacity to develop resistance. One major concern is methicillin-resistant *S. aureus* (MRSA), which has acquired resistance to β-lactam antibiotics, including methicillin. Initially emerging in medical settings, MRSA has posed significant challenges in treating infections (*11, 12*).

S. aureus secretes extracellular polymeric substances (EPS) that forms a biofilm embedded microbial cells, in a matrix composed of extracellular DNA (eDNA), proteins and polysaccharides. The remaining biofilm contains water and microcolonies (*10, 13, 14*). This biofilm confers resistance to host defenses and antibiotics (*12, 13*). *S. aureus* EPS also contains proteins including Staphylococcal Protein A (Spa), Fibrinogen Binding Protein (FnBP) A and B, Accumulation Associated Protein (Aap), Extracellular matrix Binding Protein (EmbP), *S. aureus* surface protein G (SasG) and amyloid fibers (*15, 16*). Cell wall-anchored proteins are found to be attached to cell wall peptidoglycan (PG) by trans peptidases covalently (*17*).

1.2 *Staphylococcus lugdunensis*

Staphylococcus lugdunensis (S. lugdunensis) was first described/found in 1988 in Lyon, France. *S. lugdunensis* is a CoNS, mostly found as a skin commensal, but can colonise the nasal and perineal regions (*18, 19*). Compared to other CoNS species, *S. lugdunensis* exhibits a virulence factor like *S. aureus*, and while infections are rare, it has the potential to cause fulminant infections, making it a clinically significant pathogen (*1, 20, 21*). *S. lugdunensis* infections are associated with healthcare-associated infections, such as infective endocarditis (IE), as well as skin and soft tissue infections (*18, 22-25*). Despite having fewer virulence factors than *S. aureus* and being more vulnerable to antibiotics, *S. lugdunensis* is yet able to express pathogenic mechanisms and virulence factors (*26*). *S. lugdunensis* possesses a few virulence factors with homology to factors of *S. aureus. S. lugdunensis* produces the fibrinogen binding protein to adhere to fibrinogen and a putative von Willebrand factor protein that facilitates adherence to endothelial cells (*20, 27, 28*). *S. lugdunensis* acquires heme during infection via an iron-regulated surface determinant (Isd) system, enabling it to overcome nutritional limitations. It also binds essential metals using energy-coupling factor (ECF) transporters to support its growth and virulence (*29, 30*). *S. lugdunensis* expresses surface adhesins to adhere to host matrix proteins such as fibrinogen-binding surface protein (FbI), polysaccharide intracellular adhesin (ica) and von Willebrand factor binding protein (vWbf) (*31-34*). Also, *S. lugdunensis* produces toxins such as putative β-hemolysin (*35*), putative hemolysin III (*36*) and *S. lugdunensis* synergistic hemolysins (SLUSH) peptides with delta toxin-like activity towards erythrocytes (*26, 37*).

2. Pseudomonas aeruginosa

Pseudomonas aeruginosa is a rod-shaped gram-negative bacterium. It is an opportunistic pathogen. Cells are about 1-5 μm long and 0.5–1.0 μm wide (*38, 39*). This pathogen is diverse, inhabiting water, soil, animals, and plants (including humans) (*39, 40*). This pathogen rarely causes disease in healthy people but infects immunocompromised patients (e.g., AIDS patients) as well as patients suffering from cystic fibrosis or burn injuries (*41, 42*). It is also a major contributor to hospital-acquired infections and the second common cause of pneumonia. *P. aeruginosa* demonstrates significant antibiotic resistance, largely due to its robust biofilm-forming capacity (*42, 43*).

2.1 Virulence Factors

In polymicrobial infection, *P. aeruginosa* outcompetes or dominates other pathogens with different mechanisms to adapt to changing, hostile conditions. *P. aeruginosa* possesses several virulence factors that help to target the host and cause disease. These factors include

2.1.1 Exotoxin A

P. aeruginosa produces exotoxin A, a potent toxin that inhibits protein synthesis in host cells by ADP-ribosylating elongation factor 2 (EF-2), an essential component of the translation process. This modification inactivates EF-2, effectively halting protein production in the host cell. The resulting loss of cellular function leads to cell death and contributes to tissue necrosis during infection (*44*).

2.1.2 LasA and LasB Proteases

LasA protease exhibits elastolytic activity, specifically degrading elastin, an essential component of connective tissue. The degradation facilitates bacterial invasion and contributes to tissue destruction (*45*). LasB elastase is a broad-spectrum metalloprotease that degrades various extracellular matrix components, including elastin, collagen and laminin, causing tissue damage and dissemination of bacteria (*46*). LasA enhances the elastolytic activity of LasB playing a synergistic role in virulence (*47*).

2.2 Competition Factors

P. aeruginosa utilises various strategies to outcompete *S. aureus* in polymicrobial communities which include

2.2.1 Quorum Sensing Systems

P. aeruginosa possesses intricate quorum sensing (QS) networks, including Las, RhI and Pseudomonas Quinolone Signal (PQS) systems. These systems regulate genes responsible for virulence, biofilm formation, and interspecies competition. Through QS, *P. aeruginosa* can coordinate group behaviours such as toxin production and resource acquisition, thereby enhancing its adaptability and competitiveness within polymicrobial environments (*48*).

2.2.2 4-hydroxy-2-heptylquinoline N-oxide (HQNO)

Produced under the control of the PQS system, HQNO (*49, 50*) acts as an anti-staphylococcal agent by inhibiting the electron transport chain of *S. aureus*. This inhibition suppresses the growth of *S. aureus* which leads to the formation of small colony variants (SCVs) (*51*) (*52*).

3. Interaction Between *S. aureus* and *P. aeruginosa*

3.1 Polymicrobial Infections

In polymicrobial infections, microbes compete for nutrients (iron, manganese, copper, and Zinc), pathogenicity and colonization (*53-55*). *S. aureus* and *P. aeruginosa*, both members of the ESKAPE pathogens, are primary bacteria involved in various infections, including in cystic fibrosis (CF) patients, health care-associated pneumonia and chronic wounds (*56*). The acronym ESKAPE refers to a group of clinically significant, multidrug-resistant pathogens: *Enterococcus faecium*, *S. aureus*, *Klebsiella pneumoniae*, *Acinetobacter baumanii*, *P. aeruginosa* and *Enterobacter spp*. These organisms are known for their ability to escape the action of antimicrobial drugs, contributing significantly to nosocomial infections worldwide. They possess various virulence mechanisms, including biofilm formation, antibiotic resistance, and secretion of toxins, and are considered a critical priority by World Health Organization (WHO) and Centers for Disease Control and Prevention (CDC) for research and new drug development (*57*). The Spatial organization of *S. aureus* and *P. aeruginosa* within biofilm influences their behavior (*58*). They exist in distinct niches, with *P. aeruginosa*

typically found in deeper tissues layers (*59*) where it produces virulence factors that either stabilize or eliminate *S. aureus,* located in surface of infection site (*60*).

3.2 CF as a Model of Polymicrobial Infections

CF is the typical example of biofilm-related infection of *P. aeruginosa* and *S. aureus*. CF is a genetic disorder that is hereditary and affects Caucasians, and it is caused by mutations in the CF transmembrane conductance regulator (*CFTR*) gene, which encodes for the CFTR protein (*49, 61*). This protein functions as an ion channel that transports chloride ions across cells, and it is found in epithelial cell membranes in the liver, pancreas, respiratory tract, and lungs. The impaired protein upsets the ion balance required for maintaining the normal hydrated mucus layer, which leads to increased mucus thickness that cannot be cleared by cilia (*49*). Bacteria settling within the mucus result in chronic infections and inflammation (*62*). According to an annual data report from 2020, from the CF Foundation, the lungs of CF patients get infected and colonised by multiple bacteria (*49*) throughout their lifetime and in the lungs, bacterial flora changes based on the age of patients. *S. aureus* is the most common pathogen found across all age groups but is found prominently in younger children and over time, as patients age, it is found with *P. aeruginosa* (*49*).

3.3 S. aureus SCV Adaptations

S. aureus can develop defense mechanisms to survive in the presence of *P. aeruginosa*, one of which is the formation of SCVs as mentioned above. SCVs are a subpopulation of bacteria that arise due to specific genetic mutations that result in inactivation of the respiratory chain, leading to a shift in bacterial metabolism from oxidative phosphorylation to fermentative metabolism. These variants grow at a much slower rate compared to their wild-type counterparts due to reduced efficiency of energy production through oxidative metabolism (*63, 64*). The main feature of SCVs is their resistance to oxidative stress, which allows them to survive under conditions where the host immune system, like reactive oxygen species (ROS), exerts a respiratory attack.

SCVs phenotype enhances *S. aureus* survival through increased intracellular persistence, antibiotic resistance, and biofilm formation (*51*). The size and altered

metabolic activity of SCVs make difficult to treat and a major contributor to persistent infections.

4. Nutritional Immunity

Nutritional immunity is a host defense mechanism that limits pathogen growth by restricting access to essential nutrients, particularly metals like iron. During infection, host proteins such as lactoferrin, transferrin, hepcidin and ferroportin sequester iron, reducing its availability to invading pathogens (*65*). In response, bacteria have evolved diverse iron acquisition strategies, including siderophore production and heme uptake mechanisms, to overcome these limitations (*66, 67*).

4.1 *S. aureus* Iron Acquisition

S. aureus employs multiple iron acquisition systems to thrive in iron-restricted environments.

4.1.1 Siderophore Production

S. aureus synthesises two alpha-hydroxy carboxylate siderophores, staphyloferrin A (SA) and staphyloferrin B (SB), which scavenge iron from host proteins. The HtsABC (Heme transport system) and SirABC (Staphylococcal iron-regulated) mediate the uptake of SA and SB, respectively (*30*) (*68*). Siderophore production is particularly important in iron-limited environments, such as during infection, where *S. aureus* competes with host proteins (*69*).

4.1.2 Heme Uptake System

The iron-regulated surface determinant (Isd) system allows *S. aureus* to extract iron from heme, which is abundant in host hemoglobin and other heme-containing proteins (Figure 1). The surface protein IsdB binds directly to hemoglobin while IsdA and IsdC facilitate the relay of heme through the peptidoglycan layer. Once heme reaches the membrane, it is transported into the cytoplasm by the ATP-binding cassette (ABC) transporter complex IsdDEF. Inside the cytoplasm, heme is degraded by heme oxygenases, such as IsdG and IsdI, which cleave the heme molecule to release free iron. This heme acquisition pathway is essential for *S. aureus* survival in iron-limited environments like the bloodstream and contributes significantly to its pathogenicity

(*69-71*). The ability to acquire iron from heme is critical for *S. aureus* survival in the bloodstream and for infections.

4.1.3 Ferric Uptake Regulator (Fur) System

Fur is a global transcription factor pivotal in maintaining iron homeostasis in bacteria. It regulates genes responsible for iron uptake, storage, and metabolism, ensuring a balance between iron sufficiency and toxicity (*72*). When intracellular iron levels are high, Fe^{2+} ions bind to the ferric uptake repressor (Fur) protein. This iron-bound Fur dimerises and attaches to specific DNA sequences known as “Fur boxes” located in the promoter region of iron regulated genes. Binding of Fur to these regions represses the transcription of genes involved in iron acquisition, preventing excess iron uptake and potential toxicity. Under low iron conditions, Fe^{2+} dissociates from the Fur protein (*73*). This unbound Fur undergoes a conformational change, reducing its affinity to Fur boxes and leading to its detachment from DNA. This derepression enables bacteria to enhance iron acquisition by expressing siderophore biosynthesis and transport genes, heme uptake systems, and iron transport proteins (*73-75*). In *S. aureus*, Fur regulates siderophore-mediated iron uptake and heme acquisition. It also influences virulence factors, biofilm formation and oxidative stress response, making it a key regulator beyond iron metabolism (*69*). Thus, Fur enables bacteria to balance iron acquisition and avoid toxicity, while also influencing pathogenic traits.

4.2 Iron acquisition by *S. lugdunensis*

S. lugdunensis employs multiple strategies to acquire iron from its host environment. Like CoPS, *S.lugdunensis* possesses a functional Isd system (*35, 76, 77*) and utilises the high-affinity heme uptake pathway to grow at low heme concentrations (*78, 79*).

4.2.1 Heme Acquisition and Utilisation

The Isd system in *S. lugdunensis* allows the bacteria to extract heme from hemoproteins including hemoglobin, myoglobin and hemopexin (*68*). In addition to the Isd system (Figure 1), *S. lugdunensis* possesses a unique heme acquisition mechanism known as Lugdunensis Heme Acquisition system (Lha) (*29*). This system is encoded by the *lhaSTA* operon, which facilitates energy-dependent heme uptake through an ECF transporter. This transporter allows *S. lugdunensis* to extract heme independently of surface receptors, distinguishing it from other *Staphylococcus*

species (*29*). Unlike *S. aureus*, *S. lugdunensis* cannot produce siderophores, and depends on the acquisition of xenosiderophores (siderophore produced by other microbes) in polymicrobial infection. Indeed, *S. lugdunensis* expresses the transporters HtsABC and SirABC (*30, 79*) for *S. aureus* staphyloferrrin A and staphyloferrin B siderophores, respectively. This cross-species siderophore utilization enhances *S. lugdunensis* survival in iron-limited conditions and promotes its growth in co-infections (*78*).

Figure 1: Heme Acquisition and Transport in *S. lugdunensis*: This figure illustrates the *Isd* (iron-regulated surface determinant) system in *S. aureus*, responsible for heme acquisition from host hemoproteins (Hb, Mb, Hpx). Heme is extracted by surface receptors *(IsdB, IsdJ)* and transferred through *IsdC* before being transported across

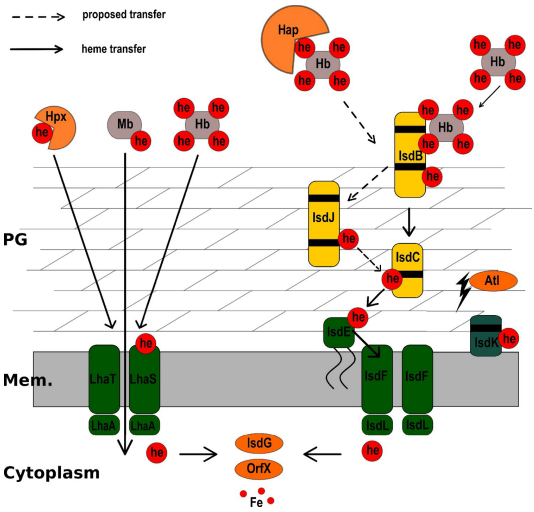

the membrane via *IsdE*, *IsdF*, and *IsdL*. Lha transporters also facilitate heme uptake. Once inside, heme is degraded by *IsdG* and *OrfX* to release iron for bacterial metabolism. Reproduced from Jochim, A. et al. (2020). An ECF-type transporter scavenges heme to overcome iron-limitation in *Staphylococcus lugdunensis*. eLife, 9, e57322.

5. *Staphylococcal* Virulence Factors

5.1 Accessory gene regulator (Agr)

QS is a bacterial communication system that enables populations to coordinate gene expression based on cell density. QS relied on the production, release, and detection of signalling molecules called autoinducers. Once these molecules reach a threshold concentration, they trigger the activation of genes involved in various processes including Phenol Soluble Modulins (PSM), virulence factor production and antimicrobial resistance.

In *S. aureus* QS is primarily regulated by accessory gene regulator (agr) locus, which encodes a two-component system, plays key role in controlling virulence and adaptation to host environment. The *agr* locus is found in all staphylococci and serves an important role in regulating virulence factors and biofilm formation. The *agr* locus comprises two divergent promoters, P2 and P3 (Figure 2) which generates two different transcripts RNAII and RNAIII respectively (*80, 81*). RNAII includes the transcript of four genes *agrB, agrD, agrC* and *agrA.* The *agrD* gene encodes the precursor of autoinducing peptide (AIP), which is processed and exported by the membrane protein AgrB. The sensor histidine kinase AgrC detects extracellular AIP and upon activation, phosphorylates the response AgrA, Phosphorylated AgrA activates transcription from both the P2 and P3 promoters, amplifying the QS signal.

RNAIII functions as a regulatory RNA that modulates the expression of numerous virulence factors. It upregulates genes encoding secreted toxins and enzymes while downregulating genes encodes secretes toxins and enzymes while downregulating genes encoding surface adhesion proteins (*80, 82*). In most staphylococci except *S. lugdunensis* and *S. saprophytic,* the *hld* gene which encodes δ-toxin is in the RNAIII transcript (*36, 82*). This gene plays a role in regulating virulence by affecting cell-cell interactions and immune evasion.

The *S. lugdunensis agr* locus shows 63% homology to that of *S. aureus*, with P2 and P3 being highly conserved regions (*82*). SLUSH peptides of *S. lugdunensis* are encoded outside of *agr* region but are still regulated by *agr* like PSMs in staphylococci. The absence of the *hld* gene in *S. lugdunensis* RNAIII did not alter the ability to function as a regulatory molecule (*82, 83*).

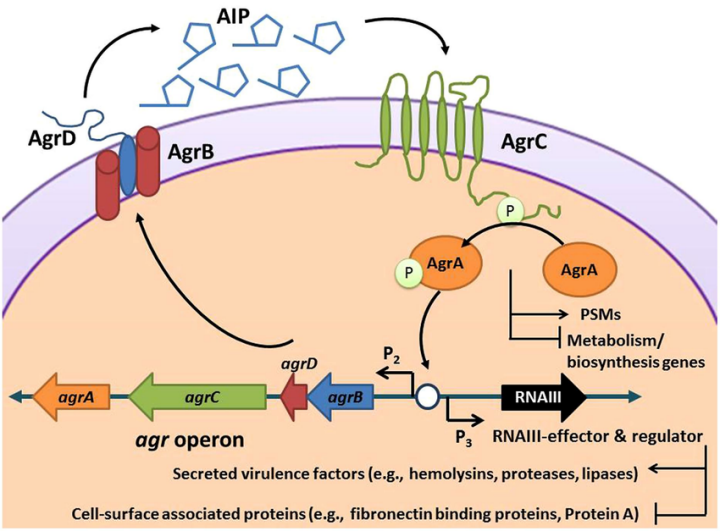

Figure 2: The *agr* Quorum Sensing System in *S. aureus:* This figure depicts the *agr* quorum sensing system, which regulates virulence in *S. aureus*. AgrD is processed by AgrB to produce AIP, which binds to AgrC, activating AgrA through phosphorylation. *AgrA* then induces *RNAIII* transcription, leading to increased secretion of virulence factors (e.g., hemolysins, proteases) and reduced expression of surface-associated proteins. This system enables *S. aureus* to coordinate virulence gene expression based on cell density. Figure is reprinted from Quave, C. L., & Horswill, A. R. (2014). Flipping the switch: Tools for detecting small molecule inhibitors of staphylococcal virulence. Frontiers in Microbiology, 5, 706.

5.2 Phenol Soluble Modulins and SLUSH

Phenol-soluble modulins (PSMs) are a family of amphipathic, alpha-helical peptides secreted by staphylococci (*84*). In *Staphylococcus epidermidis*, PSMs include PSMα, PSMβ, and PSMγ. Notably, PSMγ is identical to the δ-toxin of *S. aureus* (*85, 86*). PSMs are grouped according to their length, α- type PSMs are smaller with only 20-25 amino acids and β-PSMs are longer with 43-45 amino acids (*84, 85*). β-PSMs are surfactant-like virulence factors produced by *S. aureus*, these peptides are amphipathic and cationic as they both have hydrophilic and hydrophobic regions,

which enables to interact with and insert into lipid membranes. Once in the membrane, β-PSMs disrupt membrane integrity and form pores that lead to cell lysis, including hemolysis of red blood cells and killing of immune cells (white cells) (*87*) (*88*). *S. aureus* survives within host cells evading the immune system, and this survival is largely dependent on PSMs. PSMs contribute to pathogenesis by intracellular killing after phagocytosis (*7, 89, 90*).

S. lugdunensis is known for its hemolytic activity, which is attributed to the production of SLUSH (*Staphylococcus lugdunensis* hemolysin). SLUSH has been identified as a group of hemolytic peptides responsible for the bacterium's ability to lyse red blood cells. SLUSH peptides are encoded by three genes SLUSH-A, -B and -C with the fourth peptide OrfX present in a single locus (*36, 90*). The hemolytic action of SLUSH is similar to the mechanisms of other staphylococcal toxins, such as PSMs, which are involved in the destruction of host cells. PSMs, which are also involved in *S. lugdunensis* include peptides with both alpha-type (which form pores in host cell membranes) and beta-type (which promote cell lysis by destabilising membranes) activities.

6. Proteases

Proteases are a group of enzymes that cleave protein peptide bonds. It is categorised based on catalytic reactions into serine, cysteine, glutamic, threonine and metalloproteases (*91, 92*). Based on the site of action, they are called endopeptidase or exopeptidases. Compared to mammalian proteases, bacterial protease exhibits greater diversity in mechanism, structure, and function. Apart from their role in protein and peptide digestion, they play a role in metabolism and physiology, controlling various stages in protein synthesis, protein signalling and gene expression (*91*). The most abundant bacterial proteolytic enzymes are serine, metalloproteases, and cysteine proteases (*91, 93*).

6.1 Proteases in *S. aureus*

To access heme and other nutrients, *S. aureus* produces multiple secreted and cell wall-associated proteases: Aureolysin (Aur), a metalloprotease, degrades host structural proteins and immune factors like complement components and antimicrobial peptides (*94*). V8 protease (SspA), a serine protease, promotes tissue invasion by

breaking down extracellular matrix proteins and immunoglobulins (*94, 95*). SplA–F (serine protease-like proteins), encoded in a single operon, modulate host immune responses and may influence colonization patterns (*96*).

6.2 Proteases in *P. aeruginosa*

P. aeruginosa also produces a powerful arsenal of proteases to promote tissue damage, immune evasion, and outcompete co-infecting microbes: LasB (elastase) and LasA degrade elastin, collagen, immunoglobulins, and disrupt epithelial barriers (*44, 46*) . Protease IV contributes to virulence by degrading fibrinogen and surfactant proteins in the lung (*97*). Alkaline protease (AprA) interferes with host immune function and complements LasB in tissue destruction (*98*) . These proteases are regulated by quorum sensing (Las and Rhl systems), allowing coordinated expression in high-density communities such as biofilms.

Together, the proteolytic systems of *S. aureus* and *P. aeruginosa* are essential for virulence, nutrient acquisition (especially iron), and survival in polymicrobial infections such as those in cystic fibrosis lungs or chronic wounds (*99*).

7. Genome-scale metabolic models (GEMs)

In the age of bacterial genomics, the understanding of microbial metabolomic capacity and its impact on microbial interaction could be drastically improved by genome-scale metabolic models (GEMs) (*100, 101*). GEMs show the depth of knowledge about an organism whose genome has been sequenced, while also accentuating the knowledge gaps that will be filled by additional research, by situating the genome annotation within the context of how the biochemical components of the cell work together to consume substrates, produce energy, and grow (*102, 103*).

GEMs are reliable tools for studying bacterial systems. GEMs are an invaluable resource for comprehending the molecular connections underlying the relationship between genotype and phenotype (*103, 104*). Built from known metabolic events and metabolic genes in the target organism, GEMs are mathematical reconstructions of the metabolic network. The capacity of GEMs to model infection-relevant conditions can aid in identifying potential challenges to therapeutic interventions, particularly those arising from genetic modifications and the targeting of specific metabolic pathways. By using genome sequences, GEMs make it possible to calculate metabolic

functions at the systems level and increase the capability of pan-genome investigations to evaluate a species phenotypic variance using sequence-based analysis. A collection of gene-protein relationships that are mathematically constructed and contribute to a biological system's metabolism makes up every model. Draft reconstruction, conversion to mathematical format, refining, and network assessment are the four main phases of GEM reconstruction. After the validated model is deemed a robust GEM, the final three steps are usually repeated until predictions agree with experimental results (*104, 105*).

The method employed in genome-scale metabolic networks reconstruction, to investigate biochemical networks, is called flux base analysis (FBA). By calculating the flow of metabolites via the metabolic network, the organism growth rate or the rate of metabolite production is predicted by FBA (*106*). The first steps in FBA involve the mathematical representation of metabolic reactions. An array of the stoichiometric coefficients for every reaction, displayed as a numerical matrix, is the primary constituent of this representation. Defining a phenotype is a biological aim that is relevant to the problem under study and is the next step in the FBA process. Biomass production, or the rate at which metabolic chemicals are transformed into biomass constituents including lipids, proteins, and nucleic acids, is the goal when predicting growth. A synthetic "biomass reaction," or an additional column of coefficients in the matrix of stoichiometries, is added to model biomass generation statistically. This reaction consumes precursor metabolites at stoichiometries that closely resemble biomass production. Experimental measurements of the components of biomass serve as the foundation for the biomass response. The reaction is adjusted such that the flow through it matches the organism's exponential growth rate (μ) (*106*).

GEMs are very promising in modeling and analyzing the metabolic interaction between bacteria, such as in co-infections of *S. aureus* and *P. aeruginosa.* They allow researchers to model bacterial metabolism under different conditions, which can help identify key metabolites in bacterial interaction. By mapping interactions, GEMs could potentially uncover new targets for drug intervention, e.g., novel metabolic pathways or key enzymes implicated in bacterial survival or virulence. One of the most exciting promises is the ability of GEMs to predict how metabolic changes occur during infection, providing insight into how bacteria evolve and thrive in the nutrient-poor

conditions of the human body, particularly in chronic infections like those seen in cystic fibrosis. However, GEMs have their limitations. One of the main limitations is that GEMs are typically based on static genomic data and thus make extensive use of annotated genomes rather than actual gene expression profiles. This means that GEMs may not reflect the dynamic nature of bacterial metabolism, which can be very sensitive to environmental conditions, growth, and the specific host niche. While GEMs can make predictions based on genetic potential, they lose important regulatory aspects or metabolic fluctuation that occur in response to the host environment or stress conditions. This limitation may render it challenging to model real bacterial behaviour accurately, especially in polymicrobial infections in which multiple bacterial species are signalling to each other and the host. In addition, GEMs are typically limited by the quality of complete and accurate genomic information that is often not representative of the metabolic capacity of each bacterial species or strain.

One of the major objectives is to explore such gaps through the integration of GEMs with actual experimental data. By incorporating gene expression profiles and metabolomics data into GEM models, the gap between static genomic models and dynamic processes that take place in vivo is bridged. Here, we are concerned with the interaction between *S. aureus* and *P. aeruginosa* at the metabolic level during co-colonisation and how the interaction influences the production of essential metabolites that dictate infection outcomes. Through circumventing these disadvantages, it presents a truer and fuller depiction of bacterial metabolic networks in the context of disease, and possibly discovers novel targets for the treatment of infectious diseases.

Aim of this study

The aim of this study is to investigate the mechanisms by which *S. lugdunensis* acquires iron from the host sources, focusing specifically on how it accesses and utilizes hemoglobin following erythrocyte lysis. Specifically, we aim to understand the interplay between erythrocyte lysis, hemoglobin release and bacterial growth under iron-limited conditions. While erythrocyte lysis and the subsequent release of hemoglobin are well recognised in bacterial infections, the specific mechanisms by which bacteria induce hemolysis and acquire iron from hemoglobin and heme remain poorly understood. In Chapter 1, we examine the role of SLUSH peptides in the iron acquisition process of *S. lugdunensis* and describe their relevance for hemolysis and the release of hemoglobin. We also explore how the released hemoglobin is accessed and processed to liberate heme, which serves as the actual source of iron for bacterial uptake.

Additionally, the study will address metabolic interactions between bacterial pathogens. Specifically, it will explore the interactions between *S. aureus* and *P. aeruginosa,* two common pathogens, in conditions such as cystic fibrosis. Chapter 2 describes the use of GEMs to study metabolic interactions between *S. aureus* and *P. aeruginosa*. By utilising GEMs, we aim to predict the metabolic pathways involved in bacterial interactions under the conditions of iron limitation and competition for resources. Our research focusses on how these pathogens influence each other survival and virulence.

Chapter 2

SLUSH peptides of the PSMβ family enable *Staphylococcus lugdunensis* to use erythrocytes as a sole source of nutrient iron

Sharmila Sekar[abd], Selina Schwarzbach[abd], Mulugeta Nega[a], Dominik Alexander Bloes[a,d], Emanuel Smeds[e], Dorothee Kretschmer[abd], Timothy J. Foster[f] and Simon Heilbronner[abcdg *]

[a] Department of Infection Biology, Interfaculty Institute of Microbiology and Infection Medicine, University of Tübingen, 72076 Tübingen, Germany.

[b] Cluster of Excellence EXC 2124 Controlling Microbes to Fight Infections, 72076 Tübingen, Germany.

[c] German Center for Infection Research (DZIF), partner site Tübingen.

[d] Interfaculty Institute of Microbiology and Infection Medicine, Institute for Medical Microbiology and Hygiene, UKT Tübingen, 72076 Tübingen, Germany.

[e] Lund Protein Production Platform, Department of Biology, Lund University, Lund, Sweden

[f] Trinity College Dublin, the moyne Institute of Preventive Medicine, Dublin, Ireland

[g] Faculty of Biology: Microbiology, Ludwig-Maximilians-Universität München, Martinsried, Germany

* Corresponding author: Simon Heilbronner, LMU München, Biozentrum der LMU, Großhadernerstrasse 2-4, 82152 Martinsried; Tel: 089 2180 74611; Email: simon.heilbronner@lmu.de

Abstract:

During infection the host employs nutritional immunity to restrict access to iron. *Staphylococcus lugdunensis* has been recognized for its ability to utilize host-derived heme to overcome iron restriction. However, the mechanism behind this process involves the release of hemoglobin from erythrocytes, and the hemolytic factors of *S. lugdunensis* remain poorly understood. *S. lugdunensis* encodes four phenol-soluble modulins (PSMs), short peptides with hemolytic activity. The peptides SLUSH-A, SLUSH-B and SLUSH-C are β-type PSMs, OrfX is an α-type PSM. Our study shows the SLUSH locus to be essential for the hemolytic phenotype of *S. lugdunensis*. All four peptides individually exhibited hemolytic activity against human and sheep erythrocytes, but synergism with sphingomyelinase was observed exclusively against sheep erythrocytes. Furthermore, our findings demonstrate that SLUSH is crucial for allowing the utilisation of erythrocytes as the sole source of nutritional iron and confirm the transcriptional regulation of SLUSH by Agr. Additionally, our study reveals that SLUSH peptides stimulate the human immune system. Our analysis identifies SLUSH as a pivotal hemolytic factor of *S. lugdunensis* and demonstrates its concerted action with heme acquisition systems to overcome iron limitation in the presence of host erythrocytes.

Abbreviations: agr, accessory gene regulator; CoNS, Coagulase negative staphylococci; FPR, Formyl Peptide Receptor; Hb, Hemoglobin; Hlb, Beta- Hemolysin; Hld, Delta- hemolysin; IE, infectious endocarditis; Isd, Iron Dependent Surface Determinant; PSM, Phenol Soluble Modulins; SLUSH, Stapylococcus Lugdunensis Synergistic Hemolysin; TSA, Tryptic Soy Agar; TSB, Typtic Soy Broth

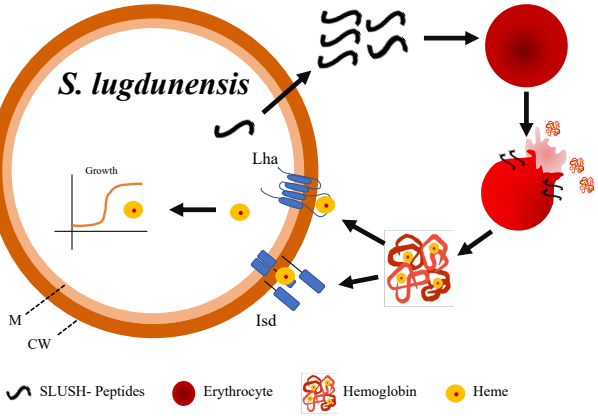

Schematic Diagram: *Staphylococcus lugdunensis* secretes SLUSH peptides to mediate the lysis of erythrocytes. Isd and Lha extract heme from the released hemoglobin and facilitate its import to overcome iron restriction and to allow proliferation.

Introduction:

Staphylococcus lugdunensis belongs to the coagulase negative staphylococci (CoNS) and was firstly described by Freney *et al* in 1988 in Lyon, France (1). It is a skin commensal that is predominantly isolated from moist areas such as the perineum, the inguinal fold and under the large toenail (2). Described as a “wolf in sheep’s clothing”, *S. lugdunensis* behaves in many ways more like the coagulase positive *S. aureus* than the other CoNS including having an apparent elevated degree of virulence. *S. lugdunensis* causes a wide range of different infections including abscesses and wound infections but is particularly associated with severe cases of infectious endocarditis (IE). Between 1 % and 5 % of IE cases are reported to be caused by *S. lugdunensis* (3) (4).

Although *S. lugdunensis* is now recognized as an important pathogen there is still remarkably little information regarding virulence factors and the molecular mechanisms of pathogenicity. Several factors putatively promoting virulence have been identified. Amongst these are the cell wall-anchored proteins Fbl and vWbl that promote adherence to the human proteins fibrinogen and von Willebrand Factor,

respectively (5-8). Additionally, an iron dependent surface determinant locus (Isd) is encoded by *S. lugdunensis*. The Isd system allows the extraction of heme form hemoglobin and its use as a source of nutritional iron (9-13). The human immune system puts enormous pressures on invading pathogens. The active depletion from human bodily fluids of easily accessible nutrients and trace elements is referred to as "nutritional immunity" (14, 15) and represents an effective antimicrobial strategy. Best studied in this regard is the role of iron (Fe^{2+}/Fe^{3+}). Iron is an important molecule for the host and the pathogen (16, 17). Within the human body, available sources of iron are actively depleted. Extracellular iron ions are bound by high-affinity iron-chelating proteins such as lactoferrin and transferrin found in lymph and mucosal secretions or within the serum, respectively (16, 18). Hemoglobin (hb) represents an abundant iron source within the host, and it is well understood that Isd systems facilitate the extraction of heme from hb to overcome nutritional immunity (19, 20). However, hb is located intracellularly within erythrocytes and is therefore not accessible unless it can be liberated from the cells (21). While it is generally accepted that hemolytic factors secreted by pathogens facilitate the release of hb from erythrocytes, the precise nature of these factors and their relevance for growth using erythrocytes as an iron source are in many cases poorly defined.

S. lugdunensis encodes three short peptides named Staphylococcus Lugdunensis Synergistic Haemolysin (SLUSH) (22). The three SLUSH peptides have a length of 43 aa and are encoded in a single locus together with a fourth peptide (OrfX) for which no function has yet been described (22). The SLUSH peptides show similar characteristics as the phenol soluble modulins (PSMs). All PSMs share an amphiphatic, α-helical structure (23) and are secreted by most staphylococcal species including *S. aureus* (24) and *S. epidermidis* (25). Two classes of PSMs are distinguished according to peptide mass, α-type PSMs (20-26 amino acids (aa) in length) and β-type PSMs (~44 aa) (24, 25). The short αPSMs of *S. aureus* display strong hemolytic effects (24, 26) and have been identified as key virulence factors of *S. aureus* in murine models (24). In addition, α- and β-type PSMs have been shown to be important for biofilm development and structuring, due to their surfactant characteristics (27, 28). *S. lugdunensis* OrfX is potentially an αPSM. In contrast SLUSH-A/B/C are β-type PSMs (29) .

Here we have investigated the role of SLUSH in promoting S. *lugdunensis* hemolysis using human and sheep erythrocytes. We show SLUSH to be the dominant hemolytic factor of *S. lugdunensis* and confirm their Agr-dependent regulation. We show that the peptides have discrete and non-synergistic hemolytic activity and are needed to allow *S. lugdunensis* to use human erythrocytes as a source of nutrient iron. Furthermore, we show that the SLUSH peptides stimulated host immune defenses.

Materials and Methods

Chemicals and reagents:

If not stated otherwise, chemicals were ordered from Sigma.

Bacterial strains and growth conditions

All strains used are listed in Table 1. Unless stated otherwise, *S. lugdunensis* and *S. aureus* were grown in tryptic soy broth (TSB) or agar (TSA) (Oxoid). *E. coli* strains were grown in lysogeny broth or agar (DIFCO). Unless stated otherwise, strains were grown at 37°C.

Table 1: Bacterial strains and plasmids

Bacterial Strain / Plasmid	Description	Reference / Source
Staphylococci		
S. lugdunensis N920143	Human clinical isolate, genome sequenced	(21)
S. lugdunensis HKU09-01	Human clinical isolate, genome sequenced	(39)
S. lugdunensis N940025	Human clinical isolate	NRC†
S. lugdunensis N910319	Human clinical isolate	NRC†
S. lugdunensis N910320	Human clinical isolate	NRC†
S. lugdunensis N930432	Human clinical isolate	NRC†
S. lugdunensis N940084	Human clinical isolate	NRC†
S. lugdunensis N940113	Human clinical isolate	NRC†
S. lugdunensis N940135	Human clinical isolate	NRC†

S. lugdunensis N940164	Human clinical isolate	NRC†
S. lugdunensis N950646	Human clinical isolate	NRC†
S. lugdunensis SL2	Human clinical isolate	(56)
S. lugdunensis SL9	Human clinical isolate	(56)
S. lugdunensis SL13	Human clinical isolate	(56)
S. lugdunensis SL27	Human clinical isolate	(56)
S. lugdunensis SL37	Human clinical isolate	(56)
S. lugdunensis SL57	Human clinical isolate	(56)
S. lugdunensis SL62	Human clinical isolate	(56)
S. lugdunensis SL71	Human clinical isolate	(56)
S. lugdunensis SL72	Human clinical isolate	(56)
S. lugdunensis HKU09-01 Δ*SLUSH*	Deletion mutant of *Slush* locus	This study
S. lugdunensis HKU09-01 Δ*SLUSHABC*	Deletion mutant of *SlushABC l*ocus	This study
S. lugdunensis HKU09-01 Δ*agrA*	Deletion mutant of *agrA* gene	This study
S. lugdunensis HKU09-01 Δ*saeRS*	Deletion mutant of *saeRS* genes	This study
Lactococci		
Lactococcus lactis NZ9000		(31)
S. aureus USA300 LAC	Clincal MRSA isolate	(57)
S. aureus USA300 LAC Δ*psm*α1-4Δ*psmβ*1-2Δ*hld*		(24)
E. coli		

DH10B	*dam*$^+$ *dcm*$^+$ Δ*hsdRMS endA1 recA1* high efficiency cloning strain	Invitrogen
Plasmids		
pIMAY	Thermosensitive vector for allelic exchange	(25)
pIMAY-Δ*SLUSH*	A deletion encompassing the entire SLUSH locus (from *orfX* ATG to TAA of *slush B*) amplified from N920143	This study
pIMAY-SLUSH-*R*	A reversion fragment containing the entire SLUSH locus with a novel *Bam*HI restriction site amplified from HKU09-01	This study
pIMAY-Δ*agrA*	Plasmid for the deletion of *agrA*	This study
pIMAY-Δ*saeRS*	Plasmid for the deletion of two component *saeRS* genes	This study

† National Reference Centre for Staphylococci, Lyon, France

Growth Curve in iron limited conditions

For growth in iron limited conditions, bacteria were grown overnight in TSB. Cells were harvested by centrifugation, washed with RPMI containing 10 µM EDDHA (LGC standards), adjusted to an OD 1 and 2,5 µL were used to inoculate 0,5 ml of RPMI + 1% casamino acids (BACTO) + 10 µM EDDHA in individual wells of a 48-well microtiter plate (NUNC). As sole iron source, 20 µM $FeSO_4$ or freshly isolated erythrocytes (10^6 cells) were added to the wells. Bacterial growth was monitored using an Epoch2 reader (300 double orbital shaking, 37°C). The OD_{600} was measured every 15 min. For growth curves with synthetic peptides, erythrocytes were prepared as mentioned above and synthetic peptides were dissolved in DMSO and diluted with erythrocyte wash buffer before being added to the cells.

Construction of SLUSH deletion and reversion cassettes

Construction of cassettes for generating deletion mutations was carried out as described previously (30). In brief, A and B primer combinations were used to amplify a 500 bp upstream sequence (up to the start codon of *orfX*) and a 500 bp sequence downstream of the stop codon of *slush-B2* (C and D primers). The PCR products were

used as templates for the spliced overlap extension (SOE) PCR using primers A and D. The resulting 1 kb fragment was gel purified, cleaved at endonuclease cleavage sites introduced with forward and reverse primers (A and D) and cloned into pIMAY (30) digested with the same endonucleases. Primer sequences are listed in Table 2.

Table 2: Oligonucleotides used in this study

Primer	**5'-3' Sequence**	**Restriction site**
SLUSH-A	actgagctctgctggcaatgcattaac	*Sac*I
SLUSH-B	cattgtagttacctcctttattgtgtgcctc	
SLUSH-C	taaaggaggtaactacaatgtaatataatgttctaaatctttgaaagacc	
SLUSH-D	gatgaattcatacagactggcaacgttcc	*Eco*RI
SLUSH-E	cgctccttttttaggatccttgttaaagtctc	*Bam*HI
SLUSH-F	gagactttaacaaggatcctaaaaaggagcg	*Bam*HI
SLUSH-OutF	ctgaatttcaaatgattcaatttattcc	
SLUSH-OutR	gatgacatacgctatgaaatatgatgc	
PFA: HKU SaeRS	gtcaaagggtaccatacagtaacg	KpnI
PRB: HKU SaeRS	catttacatcattccttgattg	
PFC: HKU SaeRS	atgatgtaaatgtgatatccttaaaactttcactagc	
PRD: HKU SaeRS	cgcaagaacgagctccggatac	SacI
PFA: HKU AgrA	gaaacatactacgggtacccgctg	Kpn I
PRB: HKU AgrA	catgtcttcacgtccttatg	
PFC: HKU AgrA	ggacgtgaagacatgtaattattagttaacatg '	
PRD: HKU AgrA	gtttgaagagctccgtggaac	SacI
SLUSH Screening F	ctgaatttcaaatgattcaatttattcc	
SLUSH Screening R	gatgacatacgctatgaaatatgatgc	

qPCR 5S rRNA F	gcaaggaggtcacacctgtt	
qPCR 5S rRNA R	gcctggcaacgtcctactct	
qPCR SLUSHA-B F	aggagtggatttacatgtcaggt	
qPCR SLUSHA-B R	acctgacatattgtaaacgctcc	

To construct the reversion cassette, Primers E and F were synthesized to create a novel *Bam*HI restriction site between *slush A* and *slush B2*. Downstream of the *slush A* stop codon, the following nucleotide exchanges were introduced to create the novel restriction site: nucleotide 24 (T to G), 25 (A to G), and 29 (G to C). Primers A and E were used to amplify the upstream sequence and the 5'-end of the locus with the nucleotide exchanges. Primers F and D were used to amplify the downstream region together with 3'-end of the locus with the nucleotide exchanges. PCR products were gel-purified and used for the SOE PCR using primers A and D. The complementation cassette was gel-purified, cleaved at the endonuclease cleavage sites introduced in primers A and D and cloned into pIMAY treated with the same endonucleases. As reported earlier, the SLUSH locus could not be cloned in *E. coli*, probably due to toxicity of the produced peptides (22). To overcome this problem, we used the Gram-positive bacterium *Lactococcus lactis* as host for the cloning procedure (31). The SLUSH locus encoded on the reversion cassette did not appear to have toxic effects on *L. lactis* and positive clones could be identified. The plasmid was isolated and used to transform *S. lugdunensis.*

Transformation

S. lugdunensis strains were transformed as described elsewhere (8). Transformation of *L. lactis* NZ9800 was carried out as described elsewhere (31)**.** Chemically competent *E. coli* strains were transformed using standard procedures.

Hemolysis on agar plates

Sheep blood agar plates (Thermoscientific) were used to analyze direct or synergistic hemolysis or the Camp test using bacterial cultures or filter disks with recombinant peptides (15 µl of 1 mg/mL). These were placed close to a streaked culture of strain RN4220. Plates were incubated for 24h at 37°C before analysis.

Isolation of erythrocytes

Human blood was obtained from healthy volunteers and mixed 1:2 with MACS buffer (pyrogen free PBS + 0.05% BSA + 2 mM EDTA). Erythrocytes were pelleted by density gradient centrifugation in a histopaque blood gradient for 20 min 380 x g at RT. The erythrocyte pellet was washed three times with erythrocyte wash buffer (21 mM Tris, 4.7 mM KCl, 2 mM $CaCl_2$, 140.5 mM NaCl, 1.2 mM $MgSO_4$, 5.5 mM Glucose, 0.5% BSA, pH 7.4) (32). Cells were stained with trypan blue (BIO RAD) and enumerated.

Quantitative hemolysis assay using culture supernatant

Bacterial strains were grown overnight in TSB. Cultures were centrifuged, the supernatant was collected and sterile filtered (0.45 µM). The supernatant was diluted in TSB to an optical density of 5. Human erythrocytes ($1x10^8$ cells/mL) were prepared as mentioned above and were diluted at a 1:2 ratio with bacterial cultures in 48 well plates to a final concentration of 0.5 x 10^8 cells/mL. To perform a control showing 100% lysis, 0.5% of TritonX-100 was used as a positive control, while erythrocyte wash buffer with TSB served as a negative control. The plate was then incubated at 37° C with agitation for 1 h. After incubation, 250 µL of samples were collected and centrifuged at 10,000 g at RT for 3 min. 100 µL of each supernatant was transferred to wells of a 96 well plates and absorbance at 570nm was measured.

Hemolysis assay with synthetic SLUSH peptides and Hlb

Human erythrocytes were prepared as before, and synthetic SLUSH peptides were dissolved in DMSO and final concentrations of 0.01, 0.05, 0.1, 0.25, 0.5, 1, 2, 5, 10 µM in erythrocyte wash buffer were added to the erythrocytes at a final concentration of 0.5 x 10^8 cells/mL. Cells were then incubated, and samples were measured at 570nm, with DMSO in wash buffer as negative control. For synergy experiments, purified β-toxin (β-toxin solution for CAMP test, Hardy Diagnostics), was used together with synthetic peptides at a dilution of 1:4 (human erythrocytes). All samples were incubated at 37°C for 1h. Hemolysis was determined by measuring absorbance at 540nm.

SLUSH peptide synthesis

Peptides corresponding to OrfX (MMIADIIGGIIKLIKTLVDTFRKK), SLUSH-A (MSGIVDAISKAVQAGLDKDWATMATSIADAIAKGVDFIAGFFN), SLUSH-B (MSGIIEAITKAVQAGLDKDWATMGTSIAEALAKGIDAISGLFG) and SLUSH-C

(MDGIFEAISKAVQAGLDKDWATMGTSIAEALAKGVDFIIGLFH) of strain N920143 were synthesized by EMC microcollections GmbH (Tübingen). The peptides were N-formylated, had a purity of at least 90% and were dissolved in DMSO.

Isolation and stimulation of human neutrophils:

Human PMNs were isolated from fresh human blood of healthy volunteers by standard Ficoll/Histopaque gradient centrifugation as mentioned in (33) and stimulated with diluted bacterial culture filtrates (final concentration 0.25%) in 96-well U-shaped bottom plates. 5×10^5 PMNs were seeded in cell culture medium (very low endotoxin RPMI 1640, 2 mM sodium pyruvate, 2 mM L-glutamine, 100 u mL^{-1} penicillin/streptomycin, 10 mM 4-(2-hydroxyethyl)-1-piperazineethanesulfonic acid (HEPES)) and incubated for 5 h at 37 °C in 5% CO_2. *S. lugdunensis* cultures were grown for 17 hours at 37°C with agitation. Subsequently, cells were harvested by centrifugation at 5000 x *g* and 4°C for 10 minutes. Obtained supernatants were sterile filtered through 0.2 µm pore-sized filters. Diluted culture filtrates exerted no toxicity towards HEK and HL60 cells as analyzed with the Cytotoxicity Detection Kit (Roche Applied Sciences). No stimulatory activity was detected in non-inoculated media at corresponding dilutions. After stimulation supernatants were collected by centrifugation for 10 Min at 250 × *g* and stored at −20 °C before use.

Quantification of cytokine production.

Cytokines were measured using ELISA kits (R&D Systems) according to the manufacturer's instructions.

Calcium influx assay with HL60 cells

S. lugdunensis cultures were grown for 17 hours at 37°C under agitation. Subsequently, cells were harvested by centrifugation at 5000 x *g* and 4°C for 10 minutes. Obtained supernatants were sterile filtered through 0.2 µm pore-sized filters and used directly for experiments or stored at -20°C. HL60 cells were grown in RPMI medium (Biochrom) 10% FCS, 20 mM HEPES (Biochrom), penicillin (100 units/ml), streptomycin (100 µg/mL, GIBCO), and 1X Glutamax (GIBCO). HL60 cells stably transfected with human receptors FPR1 or FPR2 were grown in the aforementioned composed medium supplemented with G418 (1 mg/mL, Biochrom). To analyze calcium influx, the calcium-reactive dye Fluo-3-AM (Molecular Probes) was used to stain the cells suspended in RPMI medium containing 0.05 % human serum albumin

(Biotest) as described earlier (34). Then the cells were incubated with bacterial culture supernatants for 15 s. Calcium influx into the cytoplasm was immediately measured by flow cytometry using a FACS Calibur (BectonDickinson). Peptide fMLF was used as a positive control as it is known for its high specificity for FPR1(35) (36)(37). For confirming the activity of FPR2-transfected cells the highly FPR2-specific synthetic peptide MMK1 was chosen (38)

High-performance liquid chromatography (HPLC) analysis of SLUSH peptides

S. lugdunensis HKU09-01, N940025 and the corresponding SLUSH deletion mutant strains variants were inoculated to an OD_{600} of 0.1 from an overnight culture in TSB and cultivated at 37°C. Samples were drawn after 16 h of incubation and centrifuged for 5 min at 15000 x g at 4°C. The corresponding supernatants were filtered through sterile syringe filter with 0.2 µm pore size (Sarstedt, Germany) prior to be concentrated 4x using Speedvac vacuum concentrator. SLUSH peptides were separated from the concentrated supernatant by reversed-phase chromatography using an XBridge C8, 5 µm, 4.6 x 150 mm column (Waters Corporation, Milford, MA, USA) with a fitted pre column. A linear gradient from 0.1% TFA in water (A) to acetonitrile containing 0.08% TFA (B) for 15 min with additional 5 min of 100% B at a flow rate of 1 mL/min was used and a 50 µl sample volume was injected. Peaks were detected at 210 nm. The SLUSH peptides were eluted between 18 and 23 min.

Mass spectrometric (MS) analysis and identification of SLUSH peptides

For the MS analysis of SLUSH peptides, an Agilent 1200 HPLC- MS- system consisting of 1200 diode array detector with 10 mm standard flow cell and LC/MSD Ultra Trap System XCT 6330 (Agilent, Waldbronn) was used. A sample volume of 2.5 µL was injected onto a Reprosil Gold C4 100 × 2 mm ID with a 10 × 2 mm ID precolumn (Dr. Maisch GmbH, Ammerbuch), operated at a flow rate of 400 µL/min and a temperature of 40°C. A 20-min gra- dient from 100% Water, 0.1% TFA (A) to 100% Methanol, 0.1% TFA (B) was used to separate the analytes, followed by a 5-min elution at 100% B. The mass spectrometer was operated in alternate ESI positive and negative modes with an ultra-scan range of up to 2000 with a capillary voltage of 3.5 kV. Data were analyzed with 6300 series trap control Bruker Daltonik software version 6.1, (Agilent, Waldbronn).

Results

Recombination within the SLUSH locus of *S. lugdunensis* HKU09-01

To identify factors responsible for the release of hb from erythrocytes, we screened twenty *S. lugdunensis* stains for a hemolytic phenotype. We found that 17 out of 20 strains produced distinct zones of hemolysis after 48h on Columbia agar with 5% sheep blood (Tab. 1). The complete genome sequences were available for two strains, the hemolytic strain HKU09-01 and the non-hemolytic strain N920143 (9, 39). Consequently, HKU09-01 was chosen for further investigation. Analysis of the genome sequences showed the SLUSH locus of N920143 to be 99.3% identical to that described by Donvito *et al*. (22). In contrast the SLUSH locus of HKU09-01 appears to have undergone a genetic rearrangement and annotation of the locus is incorrect (Fig 1A). The SLUSH locus of N920143 comprises the genes *orfX* as well as *slush-A*, *slush-B* and *slush-C*. A short stretch of 29 nucleotides is shared in *slush-B* and *slush-C*. Homologous recombination has taken place in HKU09-01 at this site, deleting a 193-nucleotide fragment comprising the 3' end of *slush-B* and the 5' end of *slush-C* creating a novel hybrid gene consisting of the 5'-end of *slush-B* and the 3'-end of *slush-C*. We will refer to the hybrid gene as *slush-B2*. Thus, the SLUSH locus of HKU09-01 encodes only two SLUSH peptides and OrfX. We sequenced the SLUSH locus of a second hemolytic isolate (N940025). The locus comprised all three SLUSH genes as described by Donvito *et al*. (22).

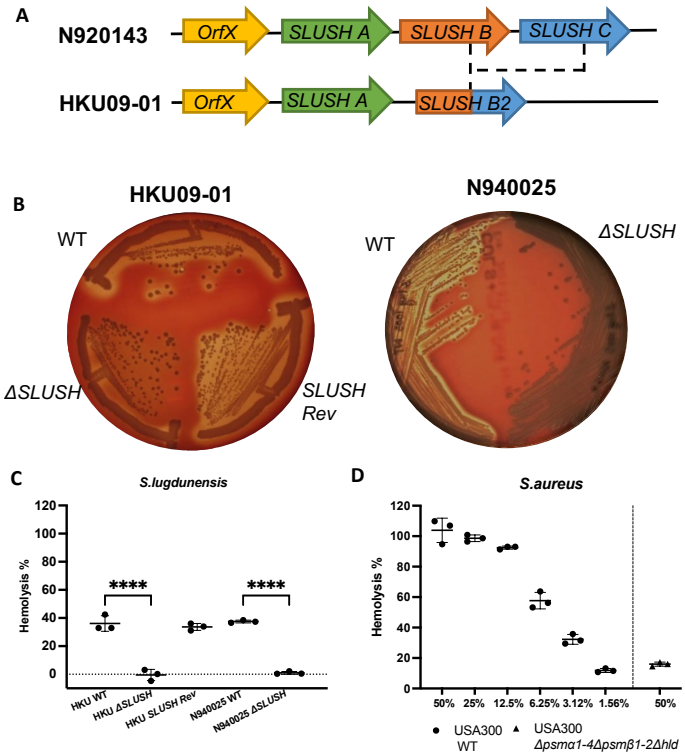

FIGURE 1: Staphylococcus *lugdunensis* hemolytic phenotype. (A) Schematic diagram of the SLUSH loci of N920143 and HKU09-01. Recombination creating the *slush B2* gene is indicated. (B) Hemolysis of HKU09-01 and N940025. Strains were streaked on Columbia agar containing 5% sheep blood. Hemolysis was assessed after 24 h incubation at 37°C. (C, D) Hemolytic titers. Dilute culture supernatants (50%) of *S. lugdunensis* (C) and two- fold dilutions of *Staphylococcus aureus* (D) were mixed with 10^8 freshly isolated human erythrocytes and incubated for 1 h at 37°C. Hemolysis was quantified by measuring absorbance at 570 nm. Relative absorbance compared to the Triton X control (100% lysis of erythrocytes) is shown. The mean and *SD* of three independent experiments are shown, and statistical analysis was performed using one- way ANOVA with Tukey 's multiple comparison test. ****$p \leq .0001$.

Additionally, the genome sequences showed the presence of intact genes encoding sphingomyelinase β-toxin (Hlb) as well as of a putative hemolysin III (40). In contrast genes encoding a putative streptolysin S-like toxin are inactivated by frameshift mutations in many strains including N920143 and HKU09-01 (9).

SLUSH is essential for the hemolytic phenotype of *S. lugdunensis*

In order to investigate the role of SLUSH peptides in the hemolytic phenotype of *S. lugdunensis,* we isolated clean deletion mutations in HKU09-01 (comprising *orfX*, *slush-A* and *slush-B2*) as well as in N940025 (comprising *orfX*, *slush-A slush-B* and *slush-C*).

Deletion of the SLUSH locus abrogated hemolysis of both strains and recombinational restoration of the deletion restored the hemolytic phenotype in HKU09-01 (Fig. 1B). This indicated that the SLUSH peptides are hemolytic factors. To further confirm this, we measured the hemolytic capacity of culture supernatants quantitatively using human erythrocytes. Dilute culture supernatants (50%) of HKU09-01and N940025 lysed ~40% of human erythrocytes within 1 h, a characteristic that was dependent on expression of SLUSH in both strains (Fig. 1C).

We sought to compare the hemolytic activity for human erythrocytes of *S. lugdunensis* to that of *S. aureus*. Hemolysis of *S. aureus* USA300 LAC under the same conditions depends on expression of the PSM peptides (PSMα1-4, δ-toxin (*hld*) and PSMβ1-2) which are structurally similar to the SLUSH peptides (25). We found 6.25% of *S. aureus* LAC culture supernatants to be sufficient for ~ 40% hemolysis, showing that the hemolytic titer of *S. aureus* exceeds that of *S. lugdunensis* by approximately one order of magnitude. Deletion of all PSM peptides reduced hemolysis dramatically (Fig.1D). However, in contrast to *S. lugdunensis Δslush*, the culture supernatants of *S. aureus* Δ*psm*α1-4Δ*psmβ*1-2Δ*hld* retained a low level of hemolysis, suggesting additional factors to contribute to lysis.

SLUSH peptides but not OrfX are detectable in culture supernatants of *S. lugdunensis*

We performed HPLC and Mass Spectrometric analyses of *S. lugdunensis* culture supernatants to assess if SLUSH peptides are produced. Using TFA/acetonitrile gradients we found in both WT strains several distinct peaks with elution times

between 16 and 23 minutes (Fig 2D and F). In the supernatant of HKU09-01 we detected four peaks, whereas six distinct peaks were detected in N940025. All peaks were absent in supernatants of the corresponding ΔSLUSH mutants, strongly suggesting that the peaks represent products of the SLUSH-loci. ESI-MS analysis using Formic acid/acetronitrile gradients allowed identification of masses corresponding to formylated SLUSH-A, SLUSH-B and SLUSH-C in N940025 as well as masses corresponding to formylated SLUSH-A and SLUSH-B2 in HKU09-01 (Sup. Figure 1). Additionally, we identified masses corresponding to non -formylated and C-terminally truncated versions of the SLUSH -peptides in (Tab. 3, Fig. S1). However, we did not identify masses corresponding to formylated, non-fomylated or truncated forms of OrfX in either strain.

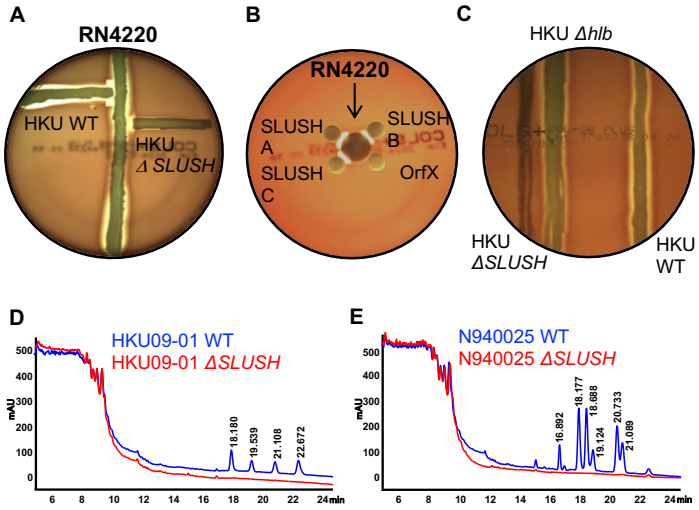

FIGURE 2: Biosynthesis of SLUSH peptides and synergism with Hlb against sheep blood erythrocytes. (A, B) Detection of SLUSH peptides in *Staphylococcus lugdunensis* culture supernatants. *S. lugdunensis* strains were grown overnight in TSB medium at 37°C. Supernatants were concentrated and analyzed by reversed-phase chromatography using a C8 column and a linear gradient from 0.1% TFA in water to acetonitrile. Peaks were detected at 210 nm. (A) HKU09- 01 and HKU09- 01 Δ*SLUSH*. (B) N940025 and N940025 Δ*SLUSH*. (C) CAMP test. *S. aureus* RN4220 and *S. lugdunensis* HKU09-01 strains were cross- streaked. (D) Synergy of individual SLUSH peptides and Hlb. SLUSH recombinant peptides (15 µL of 1 mg/mL) were spotted on filter disks and placed close to RN4220 which was spotted on the plate. (E) Relevance of *S. lugdunensis* Hlb. *S. lugdunensis* HKU09-01 strains were streaked out. Columbia agar containing 5% sheep blood was used for all experiments. Hemolysis was assessed after 24 h of incubation at 37°C

This analysis shows that *S. lugdunensis* strains produce formylated full length SLUSH-peptides along with various non-formylated and truncated variants. However, OrfX does not seem to be biosynthesized under the experimental conditions used herein.

TABLE 3. SLUSH peptides detected in culture supernatants of *S. lugdunensis.*

SLUSH peptides in	**Mass m/z**	
	Calculated	**Observed**
***S. lugdunensis* HKU09-01**		
OrfX	2747	–
SLUSH A	4446	4446
SLUSH B2	4519.26	4519.2
SLUSH A (nonformylated)	4418.07	4418
SLUSH B2 (nonformylated)	4491.25	4491
***S. lugdunensis* N940025**		
OrfX	2747	–
SLUSH A	4446	4445.7
SLUSH B	4351	4350.6
SLUSH C	4569	4569
SLUSH C (nonformylated)	4539.25	4539
SLUSH C (C-terminal truncation by one amino acid)	4436.06	4430

SLUSH peptide-mediated lysis of sheep erythrocytes is synergistic with Hlb

The hemolytic activity of several PSM peptides is reported to be synergistic with the sphingomyelinase (Hlb – β-toxin) (26). SLUSH peptides have been shown to be responsible for the "synergistic hemolytic phenotype" of *S. lugdunensis* with Hlb-

producing staphylococci (22). In agreement with this we found *S. lugdunensis* HKU09-01 to produce an increased zone of hemolysis when inoculated in close proximity to the Hlb-producing *S. aureus* strain RN4220 on Columbia-sheep-blood agar (CAMP-test) (Fig. 2A). This phenotype was dependent on SLUSH-expression.

We speculated that the individual peptides might possess different synergistic properties with Hlb. To investigate this, we synthesized each peptide with an N-terminal formyl-methionine, applied the peptides to filter discs and placed them in close proximity to RN4220 inoculated on sheep blood agar. Clear zones of hemolysis, indicating synergy, were observed for SLUSH-A, SLUSH-B and SLUSH-C but where absent for the OrfX peptide (Fig. 2B). *S. lugdunensis* does encode an intact *hlb* gene. To investigate if the hemolytic activity for sheep erythrocytes of *S. lugdunensis* depends on combined action of SLUSH and β-toxin produced by *S. lugdunensis* simultaneously, we created an isogenic *Δhlb* mutant in HKU09-01. The β-toxin deficient strain retained hemolytic activity (Fig 2C). Additionally, the Hlb deficient strain did not show increased hemolysis in close proximity to the ΔSLUSH mutant which retains the *hlb* gene. (Fig. 2C). This indicates that Hlb either lacks biological activity or is not expressed at a sufficiently high level to function in this *in vitro* test and that SLUSH alone can mediate hemolysis of sheep blood erythrocytes.

SLUSH peptides show individual and non-synergistic hemolytic properties against human erythrocytes.

The membrane composition of human and sheep erythrocytes is different. Therefore, we tested the synthetic SLUSH peptides for their hemolytic potential against human erythrocytes (Fig. 3). The three SLUSH peptides had similar, dose-dependent effects on erythrocyte integrity with 0.25-0,5 μM being sufficient to lyse ~50% of cells (Fig 3A C). In contrast, ca 10-fold higher concentrations (2-5 μM) of OrfX peptide were needed to cause ~50% lysis (Fig. 3D),

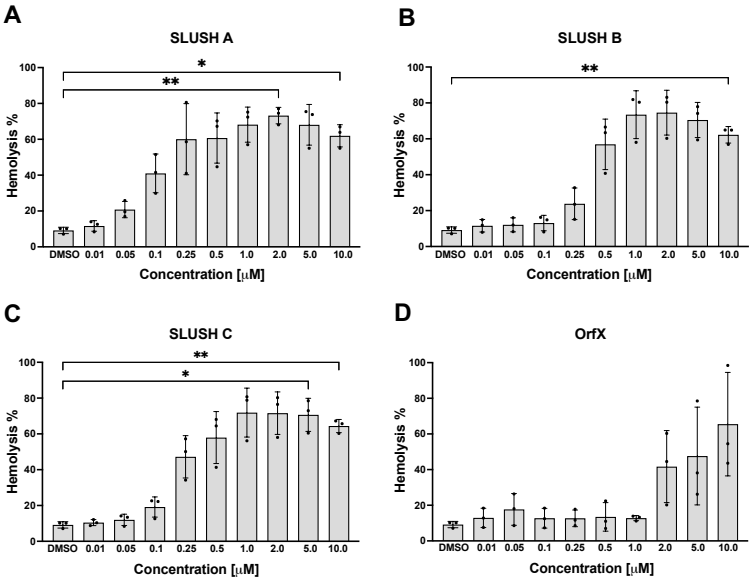

FIGURE 3: **Hemolytic capacity of individual SLUSH peptides.** (A–D) Individual hemolytic capacity of SLUSH peptides. Freshly purified human erythrocytes were incubated with increasing concentrations of synthetic SLUSH peptides for 1 h at 37°C. Absorbance at 570 nm was determined and compared to the Triton X (100% lysis of erythrocytes) control. The mean and *SD* of three independent experiments are shown. Statistical analysis was performed using one-way ANOVA with Brown–Forsythe and Welch ANOVA. * $p \leq .05$, ** $p \leq .001$

Next, we investigated if the SLUSH peptides acted synergistically with each other. For this, we repeated the hemolysis assay using human erythrocytes with pairwise combinations of two peptides in different ratios while keeping the total concentration constant. Synergism would manifest by an increase in the percentage of hemolysis above the level of the individual peptides. The results did not show synergism between the peptides (Fig. 4). Of note, the shorter OrfX peptide did not improve the hemolytic capacity of any of the three SLUSH peptides. We also assessed potential synergism between the peptides and Hlb using human erythrocytes, synthetic SLUSH peptides and recombinant Hlb (Source). Interestingly, we did not find any synergistic effects (Fig. S1) suggesting that only individual activity of the peptides is responsible for lysis

of human erythrocytes. Similarly, it has been reported that synergism between Hlb and individual staphylococcal PSM is more frequently observed against sheep erythrocytes than human erythrocytes (26).

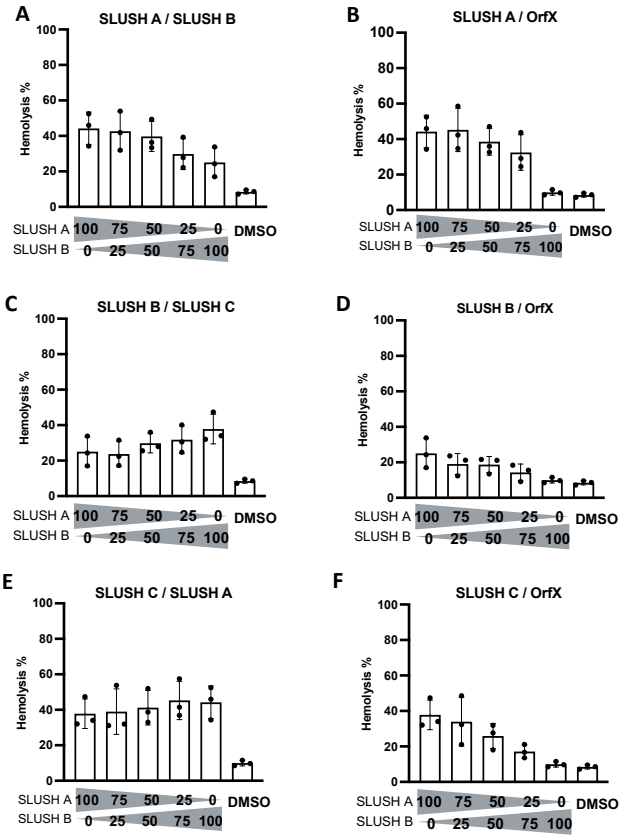

FIGURE 4: Synergism between SLUSH- peptides. (A–F) Synergistic hemolytic capacity of SLUSH peptides. Freshly purified human erythrocytes were incubated for 1 h with mixtures of synthetic SLUSH peptides with a total concentration of 0.25 µM. Absorbance at 570 nm was determined and compared to the Triton X control. The mean and *SD* of three independent experiments are shown.

SLUSH allows usage of erythrocytes as a sole source of nutrient iron.

S. lugdunensis can acquire heme from human hemoglobin (hb) (9, 10, 12, 41). However, hb is contained within erythrocytes and is not easily available. We speculated that SLUSH might be needed to release hb from erythrocytes. Wild type *S. lugdunensis* HKU09-01 and the SLUSH mutant proliferated to the same extent when $FeSO_4$ was incorporated in iron restricted minimal medium, (Fig 5A). However, the SLUSH mutants failed to grow in iron limited medium in the presence of human erythrocytes whereas the WT could grow. Thus, the SLUSH-deficient strain mimicked the phenotype of a *S. lugdunensis* Δ*isd/ΔlhaSTA* mutant which is unable to acquire heme from hemoglobin (Fig 5 B, C) (10). Supplementation with synthetic SLUSH peptides restored the ability of the mutant strain to proliferate in the presence of erythrocytes (Fig. 5D). These data suggest that SLUSH peptides are necessary and sufficient to release nutritional hb from human erythrocytes.

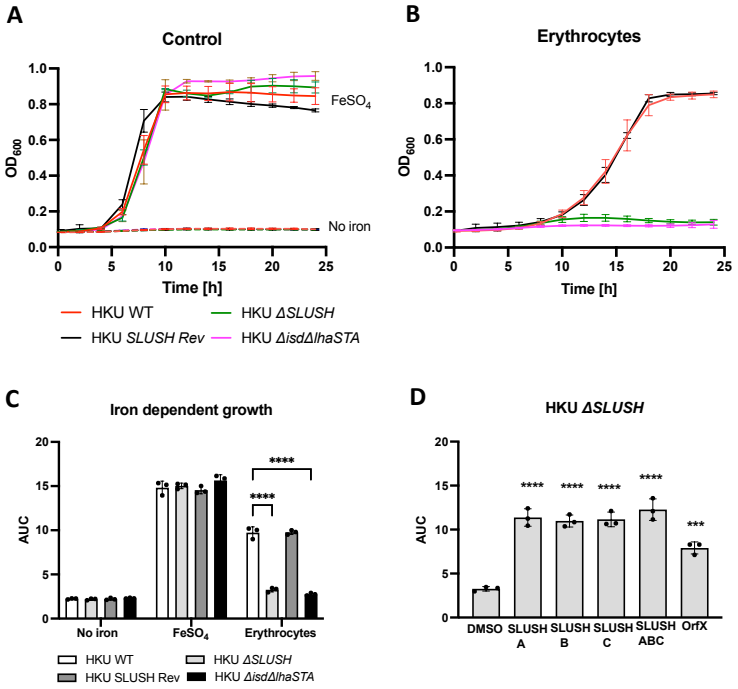

FIGURE 5: Staphylococcus *lugdunensis* growth using human erythrocytes is SLUSH-dependent. (A–D) Growth of S. *lugdunensis* using erythrocytes. 500 µL cultures were inoculated to an OD_{600} = 0.005 in iron- deficient medium (RPMI, 1% casamino acids, 10 µM EDDHA) in 48 well plates and OD_{600} was monitored every 15 min at 37°C with orbital shaking using an Epoch2 plate reader. For reasons of clarity, only values taken every 2 h are displayed. (A) Without any supplements or with 20 µM $FeSO_4$; (B) Supplementation with erythrocytes (10^6 cells/ mL); (C) Total area under the curve from graph A and B. (D) Supplementation with erythrocytes (10^6 cells/mL) and synthetic SLUSH peptides (0.25 µM). The total area under the curve is shown. The mean and *SD* from three independent experiments are shown. Statistical analysis was performed using two-way ANOVA with Tukey 's multiple comparison test. *** $p \leq .0005$, **** $p \leq .0001$.

Interestingly, we found that *S. aureus* USA300 Lac failed to grow under the same conditions in the presence of human erythrocytes (Fig.6A, B). Growth was promoted by 0.5% Triton X (Fig. 6A, B) or by addition of synthetic SLUSH peptides (Fig. 6C) into the medium suggesting a failure of *S. aureus* to produce sufficient PSMs to lyse erythrocytes under these conditions.

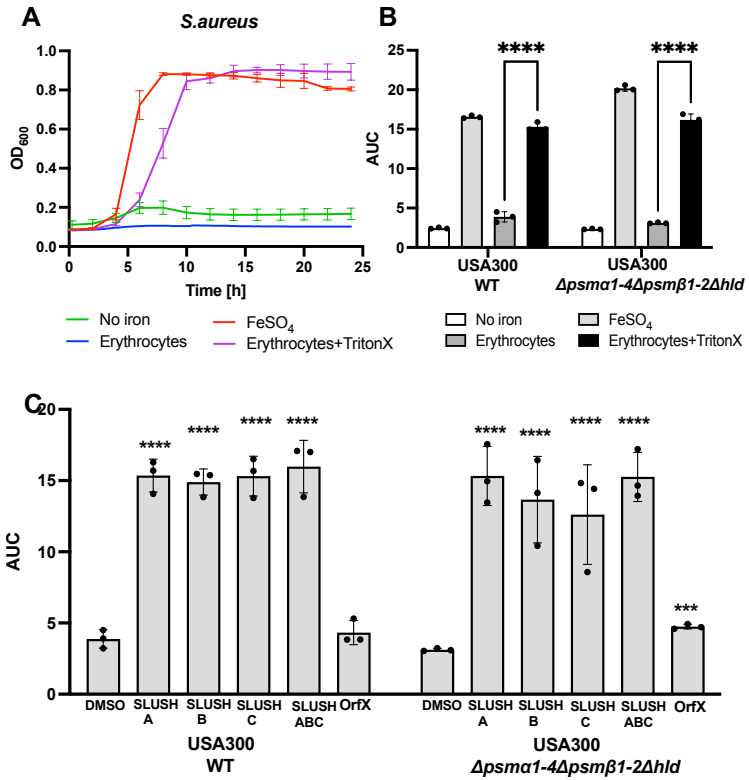

Figure 6: *Staphylococcus aureus* growth using human erythrocytes depends on external hemolytic factors. (A–C) Growth of *S. aureus* USA300 using erythrocytes. 500 µL cultures were inoculated to an OD_{600} = 0.005 in iron-deficient medium (RPMI, 1% casamino acids, 10 µM EDDHA) in 48 well plates and OD_{600} was monitored every 15 min at 37°C with orbital shaking using an Epoch2 plate reader. For reasons of clarity, only values taken every 2 h are displayed. (A) Without any supplements, with 20 µM $FeSO_4$, with erythrocytes (10^6 cells/mL) or with erythrocytes 0.5% Triton X. (B) Total area under the curve from graphs A and B. (C) Supplementation with erythrocytes (10^6 cells/mL) and synthetic SLUSH peptides (0.25 µM). The total area under the curve is shown. The mean and *SD* from three independent experiments are shown. Statistical analysis was performed using two-way ANOVA with Tukey's multiple comparison test *** $p \leq .0005$, **** $p \leq .0001$.

SLUSH-dependent growth is controlled by Agr.

To investigate the regulation of SLUSH expression, we created isogenic mutants lacking the two major regulatory loci *agr* and *saeRS* known to control multiple virulence factors in staphylococci (42, 43). Deletion of *agrA* but not of *saeRS* abolished hemolytic activity against human erythrocytes (Fig. 7A) and only the *agrA*-deficient strain failed to grow in the presence of host erythrocytes as a sole source of nutritional iron (Fig.7B).

Our experiments demonstrate that the usage of erythrocyte as a source of iron depends on the expression of SLUSH peptides which is governed by Agr activity. These experiments are congruent with recent evidence by Chin *et al.* showing Agr-dependent regulation of SLUSH (44).

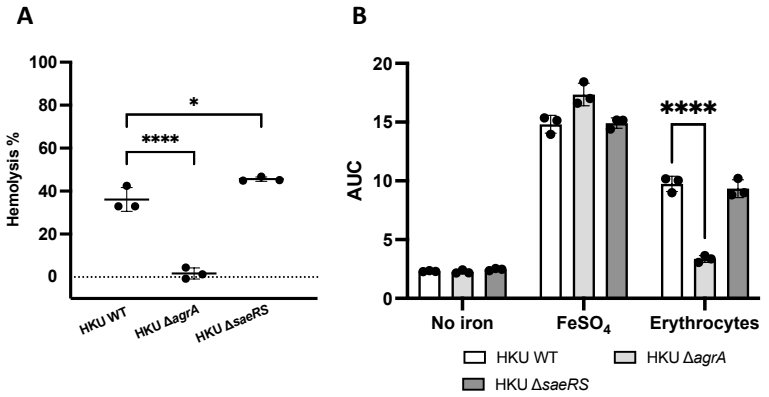

Figure 7: *SLUSH* expression depends on Agr activity. (A) Hemolytic activity of *Staphylococcus lugdunensis* HKU09-01 WT, Δ*agrA*, and Δ*saeRS*. Dilute (50%) culture supernatants were mixed with 10^8 freshly isolated human erythrocytes and incubated for 1 h at 37°C. Hemolysis was quantified by measuring absorbance at 570 nm. Relative absorbance compared to the Triton X (100% lysis of erythrocytes) is shown. The mean and *SD* of three independent experiments are shown, Statistical analysis was performed using one-way ANOVA with Tukey's multiple comparison test. ****$p \leq .0001$. (B) Iron-dependent growth of *S. lugdunensis* HKU09-01 WT, Δ*agrA*, and Δ*saeRS*. 500 µL cultures were inoculated to an $OD_{600} = 0.005$ in iron-deficient medium (RPMI, 1% casamino acids, 10 µM EDDHA) in 48 well plates and OD_{600} was monitored every 15 min at 37°C with orbital shaking using an Epoch2 plate reader. The total area under the curve from growth curves with or without iron (20 µM $FeSO_4$) and with erythrocytes (10^6 cells/mL) are shown. The mean and *SD* from three different experiments are shown. Statistical analysis was performed using two-way ANOVA with Tukey 's multiple comparison test. *$p \leq .05$, ****$p \leq .0001$.

SLUSH peptides activate human immune cells .

Bacterial proteins are formylated at the N-terminal methionine and can be recognized by the host G-protein coupled formyl peptide receptor (FPR) family (36). The innate immune system recognizes PSMs via the G-protein coupled receptor FPR2 (34), a member of the formyl peptide receptor family which is expressed on monocytes, macrophages, neutrophils and immature dendritic cells (45). This initiates pro-inflammatory neutrophil responses and chemotactic migration (23, 46) and is an important mechanism for the recognition of invading pathogens. Due to the conserved expression of PSMs among staphylococcal pathogens and the strong immune response induced by them, PSMs may be used by the immune system to distinguish between more aggressive staphylococci and less virulent species.

It has previously been reported that both synthetic SLUSH peptides and culture supernatant from a SLUSH secreting strain can activate FPR2 and induce chemotaxis of neutrophils (29). It is not known if the SLUSH peptides are the only FPR2 ligands secreted by *S. lugdunensis*. To investigate this, we incubated culture supernatants of the HKU09-01 parental strain, the isogenic ΔSLUSH mutant strain and the SLUSH revertant strain ΔSLUSH-R with FPR2 transfected HL60 cells and measured activation-associated calcium influx. Supernatants of the parent and the SLUSH-R strain induced strong calcium influx in the transfected cells whereas supernatants of the ΔSLUSH mutant showed a significant reduction (Fig. 8A). The results indicate that the SLUSH peptides are the major FPR2 ligand secreted by *S. lugdunensis*. However, the weak activation induced by the ΔSLUSH supernatant indicates the existence of at least one unidentified FPR2 ligand.

To further investigate the pro-inflammatory properties displayed by the different strains, we measured IL-8 secretion by human neutrophils upon incubation with the culture supernatants from the different strains. Stimulation with supernatants from the parent and the SLUSH-R strain induced strong IL-8 production whereas there was a significant reduction with supernatants from the ΔSLUSH mutant (Fig.8B).

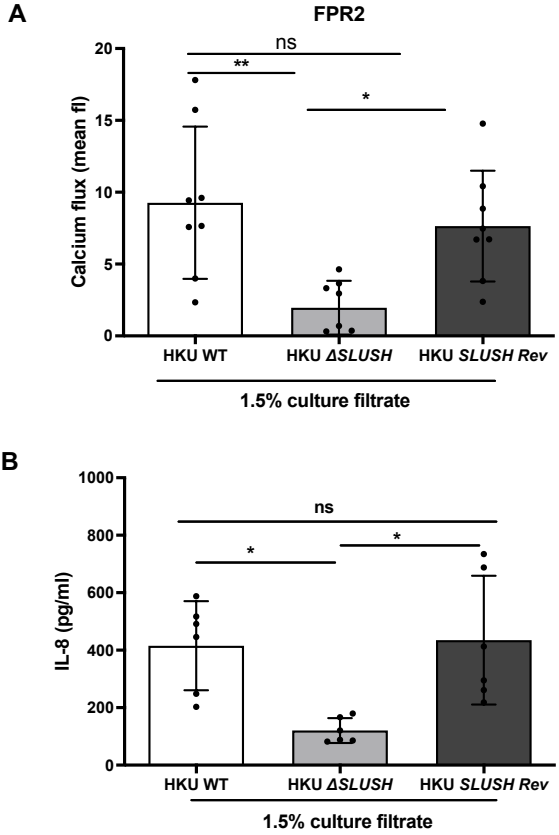

FIGURE 8 Activation of FPR2- expressing cells. (A) Calcium influx. FPR2- transfected HL60 cells were treated with 1.5% bacterial culture supernatants of *Staphylococcus lugdunensis* HKU09- 01 WT and isogenic mutants. Calcium flux was measured. (B) IL- 8 induction in human neutrophils. Freshly isolated human neutrophils were stimulated with *S. lugdunensis* culture filtrates (1.5%) for 5 h and IL- 8 in the culture medium was measured by ELISA. Data represent three to five independent experiments and three different bacterial culture supernatants. P-values were determined by one- way ANOVA with Bonferroni's post- test. *$p < .05$, **$p < .005$; ns = nonsignificant.

Discussion:

Gaining access to nutritional iron is an essential prerequisite for bacterial proliferation. In the context of nutritional immunity, pathogens face strong iron-limitation during infection and the expression of proteins allowing the extraction of heme form host-derived hemoproteins represent a hallmark of pathogens (47). *S. lugdunensis* is well equipped to acquire host-derived heme. Besides the Isd-system (48), *S. lugdunensis* expresses an energy coupling factor type transporter allowing the acquisition of heme from many different human hemoproteins (41). This suggests a special adaptation of *S. lugdunensis* towards the availability of host-derived heme. The importance of iron acquisition systems during *S. lugdunensis* infection of mice has been previously shown (49). However, hemoglobin and other host-hemoproteins are located intracellularly, and the concerted action of hemolytic toxins and heme acquisition systems is essential for this. The arsenal of putative hemolysins of *S. lugdunensis* is small compared to that of *S. aureus.* The only putative hemolysins are SLUSH, Hlb, a StreptolysinS-like toxin and haemolysin III (the last three have been revealed by genome sequencing and their function is yet to be ascertained). Toxins targeting erythrocytes in a receptor dependent fashion (50) are not encoded by *S. lugdunensis*.

We have shown here that PSM-like SLUSH peptides produced by *S. lugdunensis* are key determinants for the hemolytic activity of *S. lugdunensis* against sheep as well as human erythrocytes. We have found that recombination within the SLUSH-locus of HKU09-01 created a locus encoding two (SLUSH-A and SLUSH-B2) instead of the three peptides (SLUSH-A, SLUSH-B, SLUSH-C), peptides that were originally described previously (22). Similar, shortened loci were also identified for individual *S. lugdunensis* strains from other collections (51), indicating that the locus is prone to recombination. This is not surprising as genetic loci with repetitive nucleotide sequences are known to give rise to gene amplification and deletion events (52, 53). Interestingly, gene copy number variation of the *isd*-locus is also observed in HKU09-01 (48), which might indicate that heme acquisition systems are under selective pressure within this strain.

The PSMs of *S. aureus* are well known to destroy eukaryotic cell membranes due to their surfactant characteristics (54). The short α-type PSMs have more potent hemolytic activity than β-type PSMs (26). In contrast we found here that the SLUSH-A, SLUSH-B and SLUSH-C peptides of *S. lugdunensis* which are β-type PSMs are

more potently hemolytic than the α-type PSM OrfX. All our experiments found little effects of synthetic OrfX, rising questions regarding its biological relevance and the fact that we failed to detect masses corresponding to OrfX in culture supernatants suggests that the peptide is not produced in the same fashion as the SLUSH peptides. However, the regulatory mechanisms underlying this phenomenon are unclear. OrfX, SLUSH-A, SLUH-B and SLUSH-C appear to be located on a single polycistronic transcript and appropriate ribosomal binding sites are found upstream of each gene. Further experiments are needed to assess if posttranscriptional regulatory mechanisms prevent the biosynthesis of OrfX. Alternatively, the peptide might not be released into the supernatant or might be rapidly degraded.

We found no synergism between the different peptides indicating that each peptide functions independently of the others. Further we found potent synergistic activity of SLUSH-A, SLUSH-B and SLUSH-C with *S. aureus* Hlb against sheep blood erythrocytes. However, synergism was not observed against human erythrocytes and the Hlb-deficient mutant of *S. lugdunensis* HKU09-01 retained its hemolytic activity against sheep and human erythrocytes, suggesting that SLUSH-Hlb synergism is of little importance during infection of humans. Similar phenomena are reported for PSM molecules of *S. aureus* and *S. epidermidis* where only individual PSMs (especially δ-toxin) were found to be synergistic with Hlb against human erythrocytes (26). The role of endogenously produced Hlb for *S. lugdunensis* remains unclear. We did not measure expression profiles of *hlb* in HKU09-01. However, expression during exponential growth was verified for Hlb as well as for Hemolysin III for a range of different *S. lugdunensis* strains (51). To what extend these toxins contribute to erythrocyte lysis under varying experimental conditions remains to be investigated.

We showed that SLUSH expression is both necessary and sufficient to allow erythrocyte-dependent growth of *S. lugdunensis* under iron restricted conditions *in vitro*. This indicates that *S. lugdunensis* lyses erythrocytes efficiently to release nutritional heme from host cells. In contrast we found *S. aureus* USA300 failed to grow under the same conditions. Previous reports show that experimental demonstration of erythrocyte-dependent growth of *S. aureus* is challenging (50). This is surprising as we found that hemolytic titers produced by *S. aureus* in rich broth *in vitro* exceed those of *S. lugdunensis* by approximately one order of magnitude. However, it is evident that *S. aureus* fails to lyse erythrocytes under the experimental conditions employed here

since addition of Triton X or SLUSH peptides promoted *S. aureus* growth in the presence of erythrocytes. Most likely, differences in in the regulation of expression account for the differences between *S. aureus* and *S. lugdunensis*. SLUSH as well as PSMs of *S. aureus* are both regulated by Agr-activity (44, 54). In line with this, an *agr* mutation abolished the hemolytic phenotype and prevented growth of *S. lugdunensis* HKU09-01 in the presence of erythrocytes. Interestingly, we found no evidence of *agr* inactivation in the non-hemolytic *S. lugdunensis* strain N920143. The *agrBDCA* genes are intact and both the intergenic region between *agrB* and RNAIII which harbors P2 and P3 promoters as well as the RNAIII gene are 100% identical between N920143 and HKU09-01. Additionally, the putative promotor regions of the SLUSH-loci of N920143 and HKU09-01 are identical. This observation raises the question whether additional genetic circuits influence SLUSH expression in *S. lugdunensis*. It seems possible that, despite control by Agr, expression of PSMs occurs earlier in *S. lugdunensis* than in *S. aureus* which might allow sufficient access to hemoglobin in the very early stages of growth in our experiments. However, this hypothesis needs further investigation.

Apart of hemolysis, *S. aureus* PSMs are known to be toxic for many different eukaryotic cells and to stimulate the human immune system as they are recognized by formyl peptide receptor 2 (FRP2) (29, 34, 54). In line with this, we showed that SLUSH expression stimulated FPR2-expressing human cells and others showed th at Agr activity is involved in *S. lugdunensis* survival in whole blood and within human macrophages (44), all arguing for an important relevance of SLUSH as virulence factors in *Staphylococcus lugdunensis*. However, experimental animal models performed by others have failed to detect a decreased virulence of *agr*-deficient *S. lugdunensis* strains (44) which is surprising as PSMs of *S. aureus* are known to be key virulence factors during infection (54). The lack of attenuation of Agr-deficient *S. lugdunensis* in animal models of infection might be diverse. Firstly, it has been shown previously that the Isd-system of *S. lugdunensis* is specific for human hb, suggesting that the system is of low efficiency during infection of mice (12). Accordingly, the SLUSH-dependent release of hb might not allow *S. lugdunensis* to overcome iron-restriction during infection of mice. Secondly, expression of SLUSH *in vitro* is unclear and *S. lugdunensis* does generally show little virulence in mouse models of infection. This might suggest a general human-specificity of *S. lugdunensis*,

reducing the ability of the pathogen to proliferate within mice. Thirdly, it has been shown that PSM peptides are targets of serine protease produced by the host. *S. aureus* produces dedicated inhibitors (Eap, EapH1, EapH2) of these proteases in order to protect PSM function (55). *S. lugdunensis* does not encode similar inhibitors which might suggest more efficient inactivation of the SLUSH peptides during infection. Even in the absence of host-proteases we found various deformylated and truncated variants of the SLUSH-peptides in culture supernatants of *S. lugdunensis*, indicating that the peptides are susceptible to degradation.

Altogether our experiments show an important role of the SLUSH peptides to release hemoglobin from human erythrocytes and to facilitate the subsequent acquisition of heme-iron by the pathogen. However, improved infection models using humanized mouse lineages will be needed to validate the *in vivo* relevance of this observation.

Authors Contributions

Sekar S, Schwarzbach S, Bloes DA and Smeds E performed experiments. Nega M performed HPLC/MS analysis. Kretschmer D supervised immune stimulation experiments. Foster TJ acquired funding and supervised experiments. Heilbronner S designed the study, acquired funding, supervised experiments and wrote the manuscript. All authors edited the manuscript.

Acknowledgements

The authors thank Libera Lo Presti for critically reading and editing this manuscript. We thank Martine Pestel-Caron for providing *S. lugdunensis* strains. We acknowledge funding by the German Center of Infection Research (DZIF) to S.H (TTU 08.708). Additionally,, we acknowledge funding by the Deutsche Forschungsgemeinschaft DFG, (German Research Foundation) for personal funding (HE8381_3-1) and funding in the frame of Germany´s Excellence Strategy – EXC 2124 – 390838134 to S.H. We acknowledge the support of the Irish Research Council for Science, Engineering and Technology for an Embark scholarship (RS2000192) to S.H. and the Science Foundation Ireland for a Programme Investigator grant (08/IN.1/B1854) to TJF. We acknowledge Andreas Kulik for providing access to an Agilent 1200 HPLC-MS-system.

Data Availability Statement

The data that support the findings of this study are available in the methods and/or supplementary material of this article.

Conflict of interest:

The authors have stated explicitly that there are no conflicts of interest in connection with this article.

References:

1. J. Freney, Y. Brun, M. Bes, H. Meugnier, F. Grimont, in *International Journal of Systematic Bacteriology*. (1988), pp. 168-172.
2. L. Bieber, G. Kahlmeter, Staphylococcus lugdunensis in several niches of the normal skin flora. *Clin Microbiol Infect* **16**, 385-388 (2010).
3. K. L. Frank, J. L. Del Pozo, R. Patel, From Clinical Microbiology to Infection Pathogenesis: How Daring To Be Different Works for Staphylococcus lugdunensis. *Clinical Microbiology Reviews* **21**, 111-133 (2008).
4. P. Y. Liu *et al.*, Staphylococcus lugdunensis infective endocarditis: a literature review and analysis of risk factors. *J Microbiol Immunol Infect* **43**, 478-484 (2010).
5. J. A. Geoghegan *et al.*, Molecular Characterization of the Interaction of Staphylococcal Microbial Surface Components Recognizing Adhesive Matrix Molecules (MSCRAMM) ClfA and Fbl with Fibrinogen. *Journal of Biological Chemistry* **285**, 6208-6216 (2010).
6. M. Nilsson, A von Willebrand factor-binding protein from Staphylococcus lugdunensis. *FEMS Microbiology Letters* **234**, 155-161 (2004).
7. L. Liesenborghs *et al.*, Shear-Resistant Binding to von Willebrand Factor Allows Staphylococcus lugdunensis to Adhere to the Cardiac Valves and Initiate Endocarditis. *J Infect Dis* **213**, 1148-1156 (2016).
8. S. Heilbronner, F. Hanses, I. R. Monk, P. Speziale, T. J. Foster, Sortase A promotes virulence in experimental Staphylococcus lugdunensis endocarditis. *Microbiology* **159**, 2141-2152 (2013).
9. S. Heilbronner *et al.*, Genome sequence of Staphylococcus lugdunensis N920143 allows identification of putative colonization and virulence factors. *FEMS Microbiol Lett* **322**, 60-67 (2011).
10. S. Heilbronner *et al.*, Competing for Iron: Duplication and Amplification of the isd Locus in Staphylococcus lugdunensis HKU09-01 Provides a Competitive Advantage to Overcome Nutritional Limitation. *PLoS Genet* **12**, e1006246 (2016).
11. K. P. Haley, E. M. Janson, S. Heilbronner, T. J. Foster, E. P. Skaar, Staphylococcus lugdunensis IsdG liberates iron from host heme. *J Bacteriol* **193**, 4749-4757 (2011).
12. M. Zapotoczna, S. Heilbronner, P. Speziale, T. J. Foster, Iron-regulated surface determinant (Isd) proteins of Staphylococcus lugdunensis. *J Bacteriol* **194**, 6453-6467 (2012).
13. A. J. Farrand *et al.*, An Iron-Regulated Autolysin Remodels the Cell Wall To Facilitate Heme Acquisition in Staphylococcus lugdunensis. *Infect Immun* **83**, 3578-3589 (2015).
14. M. I. Hood, E. P. Skaar, Nutritional immunity: transition metals at the pathogen-host interface. *Nat Rev Microbiol* **10**, 525-537 (2012).
15. J. E. Cassat, E. P. Skaar, Iron in infection and immunity. *Cell Host Microbe* **13**, 509-519 (2013).
16. U. E. Schaible, S. H. Kaufmann, Iron and microbial infection. *Nat Rev Microbiol* **2**, 946-953 (2004).
17. E. D. Weinberg, Microbial pathogens with impaired ability to acquire host iron. *Biometals* **13**, 85-89 (2000).
18. D. Haschka, A. Hoffmann, G. Weiss, Iron in immune cell function and host defense. *Semin Cell Dev Biol* **115**, 27-36 (2021).

19. S. K. Mazmanian, H. Ton-That, K. Su, O. Schneewind, An iron-regulated sortase anchors a class of surface protein during Staphylococcus aureus pathogenesis. *Proc Natl Acad Sci U S A* **99**, 2293-2298 (2002).

20. S. K. Mazmanian *et al.*, Passage of heme-iron across the envelope of Staphylococcus aureus. *Science* **299**, 906-909 (2003).

21. D. L. Drabkin, Metabolism of the hemin chromoproteins. *Physiol Rev* **31**, 345-431 (1951).

22. B. Donvito *et al.*, Synergistic hemolytic activity of Staphylococcus lugdunensis is mediated by three peptides encoded by a non-agr genetic locus. *Infect Immun* **65**, 95-100 (1997).

23. M. Rautenberg, H. S. Joo, M. Otto, A. Peschel, Neutrophil responses to staphylococcal pathogens and commensals via the formyl peptide receptor 2 relates to phenol-soluble modulin release and virulence. *FASEB J* **25**, 1254-1263 (2011).

24. R. Wang *et al.*, Identification of novel cytolytic peptides as key virulence determinants for community-associated MRSA. *Nat Med* **13**, 1510-1514 (2007).

25. C. Mehlin, C. M. Headley, S. J. Klebanoff, An inflammatory polypeptide complex from Staphylococcus epidermidis: isolation and characterization. *J Exp Med* **189**, 907-918 (1999).

26. G. Y. Cheung, A. C. Duong, M. Otto, Direct and synergistic hemolysis caused by Staphylococcus phenol-soluble modulins: implications for diagnosis and pathogenesis. *Microbes Infect* **14**, 380-386 (2012).

27. S. Periasamy *et al.*, How Staphylococcus aureus biofilms develop their characteristic structure. *Proc Natl Acad Sci U S A* **109**, 1281-1286 (2012).

28. R. Wang *et al.*, Staphylococcus epidermidis surfactant peptides promote biofilm maturation and dissemination of biofilm-associated infection in mice. *J Clin Invest* **121**, 238-248 (2011).

29. M. Rautenberg, H. S. Joo, M. Otto, A. Peschel, Neutrophil responses to staphylococcal pathogens and commensals via the formyl peptide receptor 2 relates to phenol-soluble modulin release and virulence. *FASEB J*, (2010).

30. I. R. Monk, I. M. Shah, M. Xu, M. W. Tan, T. J. Foster, Transforming the untransformable: application of direct transformation to manipulate genetically Staphylococcus aureus and Staphylococcus epidermidis. *Mbio* **3**, (2012).

31. I. R. Monk, P. G. Casey, C. Hill, C. G. Gahan, Directed evolution and targeted mutagenesis to murinize Listeria monocytogenes internalin A for enhanced infectivity in the murine oral infection model. *BMC Microbiol* **10**, 318 (2010).

32. M. S. Hanson *et al.*, Phosphodiesterase 3 is present in rabbit and human erythrocytes and its inhibition potentiates iloprost-induced increases in cAMP. *Am J Physiol Heart Circ Physiol* **295**, H786-793 (2008).

33. M. C. Durr *et al.*, Neutrophil chemotaxis by pathogen-associated molecular patterns - formylated peptides are crucial but not the sole neutrophil attractants produced by Staphylococcus aureus. *Cellular Microbiology* **8**, 207-217 (2006).

34. D. Kretschmer *et al.*, Human formyl peptide receptor 2 senses highly pathogenic Staphylococcus aureus. *Cell Host Microbe* **7**, 463-473 (2010).

35. Y. Le, P. M. Murphy, J. M. Wang, Formyl-peptide receptors revisited. *Trends Immunol* **23**, 541-548 (2002).

36. W. A. Marasco *et al.*, Purification and identification of formyl-methionyl-leucyl-phenylalanine as the major peptide neutrophil chemotactic factor produced by Escherichia coli. *J Biol Chem* **259**, 5430-5439 (1984).
37. H. Fu *et al.*, Ligand recognition and activation of formyl peptide receptors in neutrophils. *J Leukoc Biol* **79**, 247-256 (2006).
38. M. Nanamori *et al.*, A novel nonpeptide ligand for formyl peptide receptor-like 1. *Mol Pharmacol* **66**, 1213-1222 (2004).
39. H. Tse *et al.*, Complete genome sequence of Staphylococcus lugdunensis strain HKU09-01. *J Bacteriol* **192**, 1471-1472 (2010).
40. G. E. Baida, N. P. Kuzmin, Mechanism of action of hemolysin III from Bacillus cereus. *Biochim Biophys Acta* **1284**, 122-124 (1996).
41. A. Jochim *et al.*, An ECF-type transporter scavenges heme to overcome iron-limitation in Staphylococcus lugdunensis. *Elife* **9**, (2020).
42. D. Kretschmer, N. Nikola, M. Durr, M. Otto, A. Peschel, The virulence regulator Agr controls the staphylococcal capacity to activate human neutrophils via the formyl peptide receptor 2. *J Innate Immun* **4**, 201-212 (2012).
43. K. Rogasch *et al.*, Influence of the two-component system SaeRS on global gene expression in two different Staphylococcus aureus strains. *J Bacteriol* **188**, 7742-7758 (2006).
44. D. Chin *et al.*, Staphylococcus lugdunensis Uses the Agr Regulatory System to Resist Killing by Host Innate Immune Effectors. *Infect Immun* **90**, e0009922 (2022).
45. I. Migeotte, D. Communi, M. Parmentier, Formyl peptide receptors: a promiscuous subfamily of G protein-coupled receptors controlling immune responses. *Cytokine Growth Factor Rev* **17**, 501-519 (2006).
46. C. Vuong *et al.*, Regulated expression of pathogen-associated molecular pattern molecules in Staphylococcus epidermidis: quorum-sensing determines pro-inflammatory capacity and production of phenol-soluble modulins. *Cell Microbiol* **6**, 753-759 (2004).
47. C. C. Murdoch, E. P. Skaar, Nutritional immunity: the battle for nutrient metals at the host-pathogen interface. *Nat Rev Microbiol* **20**, 657-670 (2022).
48. S. Heilbronner *et al.*, Competing for Iron: Duplication and Amplification of the isd Locus in Staphylococcus lugdunensis HKU09-01 Provides a Competitive Advantage to Overcome Nutritional Limitation. *Plos Genetics* **12**, (2016).
49. R. S. Flannagan *et al.*, In vivo growth of Staphylococcus lugdunensis is facilitated by the concerted function of heme and non-heme iron acquisition mechanisms. *J Biol Chem*, 101823 (2022).
50. A. N. Spaan *et al.*, Staphylococcus aureus Targets the Duffy Antigen Receptor for Chemokines (DARC) to Lyse Erythrocytes. *Cell Host Microbe* **18**, 363-370 (2015).
51. S. Ravaioli *et al.*, Searching for Virulence Factors among Staphylococcus lugdunensis Isolates from Orthopedic Infections: Correlation of beta-hemolysin, hemolysin III, and slush Genes with Hemolytic Activity and Synergistic Hemolytic Activity. *Int J Mol Sci* **24**, (2023).
52. D. Belikova, A. Jochim, J. Power, M. T. G. Holden, S. Heilbronner, "Gene accordions" cause genotypic and phenotypic heterogeneity in clonal populations of Staphylococcus aureus. *Nature communications* **11**, 3526 (2020).
53. L. Sandegren, D. I. Andersson, Bacterial gene amplification: implications for the evolution of antibiotic resistance. *Nat Rev Microbiol* **7**, 578-588 (2009).

54. A. Peschel, M. Otto, Phenol-soluble modulins and staphylococcal infection. *Nat Rev Microbiol* **11**, 667-673 (2013).

55. D. Kretschmer *et al.*, Staphylococcus aureus Depends on Eap Proteins for Preventing Degradation of Its Phenol-Soluble Modulin Toxins by Neutrophil Serine Proteases. *Front Immunol* **12**, 701093 (2021).

56. B. Chassaîn *et al.*, Multilocus sequence typing analysis of Staphylococcus lugdunensis implies a clonal population structure. *J Clin Microbiol* **50**, 3003-3009 (2012).

57. B. A. Diep *et al.*, Complete genome sequence of USA300, an epidemic clone of community-acquired meticillin-resistant Staphylococcus aureus. *Lancet* **367**, 731-739 (2006).

Supplementary Figure

Mass spectrometric (MS) analysis and identification of SLUSH peptides

A. *S. lugdunensis* N940025

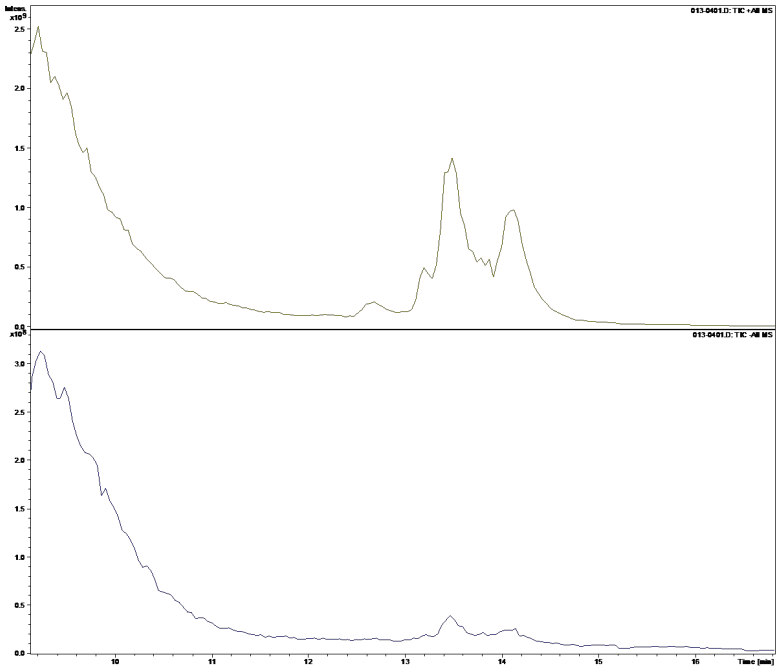

M 4446 (SLUSH A)

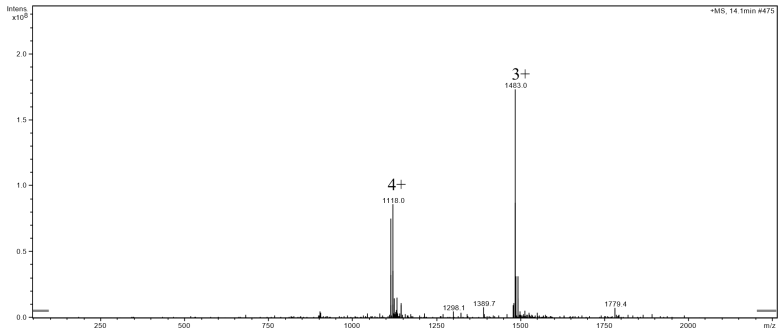

M 4350 (SLUSH B)

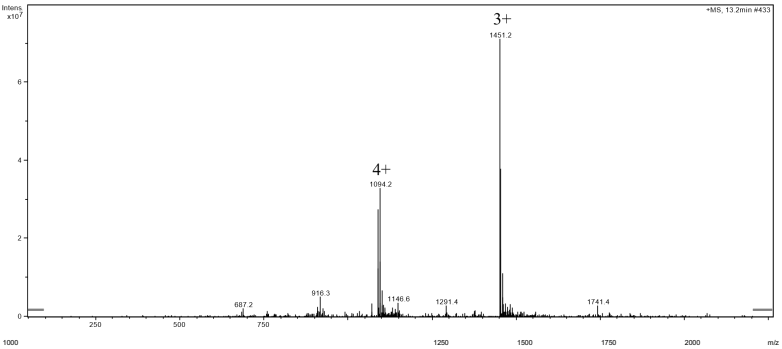

M 4539 (SLUSH C Nonformylated)

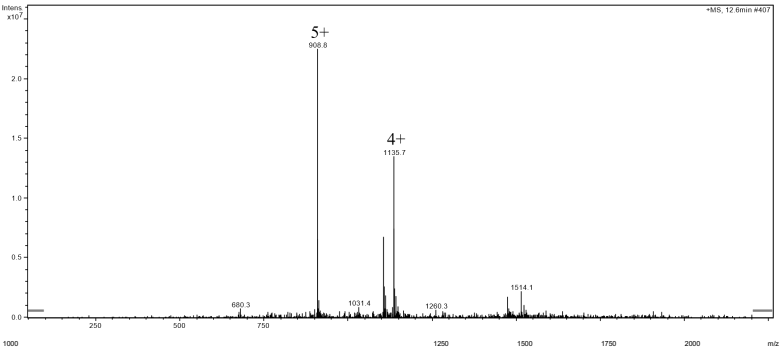

M 4569 (SLUSH C)

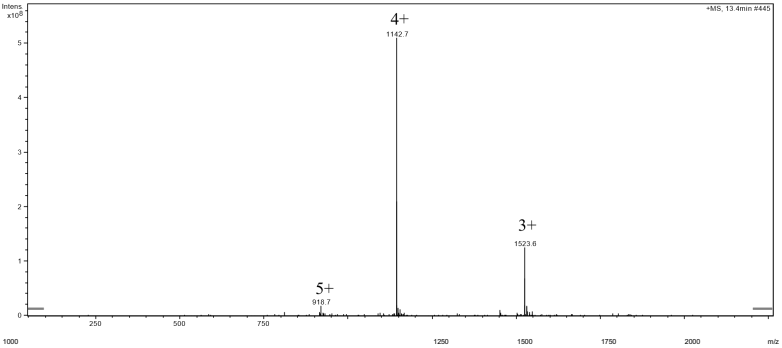

M 4430 (SLUSH C-1 aminoacid truncated)

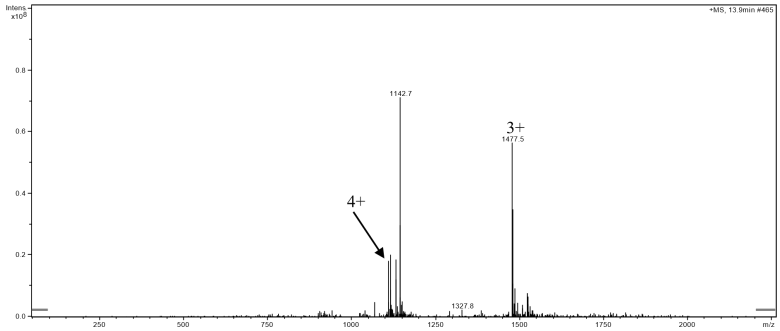

B. *S. lugdunensis* HKU09-01

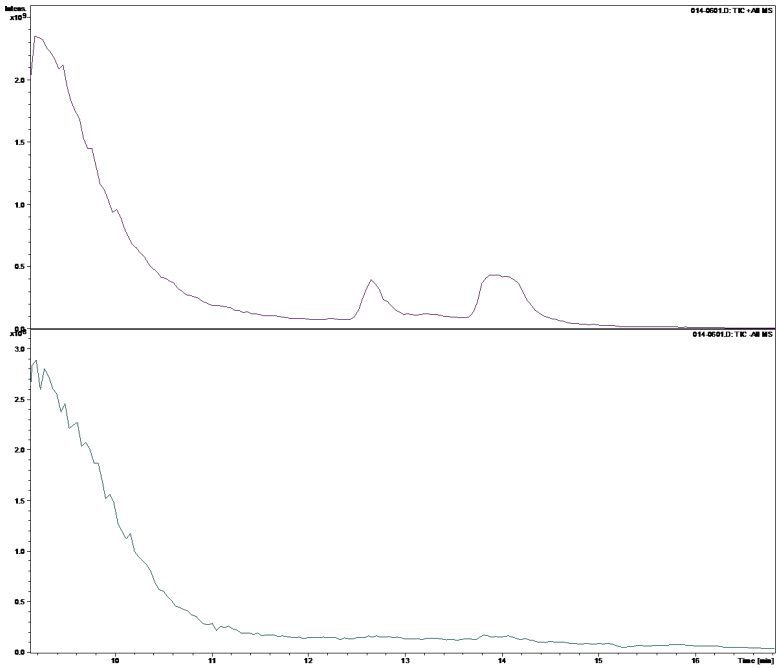

M 4418 (SLUSH A-Nonformylated)

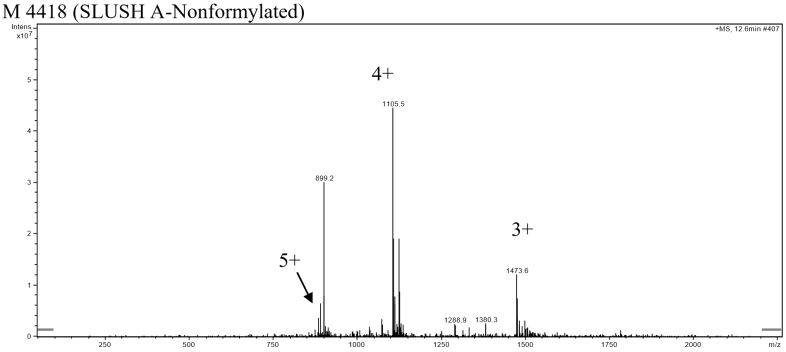

M 4491 (SLUSH B2-Nonformylated)

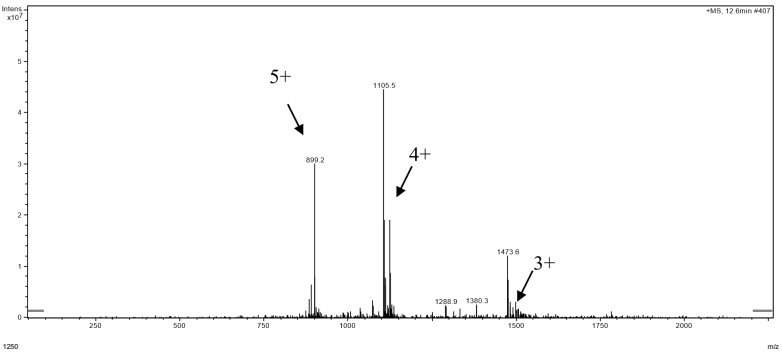

M 4519 (SLUSH B2)

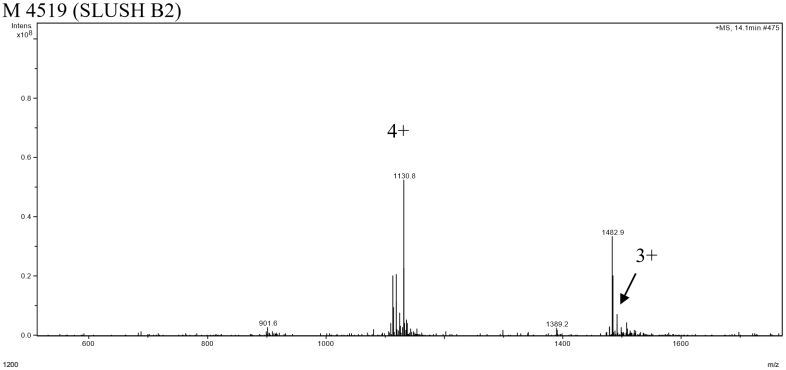

M 4445 (SLUSH A)

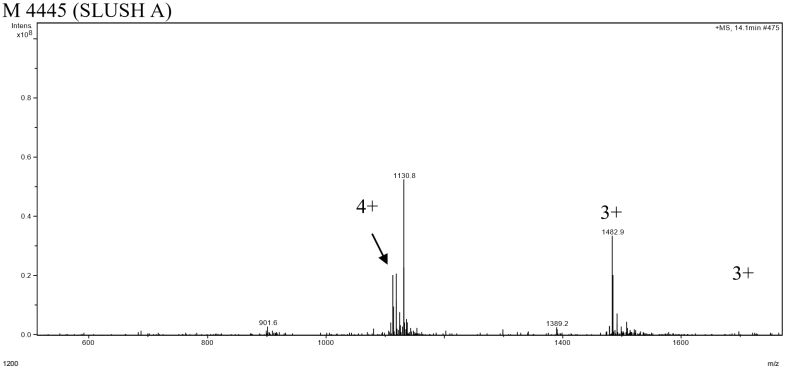

Supplementary Figure: Mass spectrometric analysis and fragment profile of SLUSH peptides in the supernatants of *S. lugdunensis* HKU09-01 (A) and *S. lugdunensis* N940025 (B). Cultures were grown overnight in TSB medium at 37◦C and supernatants were 4x concentrated before analysis. SLUSH peptides fragments were detected using HPLC-ESI-MS.

Chapter 3

Computer modelling and experimental validation of interactions between *Pseudomonas aeruginosa* and *Staphylococcus aureus.*

Sharmila Sekar[1], Nantia Leidou[2,3], Alina Renz[2,3], Andreas Dräger[2,3] and Simon Heilbronner[1,4,5]

1. Interfaculty Institute of Microbiology and Infection Medicine, 72076 Tübingen, Germany
2. Computational Systems Biology of Infection and Antimicrobial-Resistant Pathogens, Institute for Biomedical Informatics (IBMI),72076 Tübingen, Germany
3. Department for Computer Science, University of Tübingen, 72076 Tübingen, Germany
4. Ludwig-Maximilians-Universität München, Faculty of Biology, Microbiology, 82152 Martinsried, Germany
5. German Center for Infection Research "DZIF" partnersite Tübingen, Germany

Draft manuscript – Additional experiments are needed prior to submission

Abstract

35% of CF patients are co-colonised by *P. aeruginosa* and *S. aureus*. The interactions between these bacteria are well studied, yet some aspects, especially regarding their metabolic activities in the pulmonary environment, are not well understood. Genome-Scale Metabolic Models (GEMs) are used to predict these interactions, but their predictions are limited without incorporating transcriptional data. The research aims to enhance the predictive ability of metabolic models by integrating transcriptional information. This will enhance the prediction of *P. aeruginosa* and *S. aureus* metabolic interaction when co-cultured in conditions that mimic the CF lung environment. The co-culture of *P. aeruginosa* and *S. aureus* led to significant changes in gene expression, particularly in pathways related to amino acid biosynthesis and fermentation. Key metabolic products such as lactate, acetate, and formate were produced in different amounts in co-culture compared to monoculture. Notably, the gene *pvdE*, involved in *P. aeruginosa* iron acquisition, was downregulated in co-culture, suggesting *S. aureus* presence might affect *P. aeruginosa* iron metabolism and virulence. The study concludes that co-culturing *P. aeruginosa* and *S. aureus* results in the differential regulation of multiple metabolic pathways in a CF-like environment. The optimised models developed in this research will be used in future studies to predict bacterial fitness under varying environmental conditions. Despite the promising ability of GEMs, the study provides the need for further curation of the models to account for environmental factors, as model predictions and experimental results were shown to vary. This research advances the understanding of bacterial interactions in CF lungs and emphasises the potential and limitations of GEMs in predicting microbial interactions.

Introduction

To understand how microbes interact during mixed infections and to develop more effective bacterial elimination strategies, computational models can provide valuable insights. Usage of computational modelling has increased significantly, particularly with the availability of Genome-Scale Metabolic Models (GEMs). GEMs are used to predict interactions between two or even three microbes, as they have the potential to predict the cellular and metabolic behaviour of cells under defined environmental conditions (*1*). GEMs simulate the metabolic networks of biological systems at the cellular level (*2, 3*). GEMs have been successfully applied in various fields to explore cellular metabolism, inform metabolic engineering, identify essential enzymatic reactions, and facilitate systems-level genetic and metabolic analyses (*4*). A core component of GEM reconstruction is the gene-protein-reaction (GPR) association matrix (GEM) – a computational representation of an organism's mass-balanced, stoichiometry-based metabolic reactions, developed from genomic annotation data and empirically derived information. Most notably, the GEM enables the application of optimisation methods like flux balance analysis (FBA), which makes use of linear programming, to forecast metabolic flux values for a full set of metabolic reactions.

Additionally, GEMs provide a framework for integrating diverse data types, including omic datasets (e.g., genomics, proteomics, and transcriptomics). The quality and application scopes of GEMs have increased in tandem with the ongoing evolution of genome sequencing and related omics analysis techniques. Taken together, these advancements have improved our understanding of metabolism in a variety of organisms (*5*). Herein, we assess the ability of GEMs to predict interactions between *S. aureus* and *P. aeruginosa,* focusing on their metabolic competition and cooperation within a host environment.

Cystic Fibrosis (CF) is a common genetic disorder among Caucasians, affecting multiple organs. A mutation in the Cystic Fibrosis Transmembrane Conductance Regulator (CFTR) gene, which encodes a protein responsible for regulating the movement of chloride and sodium ions cross epithelial membranes (*6, 7*). One of the features of CF is the production of thick, sticky mucus that obstructs the airways, leading to chronic respiratory issues such as coughing, wheezing and frequent lung

issues. Overtime, this mucus buildup impairs gas exchange in the lungs and leads to progressive damage. In CF patients, progressive decline in normal lung function, neutrophil inflammation, and persistent bacterial infections in the mucus are the predominant causes of morbidity and mortality (*8, 9*). CF respiratory infections are known for their polymicrobial communities, which exhibit resistance to antimicrobial therapeutics. Throughout their lives, CF patients get colonised by wide range of bacterial and fungal pathogens and are also infected by viral pathogens (6, 8).

P. aeruginosa and *S. aureus* are the most common pathogens in CF patients (*10*). In addition to these pathogens, the lungs of CF patients are also freqeuntly infected with *Burkholderia cepacia*, *Haemophilus influenzae*, *Stenotrophomonas maltophilia,* and *Achromobacter xylosoxidans,* although to a lesser extent (*6, 11*). CF lungs are colonised by *S. aureus* as an early pathogen and are found across all age groups. Further, *S. aureus* is frequently found together with *P. aeruginosa* (*6*) (*10*). Increasing with age, *S. aureus* colonisation declines, while *P. aeruginosa* either remains stable or becomes more prominent (*8, 12*).

Several studies investigate interactions between *S. aureus* and *P. aeruginosa* and it is known that *P. aeruginosa* outcompetes *S. aureus*. *P. aeruginosa* inhibits the growth or lyses *S. aureus* through several mechanisms including iron sequestration and production of 2-heptyl 4-hydroxyquinoline-*N*-oxide (HQNO), which specifically inhibits *S. aureus* respiration (*8, 9*). The state of coexistence could thus represent a trade-off allowing both pathogens to benefit mutually and maintain equilibrium. *P. aeruginosa* alters its carbon metabolism in response to *S. aureus*, reflecting how bacterial species dynamically adapt their nutrient utilisation strategies- particularly carbon sources to support survival and growth in polymicrobial environments. Here, *P. aeruginosa* uses the acetoin produced by *S. aureus* as a nutrient source for its metabolism (*7, 9*). The metabolic exchange between the two pathogens is observed as they adapt to the CF lung environment, enabling their cooperation and mutual survival in the host *(9, 11)*.

The objective of this project was to evaluate the translatability of GEMs in *in vitro* co-culture experiments, specifically within the context of cystic fibrosis (CF). We focused on the interactions between *S. aureus* and *P. aeruginosa* in Artificial Sputum Medium (ASM), a nutrient-rich environment designed to mimic the conditions of the CF lung. To gain insight into metabolic shifts during bacterial co-culture, we performed transcriptomic analyses on both single and mixed cultures, identifying dysregulated

genes that aligned with model predictions. Additionally, we conducted growth curve experiments with *S. aureus* mutants to determine their influence on *P. aeruginosa* growth. However, no significant differences were observed between mixed and single cultures, suggesting that the predicted metabolic interactions had limited impact under the tested conditions.

Given that ASM contains proteins, amino acids, and DNA, we also examined the role of differentially regulated proteases and DNases. Despite their potential function in nutrient acquisition and bacterial competition, protease mutants did not significantly alter growth patterns in co-culture. These findings highlight the complexity of bacterial interactions in CF-like environments and underscore the need for further refinement of GEM predictions to capture the nuances of interspecies metabolic dependencies better.

Materials and Methods

Bacterial Strains and Growth Conditions

All strains used are listed in Table 1. Methicillin-resistant *Staphylococcus aureus* (MRSA) strain substr. USA300 TCH1516 (also named USA300-HOU-MR) was originally isolated from an outbreak in Houston, Texas. MRSA USA300 LAC was originally isolated from the Los Angeles County jail. MRSA USA300 LAC contains three small plasmids, one encoding resistance to tetracycline and another encoding erythromycin resistance. The third plasmid is cryptic. For ease of genetic manipulation and to avoid interference, all three plasmids were cured, yielding strain *S. aureus* USA300 JE2 (*13-15*). The burn wound *P. aeruginosa* isolate PA14, also known as UCBPP-PA14. Originating as a study on the relationship between plant pathogens and human infections, PA14 research has evolved into a highly favored model for pathogenicity and severe *P. aeruginosa* infections (*16*). *S. aureus* was grown in tryptic soy broth (TSB) or Agar (TSA) (Oxoid), *E. coli* and *P. aeruginosa* strains were grown in Luria-Bertani L-broth or L-agar (DIFCO) or ASM (Artificial Sputum Medium) to mimic Cystic Fibrosis Conditions. Strains from Nebraska transposon mutant library (NTML) for USA300/JE2 and for PA14 strains, PA14 Transposon insertion mutant library was used. Unless stated otherwise, strains were grown at 37°C.

Growth Kinetics and Co-Cultivation

Growth of Single culture (JE2/PA14) or Mixed culture (JE2 and PA14) was done with TSB/LB/ASM medium. Optical Density (OD600) /CFU correlation was done for the strains, and mixed culture, the strains are mixed in a ratio, so they have a similar number of bacteria. For JE2 Optical Density of 0.025 and PA14 Optical Density of 0.017 was used. Every hour, the sample was taken, washed and resuspended in PBS, then OD600 was measured, and the sample was plated in different dilutions on selective agar (TSB agar+7% NaCl) for JE2 and LB agar for PA14 using a spiral plate reader (Eddy jet spiral plater). The plates were then incubated for 18-24 h, and colony-forming units are calculated using SphereFlash® (Automatic Colony Counter).

ASM Medium Preparation

ASM was prepared as described in (*17*), 1 L ASM contained 5 g of pig mucin (type 2), 4 g of low molecular weight salmon sperm DNA, 5.9 mg of DTPA, 5 g of NaCl, 2.2 g of KCl, and 1.81 g of Tris base, 5 g of casamino acids and adjusted to pH 7.0. ASM was sterilisation at 121°C for 15 min. After sterilisation, 5 mL of egg yolk emulsion was added under sterile conditions. All products are from Merck. For ASM agar, the medium was prepared as mentioned above, and agar (2X concentrated) was mixed with the medium and poured into the plates.

Construction of Gene Deletion Mutants

For generating deletion mutations, the construction of cassettes was carried out as previously described (*18*). A and B primer combinations were used to amplify a 500 bp upstream sequence (up to the start codon of the gene of interest) and a 500 bp sequence downstream of the stop codon (C and D primers). The PCR products were used as templates for the spliced overlap extension (SOE) PCR using primers A and D. The resulting 1 kb fragment was gel-purified, cleaved at endonuclease cleavage sites introduced with forward and reverse primers (A and D) and cloned into pIMAY, (*18*) digested with the same endonucleases. Primer sequences are listed in Table 2.

Transformation and Allelic Replacement

S. aureus strains were transformed as described elsewhere (*19*). Chemically competent *E. coli* strains were transformed using standard procedures.

Fermentation Assay

To assess the accumulation of fermentation products, cells were grown in ASM medium, and samples were collected at timepoints 0 h, 5 h and 24 h from mixed culture and single cultures. D-Lactate (MAK064), Succinate, Acetate and Formate production in the ASM was measured using Assay Kits (D-Lactate (MAK064), Succinate, Acetate and Formate kits from Sigma-Aldrich following the manufacturer's guidelines. ASM medium was used as a control for the measurements.

Spot Assay

The aim of this experiment was to evaluate the ability of bacterial strains to produce DNase and proteolytic enzymes, thereby assessing their enzymatic activity and capacity to degrade nucleic acids and proteins. DNase agar was prepared using DNase Test agar from BD Difco™. For proteolysis assessment, LB agar was supplemented with 1% skimmed milk. Overnight cultures were grown in ASM, TSB, or LB medium, diluted to an OD600 of 1, and then spotted onto the prepared agar plates. After drying, the plates were incubated at 37°C for 24 h. The presence of a clear halo around colonies indicated proteolytic activity on the skim milk agar, while a clear zone on DNase agar confirmed DNase production.

Iron-Restricted Spot Assay

To inhibit siderophore-independent growth, iron-depleted agar plates (0.5 L) were prepared by dissolving 5.4 g of RPMI-1640 powder (Gibco™) and 5 g of Casamino acids (Difco) in 250 mL of ddH_2O. Afterwards, 22.5 g of Chelex-100 resin (Bio-Rad) was added, and the mixture was incubated with stirring for 18 h at 4°C. After the incubation, Chelex was removed by sterile filtering through a 0.25 µm filter (pore size), and 10 µM EDDHA (Ethylenediamine-N, N'-bis (2-hydroxyphenylacetic acid)) (Fluorochem) was added, followed by an additional incubation for 30 minutes at 37°C on a shaker.

Agar solution (2X concentrated) was prepared separately. The RPMI medium was warmed to 60°C and mixed with agar, and plates were prepared. Bacteria were grown overnight in TSB/LB. The overnight culture (1 mL) was washed twice with RPMI medium, and the optical density at 600 nm (OD_{600}) was measured. For the spot assay, the lawn OD was adjusted to 0.05, and for the spots, the OD was set in RPMI medium

(1X RPMI + 1% Casamino acids + 10 µM EDDHA). The strains for the lawn were scratched using a cotton swab, and after drying, 5 µL of bacteria was spotted and incubated at 37°C for 18 h.

RNA Isolation

Bacterial Cultures of USA300 and PA14 were inoculated in ASM, SNM3 and TSB/LB with an initial OD600 of 0.05 from overnight cultures and grown at 37°C with agitation. Samples were collected at an exponential phase with an OD600 of 0.2, centrifuged at 5.000 g for 10 min, 4°C. The cell pellet was resuspended in 1 mL Trizol (Invitrogen™) and transferred to prefilled screw-cups (Zirconia/Silica beads). Cells were disrupted using Fastprep24 and two cycles of 30 s at 6500 rpm (6.5 m/s). 200 µL of chloroform was added, followed by centrifugation at 12.000 g for 15 min at 4°C. 600 µL of the aqueous phase was collected, and 500 µL of isopropanol was added. The sample was incubated at RT for 10 min and centrifuged (12.000 g for 30 min at 4°C). The pellet was washed again with 75% EtOH (95-99% purity) and resuspended in nuclease-free water. The RNA was purified using the Nucleospin RNA cleanup and concentration kit (MACHEREY-NAGEL).

RNA Isolation for Transcriptomics

For transcriptomics, 100 mL samples (ASM/SNM3 medium) were harvested at an OD600 0.2 culture grown at 37° C and mixed with 1/9 volume of Ethanol/Phenol solution (stabilised with Tris-EDTA-pH 6.5 (AppliChem)), centrifuged at 20.000 g at 4°C for 15 min. Then the supernatant was mixed with TRIZOL, and RNA was isolated from the above-mentioned protocol. A fold change threshold of >2 or <−2 was applied to identify genes with substantial expression differences. This allowed us to focus on those with significant transcriptional changes, streamlining the analysis and narrowing down the list of candidate genes for further validation.

RT-qPCR

200 ng of RNA was used to synthesise cDNA using Superscript™ IV Vilo (Invitrogen). Quantitative PCR was then performed in Quantstudio™ Real-time PCR system, with diluted cDNA or undiluted cDNA, primers (Table 2) and SYBR Master mix (Applied Biosystems).

Table 1: Bacterial Strains and Plasmids

Bacterial Strain / Plasmid	Description	Reference / Source
Staphylococci		
S. aureus USA300/JE2	Plasmid curated LAC strain	(*18*)
S. aureus JE2Δ*sspAB*	Deletion mutant of *sspAB* locus	This study
S. aureus JE2Δ*splABCDEF*	Deletion mutant of *splABCDEF* locus	This study
S. aureus JE2 adhE::ery /JE2_0151	Transposon mutant of the *adhE*	(*20*)
S. aureus JE2_*1214*	Transposon mutant of the gene 1214	(*5, 20*)
S. aureus JE2_*1329*	Transposon mutant of the gene 1329	(*20*)
S. aureus JE2_*1642*	Transposon mutant of the gene 1642	(*20*)
S. aureus JE2_*0914*	Transposon mutant of the gene 0914	(*20*)
S. aureus JE2 *Δsfa*	Markerless deletion of the entire sfa locus (staphyloferrin A biosynthesis genes; sfaA-D)	(*21*)
S. aureus JE2 *Δsba*	Markerless deletion of the entire sbn locus (staphyloferrin B biosynthesis genes; sbnA-I)	(*21*)
S. aureus JE2 *ΔsfaΔsbn*	Markerless deletion of the entire sfa and sbn locus	(*22*)
P. aeruginosa		
UCBPP-PA14	Human clinical isolate	(*23*)
PA14 *ΔeprS*	Deletion mutant of *eprS* gene	(*24, 25*)
PA14_*18750*	Transposon mutant of gene 18750	(*26*)
PA14_*23080*	Transposon mutant of gene 23080	(*26*)
PA14_*ΔpvdA*	Transposon mutant of gene *pvdA*	(*26*)
PA14_*ΔpvdD*	Transposon mutant of gene pvdD	(*26*)
PA14_*ΔpvdE*	Transposon mutant of gene pvdE	(*26*)
PA14_*ΔpvdF*	Transposon mutant of gene pvdF	(*26*)
Plasmids		
pIMAY	Thermosensitive vector for allelic exchange	(*18*)
pIMAY-Δ*sspAB*	Plasmid for deletion of *sspAB*	This study
pIMAY--Δ*splABCDEF*	Plasmid for deletion of entire *spl* protease locus	This study

Table 2: Oligonucleotides Used In This Study

Primer	5'-3' Sequence	Restriction site
PFA: JE2 SSpAB	ghattcggtaccggatttgtaaggatttc	KpnI
PRB: JE2 SSpAB	catctaaaaacctccaaaaaatttatttac	
PFC: JE2 SSpAB	ggtttttagatgtaaaaagtaatatagatattg	
PRD: JE2 SSpAB	ggtttttagatgtaaaaagtaatatagatattg	SacI
PFA: JE2 SplA-F	gtttgaattagcaggtaccatactaagtaatg	KpnI
PRB: JE2 SplA-F	catattttacctccttccaaatttatttttata	
PFC: JE2 SplA-F	catattttacctccttccaaatttatttttata	
PRD: JE2 SplA-F	tatatcgagctcttgcgtttcaatttcacg	SacI
qPCR PA14 gapA F	acaccaacgaccagaacctc	
qPCR PA14 gapA R	cctcgtctacgctggtatcc	
qPCR PA14 phhC F	accagttcctgctcgaagaa	
qPCR PA14 phhC R	accagttcctgctcgaagaa	
qPCR PA14 pirS F	accagttcctgctcgaagaa	
qPCR PA14 pirS R	ggcaagtgcattgaggttg	
qPCR PA14 rhlI F	ctctctgaatcgctggaagg	
qPCR PA14 rhlI R	gacgtccttgagcaggtagg	
qPCR PA14 eprS F	agcatcgacagctaccacct	
qPCR PA14 eprS R	agcatcgacagctaccacct	
qPCR PA14 rpoD F	accgtcgtggctacaaattc	
qPCR PA14 rpoD R	ggcgatcttcagtaccttgc	
qPCR PA14 gyrB F	aaattcaagatcgccaccac	
qPCR PA14 gyrB R	gattctccagcaggaagtcg	
qPCR PA14 hmgA F	agaaatacctcggcgagctg	
qPCR PA14 hmgA R	tgcgggttgaaggtggatac	
qPCR JE2 leuA F	tgaacgagcaggtaatgcag	
qPCR JE2 leuA R	acgccatcttggtgaatacc	
qPCR JE2 ilvC F	tgcaaaaggtattggtgcaa	
qPCR JE2 ilvC R	tctggttgataacccgcttc	
qPCR JE2 sspA F	acgatcgtcaccaaatcaca	
qPCR JE2 sspA R	ttgcagaagggaatgctttt	
qpCR JE2 rpoD F	caagcaatcactcgtgcaat	
qPCR JE2 rpoD R	caggttcttgcgcaattttt	
qPCR JE2 gyrB F	ggtgctgggcaaatacaagt	
qPCR JE2 gyrB R	tgggataccacgtccgttat	
qPCR JE2_0151 F	acgcatgcaatggaatcata	

qPCR JE2_0151 R	aaatgccataccagccaaag	
qPCR JE2_1214 F	aagcttcgggatatggcttt	
qPCR JE2_1214 R	aagcttcgggatatggcttt	
qPCR JE2_1329 F	ggtttcttctcagcgtttgc	
qPCR JE2_1329 R	acctgtttcagggattgcag	

Results

To study GEM prediction and experimental observation, we used *S. aureus* strain JE2 and *P. aeruginosa* UCBPP-PA14 as metabolic models are readily available, both are genetically approachable, and transposon mutant libraries are available.

P. aeruginosa PA14 and *S. aureus* JE2 show competitive behaviour on solid agar surfaces.

Previous studies have shown that different *S. aureus* and *P. aeruginosa* strains can exhibit either collaborative or competitive interactions (*9*). To investigate this phenomenon with our specific strains, we performed a competitive assay by plating a lawn of *S. aureus* on TSB agar and then spotting *P. aeruginosa* on top. After incubation, a clear inhibition halo was observed around the PA14 spot, indicating a competitive interaction in solid media (Figure 1A).

To further explore these interactions in a more physiologically relevant environment, we grew JE2 and PA14 in ASM under monoculture and co-culture conditions. Growth was assessed by both optical density (OD600) and colony-forming units (CFU/mL) (Figures 1B-D). Both JE2 and PA14 exhibit enhanced growth in mixed cultures compared to single culture (Figure 1B, C &D). These interactions could be due to nutrient sharing.

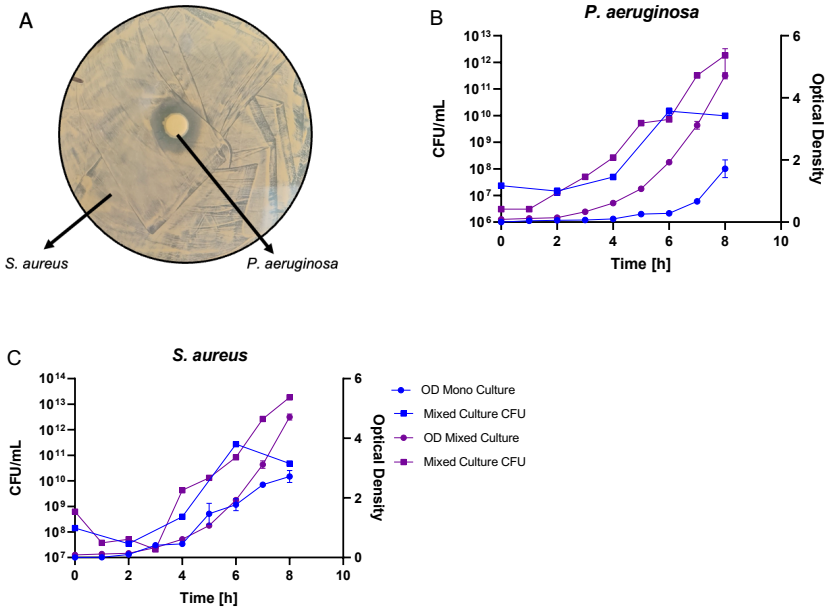

Figure 1. Interaction Between *S. aureus* and *P. aeruginosa*

(A) *S. aureus* (100 µL culture) was spread as a lawn on an agar plate and allowed to dry. *P. aeruginosa* (10 µL) was then spotted at the center. Plates were incubated at 37 °C for 24 hours. The presence of a halo indicates potential competitive interaction between the strains.

(B) (B & C) Growth analysis of *P. aeruginosa* PA14 and *S. aureus* JE2 in monoculture and co-culture in artificial sputum medium (ASM). Optical density (OD600) and colony-forming units (CFU) were measured. CFUs were determined by plating on TSB + 7% NaCl for *S. aureus* and on LB agar for *P. aeruginosa*. No statistically significant differences were observed. The mean and *SD* from three independent experiments are shown.

Medium-dependent growth - Effect of Nutritional Media on the Growth and Interactions of *S. aureus* and *P. aeruginosa*

The primary goal of this experiment was to assess whether computational models can accurately predict the effects of co-culture on *S. aureus* and *P. aeruginosa* under nutritional conditions such as ASM. With the growing importance of understanding bacterial interactions, especially in mixed-species environments, we aimed to determine whether these models align with the observed growth dynamics in

laboratory settings. To this end, we provided detailed nutritional content information for ASM media to a bioinformatics team. They applied their GEMs and expertise to model the growth kinetics of both bacterial species in monoculture and mixed culture scenarios.

The models predicted several key outcomes regarding the growth of *S. aureus* and *P. aeruginosa* in ASM medium. For *S. aureus*, the predicted biomass gain was only slightly reduced in mixed culture compared to monoculture (Fig. 2A), suggesting that while there may be minor competition, *P. aeruginosa* and its metabolic byproducts do not drastically impair *S. aureus* growth. However, this finding contrasts with the inhibition observed in close proximity on solid media (Fig. 1A), highlighting how spatial structure alters interaction dynamics.

In contrast, *P. aeruginosa* was predicted to benefit substantially from coculture, with a large increase in biomass gain in mixed conditions compared to monoculture (Fig. 2B). Notably, the data are presented as the inverse of biomass gain (1/gain), which approximates generation time; thus, a lower value indicates faster growth. This significant drop in 1/gain in the mixed condition illustrates that *P. aeruginosa* grows considerably faster when co-cultured with *S. aureus*.

To test the accuracy of model predictions, we performed growth curve analyses of JE2 and PA14 in single and co-culture in ASM medium (Figure 1B) and calculated the generation time of each bacterium. In monoculture, JE2 exhibited a shorter doubling time than PA14, consistent with data from model predictions. However, in co-culture, the model data showed that *P. aeruginosa* would benefit substantially, growing faster than *S. aureus,* whereas experimentally, PA14 continued to grow more slowly than JE2. Thus, while the model correctly captured growth trends in monoculture, its data for co-culture did not align with our experimental findings.

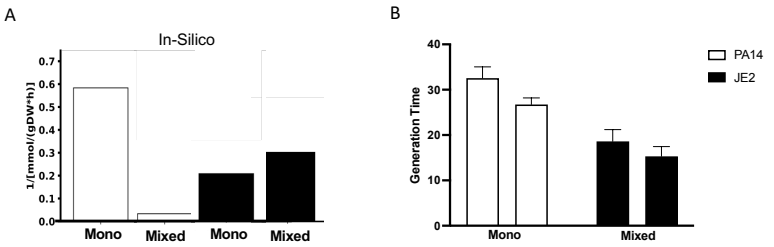

Figure 2: Growth Kinetics of *S. aureus* and *P. aeruginosa*

A. Predicted gain of biomass from genome-scale metabolic models (GEMs) for *S. aureus* and *P. aeruginosa* in single and mixed cultures grown in ASM media, reciprocal values are displayed to allow direct comparison to measured generation times displayed in B.

B. Generation time of *S. aureus* and *P. aeruginosa* calculated from growth curves in ASM media for single and mixed cultures. Doubling times are expressed in minutes. Error bars represent mean ± standard deviation (SD) of three repetitive experiments.

Experimental Validation of Genome-Scale Metabolic Model Predictions

To test whether GEMs could accurately predict metabolic pathways shaping the interaction between *S. aureus* and *P. aeruginosa*, we utilised a series of gene-deletion GEMs developed by Prof. Dräger's group. These GEMs were designed for both organisms, with each model lacking one metabolic gene at a time. The WT *S. aureus* GEM was combined with all individual *P. aeruginosa* deletion GEMs to simulate the growth rates of both organisms in co-culture within ASM media. Similarly, the *P. aeruginosa* WT GEM was paired with all individual *S. aureus* deletion GEMs. Any gene deletions that significantly impacted the growth characteristics of the WT partner strain were considered to potentially mediate interspecies interactions. Predicted gene deletions and gene knockouts for *S. aureus* are shown in Tables 3 and 4.

Table 3: *S. aureus* Single Gene Deletions

KEGG ID	Gene Name	Growth reduction [in %]
SAUSA300_0757	pgk	15.11
SAUSA300_0756	gap	15.11
SAUSA300_0760	eno	11.72
SAUSA300_0758	tpiA	11.65
SAUSA300_0151	adhE	10.59
SAUSA300_1657	ackA	10.59
SAUSA300_0570	pta	10.59
SAUSA300_1329	Amino acid permease	10.48
SAUSA300_1214	Threonine aldolase	10.48

Table 4: *S. aureus* Single Reaction Knockouts

BiGG ID	Name	Reaction	Genes	E.C. Number	Growth reduction [in %]
GLYt2	Glycine transport in via proton symport	Glycine_e + H_e <=> Glycine_c + H_c	SAUSA300_1642, SAUSA300_0914	-	15.23
SH_gly_e	Shuttle reaction of glycine	Inter-species exchange of glycine	-	-	15.23
GAPD	Glyceraldehyde-3-phosphate dehydrogenase	D-Glyceraldehyde 3-phosphate + Phosphate + NAD+ <=> 3-Phospho-D-glyceroyl phosphate + NADH + H+	SAUSA300_0756	1.2.1.12	15.11
PGK	Phosphoglycerate kinase	ATP + 3-Phospho-D-glycerate <=> ADP + 3-Phospho-D-glyceroyl phosphate	SAUSA300_0757	2.7.2.3	15.11
PGM	Phosphoglycerate mutase	2-Phospho-D-glycerate <=> 3-Phospho-D-glycerate	SAUSA300_0759, SAUSA300_0375, SAUSA300_2362	5.4.2.12, 5.4.2.11	11.72
ENO	Enolase	2-Phospho-D-glycerate <=> Phosphoenolpyruvate + H2O	SAUSA300_0760	4.2.1.11	11.72
TPI	Triose-phosphate isomerase	D-Glyceraldehyde 3-phosphate <=> Glycerone phosphate	SAUSA300_0758	5.3.1.1	11.65
ACKr	Acetate kinase	ATP + Acetate <=> ADP + Acetyl phosphate	SAUSA300_1657	2.7.2.1	10.59
ACALD	Acetaldehyde dehydrogenase	Acetaldehyde + CoA + NAD+ <=> Acetyl-CoA + NADH + H+	SAUSA300_0151	1.2.1.10	10.59
PTAr	Phosphotransacetylase	Acetyl-CoA + Phosphate <=> CoA + Acetyl phosphate	SAUSA300_0570	2.3.1.8	10.59
THRSEREx	L-serine/L-threonine exchange.	serine_c + threonine_e <=> sodium_e + threonine_c	SAUSA300_1329	-	10.48
THRAr	Threonine aldolase	L-Threonine <=> Glycine + Acetaldehyde	SAUSA300_RS06585	4.1.2.48	10.48
SH_thr L_e	Shuttle reaction of L-threonine	Inter-species exchange of L-threonine	-	-	10.48

The analysis revealed that *P. aeruginosa* gene products (Table 5) that promote the growth of *S. aureus* were only observed in the absence of oxygen, indicating that these interactions may be oxygen-dependent. Conversely, the *S. aureus* genes that inhibited *P. aeruginosa* growth were primarily associated with carbon metabolism. Given the conditions required for *P. aeruginosa* gene products (anaerobic or low oxygen), we

focused on validating the predictions related to *S. aureus* genes, which did not require any special environmental conditions.

Table 5: *P. aeruginosa* Single Gene Deletions

KEGG ID	Gene Name	Growth reduction [in %]
PA14_41560	nasA	100.0
PA14_13040	cioB	100.0
PA14_13030	cioA	100.0
PA14_22890	gapA	4.13
PA14_07190	pgk	4.13

Since many of the predicted genes from the models are involved in energy pathways and are challenging to mutate, we used the USA300/JE2 Nebraska mutant library to identify transposon mutants for further investigation. Specifically, we focused on the single gene deletions from Table 3, predicted by the models to decrease *P. aeruginosa* growth by 10% in co-culture with *S. aureus* in ASM.
The selected genes include

- SAUSA300_0151(*adhE*) – encodes aldehyde alcohol dehydrogenase, a key enzyme in fermentation and redox balance.
- SAUSA300_1214 – encodes threonine aldolase
- SAUSA300_1329 – encodes aminoacid permease

And single gene reactions predicted to impact glycine transport via proton symport are

- SAUSA300_0914
- SAUSA300_1642

By investigating these mutants, we aimed to validate whether disrupting these metabolic pathways in *S. aureus* would indeed alter the *P. aeruginosa* growth as predicted by models.

The *S. aureus* transposon mutants, obtained from the Nebraska Transposon Mutant Library (NTML), were cultivated both in single culture within ASM media and in co-culture with *P. aeruginosa* PA14. The growth kinetics of these mutants were compared to those of *S. aureus* JE2 WT with *P. aeruginosa* PA14 WT under the same conditions. In contrast to the predictions of the GEMs, we observed no differences in

P. aeruginosa growth when co-cultured with either *S. aureus* WT or any of the *S. aureus* transposon mutants (Figure 3).

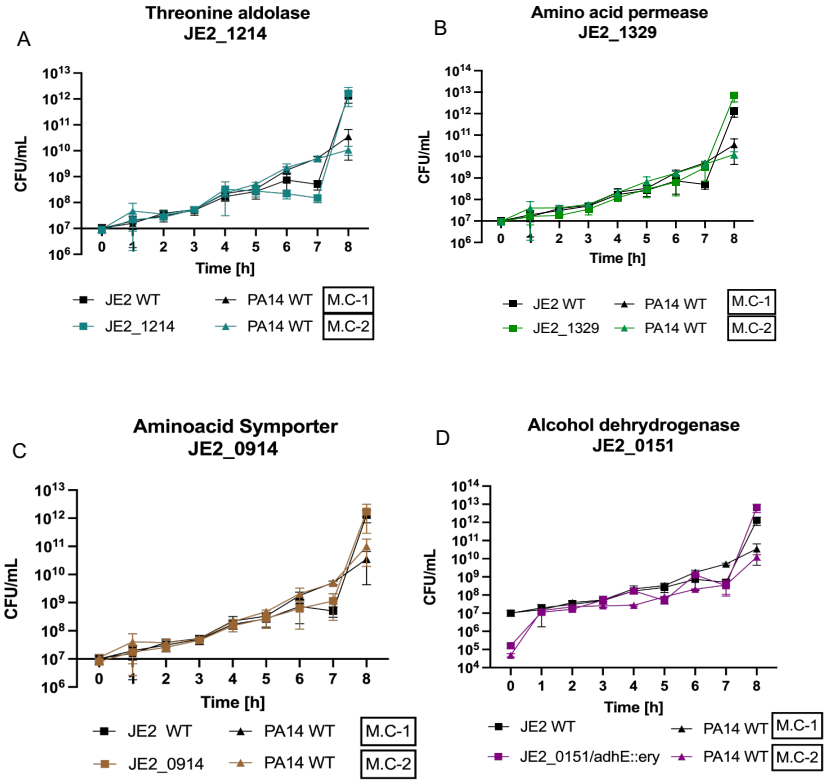

Figure 3: Growth activity of transposon mutants

A-D O/N cultures of JE2WT, JE2 transposon mutants and PA14 were grown in TSB/LB media. OD of 0.025 for JE2 and 0.017 for PA14 was used for growth curves in ASM. Samples were taken every hour, washed, resuspended in PBS, and OD600 was measured and plated on selective agar for CFU counting after incubation. **A.** JE2_0151 + PA14 WT **B.** JE2_1214 + PA14 WT **C.** JE2_0914 + PA14 WT **D.** JE2_1329 + PA14 WT. The mean and *SD* from three independent experiments are shown.

This suggests that while the GEMs offer valuable insights into metabolic pathways potentially involved in interspecies interactions, these models may not fully capture the complexity of real-world biological systems. Factors such as nutrient availability,

cross-feeding, and bacterial communication networks could influence the outcomes in ways that the models do not predict.

Transcriptomic Insights into *S. aureus* and *P. aeruginosa* Co-Culture - Use of Transcriptomics to Improve Models

The discrepancy between the model predictions and our experimental data in co-culture highlights an important limitation: while GEMs offer valuable predictions, their accuracy depends heavily on the quality and completeness of the input data. Refining these models, particularly to capture complex interspecies interactions, requires detailed mechanistic insight and improved integration strategies, which remain a task for dedicated bioinformaticians and are not further addressed in this study.

To explore bacterial interactions from a complementary angle, we did transcriptomic analysis in a more conventional framework to identify differentially expressed genes and relevant metabolic pathways. Integrating transcriptomic data into GEMs is a critical step toward enhancing their predictive power. Unlike GEMs, which assume that a bacterium exploits its full metabolic potential, transcriptomics reveals the actual metabolic activity under specific environmental conditions. This is crucial for improving the accuracy of models, particularly in complex co-culture environments like the interaction between *S. aureus* and *P. aeruginosa.* Transcriptomic data reflect the gene expression profiles in response to environmental changes, nutrient availability, competition, and interspecies interactions.

We performed transcriptomic analysis of the interaction between *S. aureus* and *P. aeruginosa* in ASM medium, comparing their gene expression profiles in monoculture versus co-culture. This approach allowed us to examine how each bacterium adjusts its metabolic activity in response to the presence of the other. Our analysis revealed substantial shifts in gene expression, highlighting the metabolic reprogramming that occurs during interspecies interactions. These findings reinforce the value of transcriptomic data for improving metabolic models.

Global Transcriptional Responses

Transcriptomic data revealed metabolic shifts in *S. aureus* and *P. aeruginosa* in monoculture and co-culture, influencing multiple pathways, including acetate metabolism, siderophore biosynthesis and protease production (Figure 4). Additionally, DNases were not found to be differentially expressed in the co-culture of

JE2 and PA14, in contrast to the proteases. The data revealed the upregulation of protease genes in *S. aureus,* including *sspA* and *sspB,* which encode precursors to cysteine proteases and V8 protease, both exhibiting a 3.5-fold increase in expression in co-culture. Additionally, genes encoding the *S. aureus* protease *splABCDEF* and *P. aeruginosa* protease EprS were differentially expressed, suggesting their role in protein degradation.

Acetate metabolism was differentially regulated, with associated genes being down-regulated in *P. aeruginosa* and up-regulated in *S. aureus* in co-culture. Interestingly, only *P. aeruginosa* is responsible for exporting formate, although no differentially expressed genes related to the formate export protein were detected in either species.

Iron acquisition was also affected, as the gene for staphyloferrin B (*sbnC*) biosynthesis in *S. aureus* showed an 8-fold upregulation, where the gene for pyoverdine biosynthesis (*pvdA*) in *P. aeruginosa* was downregulated by 5-8 times when the species were grown in co-culture.

Species-Specific Transcriptional Responses

S. aureus

In mixed culture *S. aureus* exhibited upregulation of genes such as *leuA, ilvC*, and *sspA* (Figure 4A), which are involved in amino acid biosynthesis. This upregulation likely represents a response to interspecies competition and nutrient shifts, with *S. aureus* increasing its biosynthetic and proteolytic activity to optimise survival in a shared environment.

P. aeruginosa

P. aeruginosa displayed downregulation of several genes involved in amino acid biosynthesis (*gapA*, *phhC*, *pirS*, *hmgA*) and quorum sensing (*rhlI*) in co-culture compared to monoculture (Figure 4B). This transcriptional profile suggests that

P. aeruginosa may benefit from metabolic cross-feeding, obtaining amino acids from *S. aureus* and thereby reducing its biosynthetic burden.

A

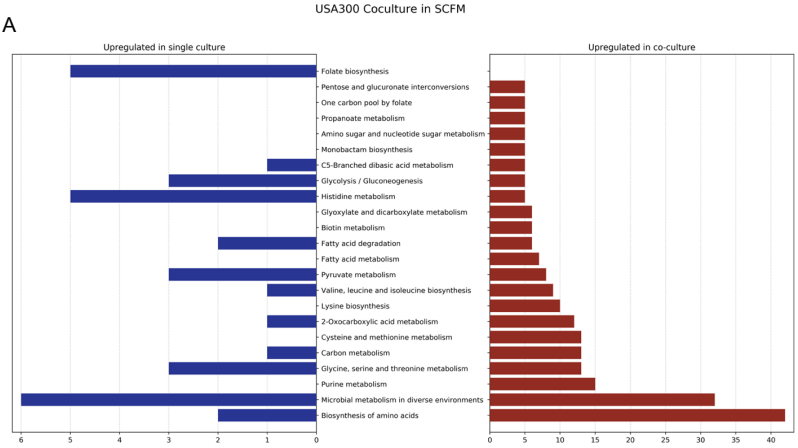

B

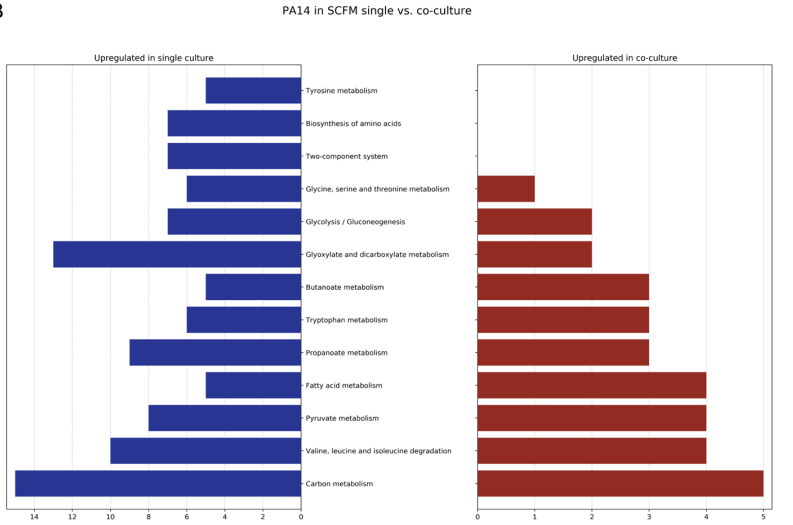

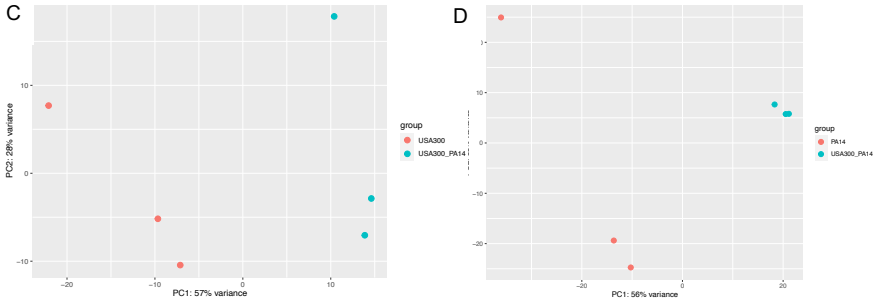

Figure 4: Transcriptomic Analysis of *S. aureus* and *P. aeruginosa*

Differentially expressed metabolic pathways identified from transcriptomic profiling of mono- and co-culture conditions in ASM.

(A) Bar graphs show pathways upregulated in *S. aureus* JE2 (USA300) during single culture (left, blue) and co-culture with *P. aeruginosa* (right, red).

(B) Corresponding analysis for *P. aeruginosa* PA14, showing pathways upregulated in single culture (left, blue) and co-culture (right, red). Pathway enrichment was based on gene expression data; the number of differentially expressed genes per pathway is shown on the x-axis.

(C&D) PCA analysis of *S. aureus* and *P. aeruginosa* single and co-culture in ASM

qRT-PCR Validation

To validate the transcriptomic data, quantitative real-time PCR (qRT-PCR) was performed on selected genes (Figure 5, Table 6 and Table 7). The qRT-PCR results confirmed the differential expression patterns observed in the RNA-seq data, including the upregulation of *sspA* in *S. aureus* and the downregulation of *gapA*, *pirS*, *rhlI*, and *eprS* in *P. aeruginosa* during co-culture. Notably, the expression of *phhC* and *hmgA* did not follow the expected downregulation trend, indicating possible discrepancies between RNA-seq and qRT-PCR results for these genes.

These results confirm the validity of key gene expression changes observed in the RNA-seq dataset, supporting the conclusion that interspecies interaction elicits specific transcriptional responses in both organisms.

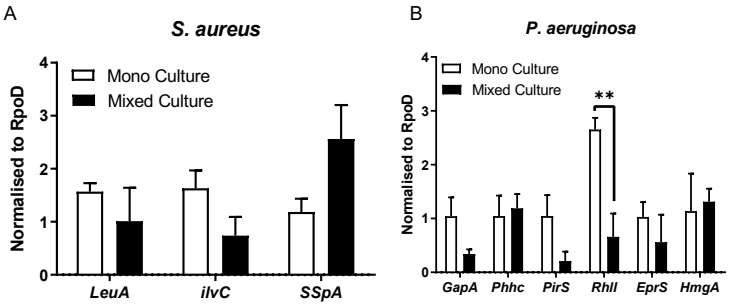

Figure 5: Gene Expression Analysis by qPCR

(A & B) Quantification of *P. aeruginosa* and *S. aureus* Gene Expression. Gene expression levels of *P. aeruginosa* and *S. aureus* in both single and mixed cultures were quantified using quantitative PCR (qPCR). The data were normalised to the expression levels of the housekeeping gene (*rpoD*), allowing for the assessment of differential gene regulation in response to co-culture conditions. The mean and *SD* from three independent experiments are shown. Mean and SD are from three independent experiments. Statistical analysis was performed using two-way ANOVA with Sidak's multiple comparison test. ** $p \leq .001$.

Table 6: USA300 Co-culture upregulated genes

Pathway	Locus tag	Gene name	Log2FC
Aminoacid Biosynthesis	SAUSA300_2010	*leuA*	2,62
	SAUSA300_2009	*ilvC*	2,64
Proteases	SAUSA300_0951	*sspA*	4

Table 7: PA14 co-culture downregulated genes

Pathway	Locus tag	Gene name	Log2FC
Aminoacid Biosynthesis	PA14_22890	*gapA*	-3,46
	PA14_53010	*phhC*	-2,86
Two-Component system	PA14_52240	*pirS*	-4,62
	PA14_19130	*rhlI*	-4,07
Proteases	PA14_18630	*eprS*	-3,47
Tyrosine metabolism	PA14_38510	*hmgA*	-4,98
	PA14_53010	*phhC*	-2,86

These data provide a deeper understanding of the interactions between *S. aureus* and *P. aeruginosa* in co-culture and offer important insights into the transcriptomic adaptations that occur in response to mixed-species environments.

Role of Proteases in *S. aureus* and *P. aeruginosa* Interactions in Protein-Rich ASM Medium

Given that ASM contains high levels of protein, we hypothesised that the secretion of public good like proteases could play a role in the interactions between *S. aureus* and *P. aeruginosa*. We postulated that proteases could be beneficial by breaking down extracellular proteins, facilitating nutrient acquisition. If the genes encoding these proteases were deleted, we anticipated that the bacteria would be unable, or severely restricted, in their ability to utilise extracellular proteins from the medium for growth. *S. aureus sspA* and *sspB* genes encoding the proteases V8 protease (SspA) and staphopain B (SspB) reside in the same operon, a mutant strain (JE2 *ΔsspAB*) was constructed with both genes deleted (*27*). The *spl* operon in *S. aureus* encodes six extracellular serine proteases: SplA, SplB, SplC, SplD, SplE, and SplF. A mutant strain lacking all six proteases (JE2 *ΔsplABCDEF*) was also generated, and growth in high protein ASM medium was analysed. The growth curves of JE2 *ΔsspAB*, JE2 *ΔsplABCDEF*, and wild-type JE2 (WT) in single and co-culture with PA14 WT were analysed (Figure 6). Contrary to our hypothesis, no growth reduction was observed in the mutants, nor were there any significant differences in colony formation between the strains. This suggests that protease activity is not a critical factor for PA14 growth under our conditions, indicating that PA14 does not rely on JE2 proteases for nutrient acquisition.

We hypothesised that EprS protease in *P. aeruginosa* could enhance *S. aureus* growth in co-culture, as it was downregulated in transcriptomics data. However, the growth *S. aureus* in coculture with EprS proficient or deficient strains did not differ significantly. of co-cultures of *S. aureus* WT with PA14 *ΔeprS* (Figure 6C) showed no alterations or growth defects

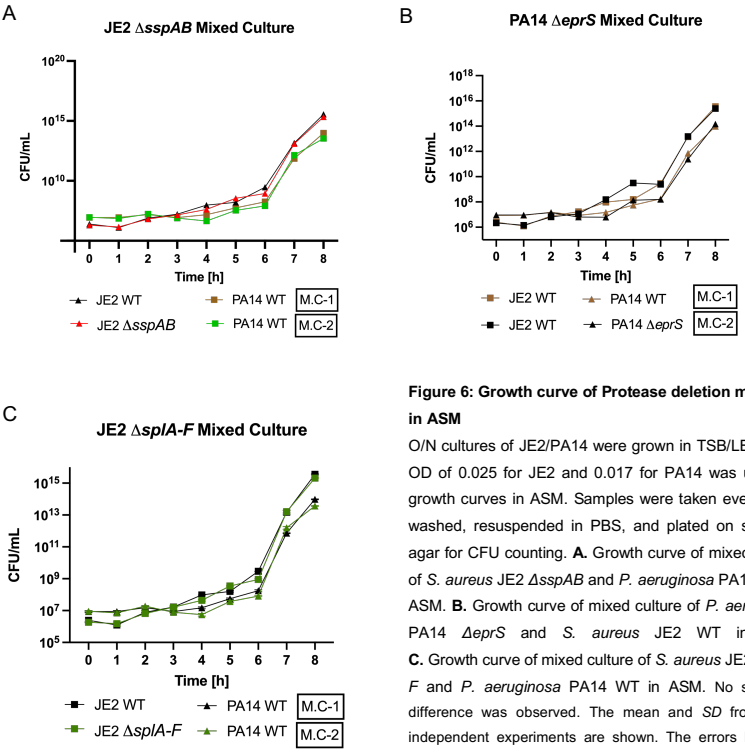

Figure 6: Growth curve of Protease deletion mutants in ASM

O/N cultures of JE2/PA14 were grown in TSB/LB media. OD of 0.025 for JE2 and 0.017 for PA14 was used for growth curves in ASM. Samples were taken every hour, washed, resuspended in PBS, and plated on selective agar for CFU counting. **A.** Growth curve of mixed culture of *S. aureus* JE2 *ΔsspAB* and *P. aeruginosa* PA14 WT in ASM. **B.** Growth curve of mixed culture of *P. aeruginosa* PA14 *ΔeprS* and *S. aureus* JE2 WT in ASM. **C.** Growth curve of mixed culture of *S. aureus* JE2 *ΔsplA-F* and *P. aeruginosa* PA14 WT in ASM. No statistical difference was observed. The mean and *SD* from three independent experiments are shown. The errors bars are small to be seen.

Metabolic product analysis

To further explore potential metabolic shifts, we measured the production of several key metabolic end products — including lactate, acetate, formate, and succinate in cultures of from *S. aureus* (JE2), *P. aeruginosa* (PA14), and their co-culture in ASM media.

We selected three specific timepoints—0, 5, and 24 hours—and measured these metabolites in the supernatant. These compounds are primarily produced by *S. aureus* via fermentation during glucose-rich growth phases and can be

reassimilated later during aerobic metabolism when glucose becomes limiting. This time-course approach allowed us to monitor both the accumulation and potential re-utilisation of fermentation products, providing insight into dynamic metabolic interactions.

As shown in Figure 6, we observed no significant differences in the levels of D-lactate, acetate, and formate between the single cultures and the co-culture. Despite transcriptomic data suggesting altered acetate metabolism, these findings indicate that the overall levels of these metabolites in the extracellular medium remained stable between conditions.

Since *P. aeruginosa* is a strict non-fermenter, it is unlikely to produce significant quantities of lactate or formate. Acetate production can occur via overflow metabolism under aerobic conditions, but its levels are typically low. The observed increase in acetate in *P. aeruginosa* cultures may therefore reflect experimental variability, contamination from media components, or minor aerobic overflow. Further validation—such as isotopic labelling or enzymatic assays—would be necessary to confirm the metabolic origin and dynamics of acetate in these conditions.

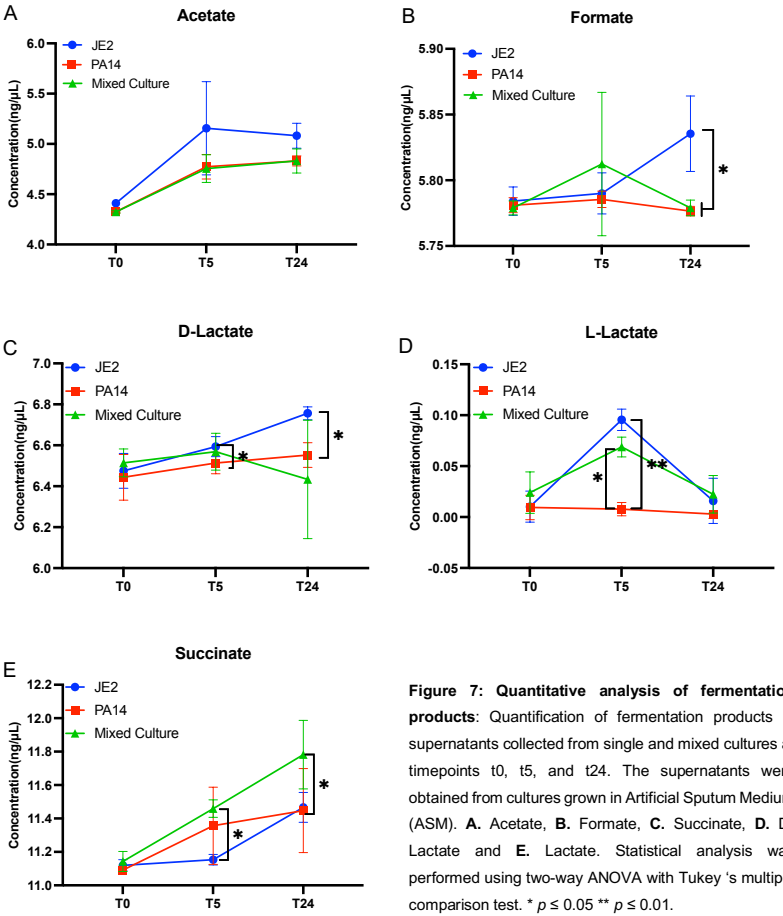

Figure 7: Quantitative analysis of fermentation products: Quantification of fermentation products in supernatants collected from single and mixed cultures at timepoints t0, t5, and t24. The supernatants were obtained from cultures grown in Artificial Sputum Medium (ASM). **A.** Acetate, **B.** Formate, **C.** Succinate, **D.** D-Lactate and **E.** Lactate. Statistical analysis was performed using two-way ANOVA with Tukey 's multiple comparison test. * $p \leq 0.05$ ** $p \leq 0.01$.

Iron limitation during co-culture

We hypothesised that *P. aeruginosa* might consume staphyloferrins to satisfy its own iron needs, thus causing an increase in iron limitation for *S. aureus.* To test this, we performed an iron-limited spot assay (Figure 8). First, we assessed whether *S. aureus* could benefit from *P. aeruginosa* siderophores. We created lawns of

S. aureus JE2 wild-type (WT) and siderophore-deficient mutants: *Δsfa* (unable to produce staphyloferrin A), *Δsfb* (unable to produce staphyloferrin B), and *ΔsfaΔsfb* (unable to produce both siderophores). Onto these lawns, we spotted *P. aeruginosa* strains (PA14 WT, Pyoverdine-deficient mutants PA14 *ΔpvdE* and PA14 *ΔpvdD*) to test if *S. aureus* could use *P. aeruginosa* siderophores (Figure 8A). No enhanced *S. aureus* growth was observed surrounding any of the P. aeruginosa strains, indicating that *S. aureus* does not utilise P. aeruginosa siderophores under these conditions. As a control, *S. aureus* JE2 WT was also spotted on a lawn of the *S. aureus ΔsfaΔsfb* double mutant, confirming that JE2 WT does not benefit from its siderophores under these conditions and ruling out generalised cross-feeding.

Next, we reversed the setup to assess whether *P. aeruginosa* could utilise *S. aureus* staphyloferrins. We prepared lawns of *P. aeruginosa* pyoverdine-deficient mutants (*ΔpvdE* and *ΔpvdD*), which are impaired in their siderophore production and dependent on alternative iron sources. Onto these lawns, we spotted *S. aureus* JE2 WT and siderophore mutants. Interestingly, both WT and *Δsfa* strains (which still produce staphyloferrin B) supported *P. aeruginosa* growth, while *Δsfb* and *ΔsfaΔsfb* did not (Figure 8B). This suggests that *P. aeruginosa* is capable of consuming staphyloferrins B (Sbn) produced by *S. aureus* in a co-culture, highlighting a potential interspecies competition for iron, where *P. aeruginosa* may exploit *S. aureus* siderophores to meet its iron demands.

These findings underscore the complexity of microbial interactions in co-culture environments, where iron acquisition strategies could influence bacterial growth and the competitive dynamics between the species. Our results also suggest that the regulation of siderophore biosynthesis in both species may be an adaptive response to iron limitation in co-culture. Further studies could investigate how *P. aeruginosa* consumption of staphyloferrins might affect the virulence or survival of *S. aureus* under these conditions, as well as the broader implications for microbial community interactions in iron-limited environments.

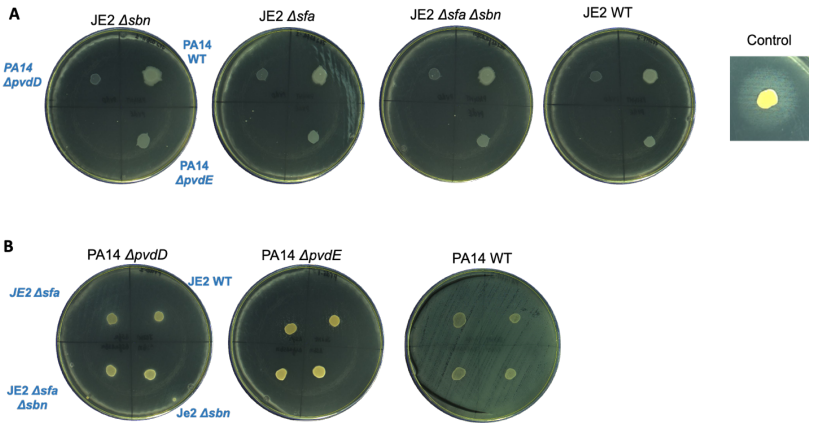

Figure 8: RPMI-Spot assay to assess siderophore-mediated interactions between *S. aureus* and *P. aeruginosa*.
A. *S. aureus* JE2 WT as a lawn, and *P. aeruginosa* PA14 WT and siderophore mutants (e.g., *ΔpvdD* and *ΔpvdE* for pyoverdine deficiency) were spotted on top.
B. *P. aeruginosa* PA14 WT was grown as a lawn, and *S. aureus* JE2 WT and siderophore mutants (e.g., *Δsfa, Δsir,* and *Δsbn)* were spotted. Minimal or reduced growth of *P. aeruginosa* pyoverdine-producing strains was observed around *S. aureus* JE2 WT and JE2 *Δsfa* spots, suggesting potential iron competition or inhibition. As a control, *S. aureus* JE2 WT was spotted on a lawn of *S. aureus* siderophore mutant.

Degradation of Complex Nutrients

In our study, we examined the degradation capabilities of *S. aureus* (USA300/JE2) and *P. aeruginosa* (PA14) using spot assays on agar plates supplemented with DNase, mucin, and protease to evaluate their ability to degrade these complex nutrients.

The results indicate a distinct difference in proteolytic activity between the two species. Cultures of *P. aeruginosa* PA14 displayed a significantly higher level of proteolytic activity than *S. aureus* JE2. This difference was visible on protease agar plates, where *P. aeruginosa* with large degradation zones showcased its enhanced ability to break down complex proteins compared to *S. aureus*. Conversely, *S. aureus* showed minimal to no detectable proteolytic activity under the same conditions (Figure 9).

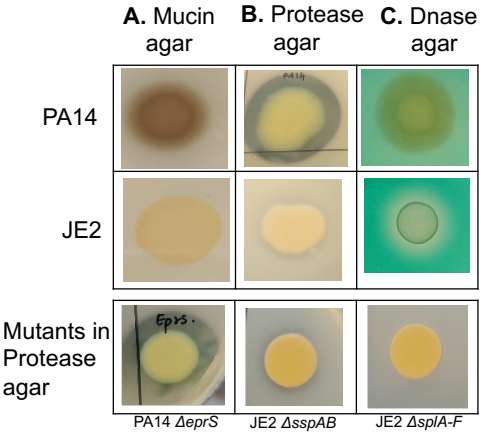

Figure 9: Spot assay

Overnight cultures of PA14 and JE2 were grown in TSB, or LB media, diluted to an OD of 1, and spotted onto **A. Mucin, B. Protease**, and **C. DNase** agar plates. In the bottom panel, protease mutants (PA14 *ΔeprS, JE2 ΔsspAB and* JE2 *ΔsplA-F)* were spotted on protease agar. After 24 hours of incubation at 37 °C, images were captured to assess enzymatic activity.

When assessing DNase activity, *P. aeruginosa* cultures showed weak or no observable degradation of DNA, suggesting a limited capacity to secrete extracellular DNases under the tested conditions. Similarly, *S. aureus* JE2 exhibited only minimal DNase activity. These findings indicate that neither organism demonstrates robust DNase-mediated degradation under the conditions tested, despite their potential to express DNases in other contexts.

In contrast, when evaluating mucin degradation, neither *P. aeruginosa* nor *S. aureus* JE2 showed significant mucin lysis activity. Furthermore, no observable changes were detected in the degradation of mucin, DNA, or general proteolytic activity across strains, even when specific proteases were differentially expressed. This suggests that the loss or variation of individual proteases does not markedly impact the overall ability of these bacteria to degrade complex host-derived nutrients like mucins or extracellular DNA under these experimental conditions.

Discussion

This study investigated the metabolic interactions between *S. aureus* and *P. aeruginosa* using GEMs and experimental validation. While computational models are powerful tools for predicting bacterial growth and metabolism, our findings highlight their limitations in accurately capturing complex interspecies interactions.

Growth Competition and Model Limitations

Our results demonstrate that *S. aureus* and *P. aeruginosa* compete for growth and survival in co-culture (Figure 1). Doubling time calculations revealed discrepancies between GEM predictions and experimental data. These false-negative predictions suggest that the current models do not fully account for nutrient availability, metabolic flexibility, or adaptive stress responses. Similar modeling challenges have been reported in other studies, where GEMs struggle to predict growth in complex environments due to incomplete media compositions or overlooked regulatory constraints (*28, 29*).

Incorporation of transcriptomics data from single and mixed cultures in ASM media have the potential to improve the accuracy of predictions. However, integrating transcriptomic insights into GEMs remains an ongoing challenge due to the complexity of regulatory networks and the dynamic nature of gene expression. Prior studies have also highlighted the difficulty of aligning transcriptomic data with metabolic models, particularly when dealing with condition-dependent gene regulation and post-transcriptional modifications (*30*). These tasks are needed to be done in Prof. Drager's lab, and it is beyond our expertise.

Metabolic Interactions: Expected vs. Observed Trends

From transcriptomics data, we found specific pathways to be differentially regulated in co-culture, particularly amino acid biosynthesis, two-component signaling systems, proteases, and tyrosine metabolism. However, RT-PCR validation (Figure 5) revealed discrepancies, especially for *P. aeruginosa*, where predicted gene downregulation (*phhC* and *HmgA)* in co-culture was not observed experimentally. These discrepancies are likely attributable to technical variability between replicates, differences in sensitivity between RNA-Seq and RT-PCR, or the complexity of temporal gene expression dynamics. Therefore, while transcriptomics provides

valuable insights into potential regulatory shifts, careful experimental validation remains essential to confirm biological relevance.

Studies have extensively documented the competitive dynamics between *S. aureus* and *P. aeruginosa*, showing that *P. aeruginosa* produces antimicrobial compounds like HQNO, siderophores, and rhamnolipids, which inhibit *S. aureus* respiration and growth (*31, 32*). The transcriptomic data revealed some regulatory shifts, but they did not account for the complete metabolic changes induced by competition (*33*). Previous research indicates that GEMs often fail to integrate these complexities, limiting their ability to predict interspecies dynamics (*33*).

Nutrient Cross-Feeding and Fermentation Dynamics

Our study also explored the potential for metabolic cross-feeding, where *S. aureus* ferments glucose under oxygen-limiting conditions to produce acetate, which can then be utilised by *P. aeruginosa*. Although models predicted shifts in acetate metabolism, experimental metabolite profiling (Figure 8) did not detect significant differences between single and mixed cultures. This discrepancy might be due to challenges in detecting fermentation products or the activation of the additional compensatory metabolic pathways that were not accounted for in experimental conditions.

Importantly, *P. aeruginosa* is a non-fermenter and does not produce acetate. The observed gene expression changes likely reflect acetate degradation rather than its production. This distinction highlights the need for careful interpretation of transcriptomics data and need for experimental validation.

Iron Acquisition and Public Goods Sharing

Iron competition plays a crucial role in *S. aureus - P. aeruginosa* interactions. Our transcriptomic data indicated upregulation of *S. aureus* siderophore biosynthesis genes in co-culture, which was confirmed through spot assays on iron-restricted media. *P. aeruginosa* mutants lacking pyoverdine limited but detectable growth when co-cultured with *S. aureus*, suggesting that it uses *S. aureus* siderophores to meet its iron requirements. This supports previous findings that *P. aeruginosa* can use siderophores produced by other species, allowing it to suppress its siderophore production (*34*). However, GEMs did not predict this interaction, likely due to the lack of explicit modeling for siderophore uptake and utilisation pathways.

Improving Predictive Models for Microbial Interactions

Despite their potential, GEMs remain limited in predicting microbial interactions due to gaps in genetic, regulatory, and environmental data. Our study underscores several key challenges include False-negative predictions (e.g., underestimated *P. aeruginosa* growth), likely due to incomplete media formulations and missing adaptive mechanisms. Difficulty in integrating transcriptomics into metabolic models, reflecting a broader issue in systems biology where gene expression data do not always translate directly into metabolic flux predictions.

Future efforts should focus on incorporating regulatory networks: Adding transcriptional regulation layers to GEMs to capture stress responses and quorum sensing. Additionally, dynamic modelling approaches such as flux balance analysis with regulatory constraints (FBA-RC) to refine predictions. To improve model accuracy, more comprehensive media formulations are needed to ensure that in silico environments better reflect experimental conditions. In future studies, it may be beneficial to conduct more detailed assays using various forms of complex proteins and carbohydrates, as well as other public goods, to assess the degradation abilities of both bacteria further. Additionally, exploring how the environmental context (e.g., oxygen availability, pH, nutrient availability) influences these metabolic processes could provide deeper insights into the ecological roles of these organisms and their potential interactions in natural and clinical settings. Investigating the impact of these differences on biofilm formation, virulence, and overall fitness in a co-culture environment could also uncover additional layers of complexity in how *S. aureus* and *P. aeruginosa* interact.

These findings not only improve our understanding of the metabolic strategies these pathogens employ but also create new opportunities for investigating therapeutic interventions designed to disrupt their nutrient acquisition mechanisms, potentially offering new targets for drug development.

Conclusion

Our findings emphasise the iterative nature of computational and experimental microbiology. While GEMs provide valuable insights into bacterial metabolism, their predictive power remains constrained by incomplete regulatory information and environmental complexity. By integrating transcriptomics, metabolomics, and refined modelling approaches, we can improve our understanding of microbial interactions and enhance the applicability of GEMs in biomedical and biotechnological research.

By integrating these transcriptomic insights, Prof. Dräger's lab aims to improve GEMs and refine predictions of metabolic shifts and growth dynamics in co-culture conditions. This approach not only enhances the understanding of bacterial metabolism in mixed environments but also provides a powerful tool for investigating the impact of interspecies interactions, which may help uncover new therapeutic targets for disrupting pathogen cooperation and competition.

References

1. D. D. Payne *et al.*, An updated genome-scale metabolic network reconstruction of Pseudomonas aeruginosa PA14 to characterize mucin-driven shifts in bacterial metabolism. *NPJ Syst Biol Appl* **7**, 37 (2021).
2. F. Bauerle, G. O. Dobel, L. Camus, S. Heilbronner, A. Drager, Genome-scale metabolic models consistently predict in vitro characteristics of Corynebacterium striatum. *Front Bioinform* **3**, 1214074 (2023).
3. M. Jalili, M. Scharm, O. Wolkenhauer, A. Salehzadeh-Yazdi, Metabolic function-based normalization improves transcriptome data-driven reduction of genome-scale metabolic models. *npj Systems Biology and Applications* **9**, (2023).
4. A. M. Feist, B. O. Palsson, The biomass objective function. *Curr Opin Microbiol* **13**, 344-349 (2010).
5. C. Gu, G. B. Kim, W. J. Kim, H. U. Kim, S. Y. Lee, Current status and applications of genome-scale metabolic models. *Genome Biol* **20**, 121 (2019).
6. L. Biswas, F. Gotz, Molecular Mechanisms of Staphylococcus and Pseudomonas Interactions in Cystic Fibrosis. *Front Cell Infect Microbiol* **11**, 824042 (2021).
7. P. Briaud *et al.*, Impact of Coexistence Phenotype Between Staphylococcus aureus and Pseudomonas aeruginosa Isolates on Clinical Outcomes Among Cystic Fibrosis Patients. *Front Cell Infect Microbiol* **10**, 266 (2020).
8. D. H. Limoli *et al.*, Pseudomonas aeruginosa Alginate Overproduction Promotes Coexistence with Staphylococcus aureus in a Model of Cystic Fibrosis Respiratory Infection. *mBio* **8**, (2017).
9. P. Briaud *et al.*, Coexistence with Pseudomonas aeruginosa alters Staphylococcus aureus transcriptome, antibiotic resistance and internalization into epithelial cells. *Sci Rep* **9**, 16564 (2019).
10. M. A. Alford, S. Mann, N. Akhoundsadegh, R. E. W. Hancock, Competition between Pseudomonas aeruginosa and Staphylococcus aureus is dependent on intercellular signaling and regulated by the NtrBC two-component system. *Sci Rep* **12**, 9027 (2022).
11. L. Camus, P. Briaud, F. Vandenesch, K. Moreau, How Bacterial Adaptation to Cystic Fibrosis Environment Shapes Interactions Between Pseudomonas aeruginosa and Staphylococcus aureus. *Front Microbiol* **12**, 617784 (2021).
12. P. D. Lister, D. J. Wolter, N. D. Hanson, Antibacterial-resistant Pseudomonas aeruginosa: clinical impact and complex regulation of chromosomally encoded resistance mechanisms. *Clin Microbiol Rev* **22**, 582-610 (2009).
13. Y. Gao, S. Poudel, Y. Seif, Z. Shen, B. O. Palsson, Elucidating the CodY regulon in Staphylococcus aureus USA300 substrains TCH1516 and LAC. *mSystems* **8**, e0027923 (2023).
14. K. G. Hulten *et al.*, Three-year surveillance of community onset health care-associated staphylococcus aureus infections in children. *Pediatr Infect Dis J* **25**, 349-353 (2006).
15. N. P. Vitko, A. R. Richardson, Laboratory maintenance of methicillin-resistant Staphylococcus aureus (MRSA). *Curr Protoc Microbiol* **Chapter 9**, Unit 9C 2 (2013).
16. A. Grace, R. Sahu, D. R. Owen, V. A. Dennis, Pseudomonas aeruginosa reference strains PAO1 and PA14: A genomic, phenotypic, and therapeutic review. *Front Microbiol* **13**, 1023523 (2022).
17. D. Sriramulu, Artificial Sputum Medium. *Protocol Exchange*, (2010).

18. I. R. Monk, I. M. Shah, M. Xu, M. W. Tan, T. J. Foster, Transforming the Untransformable: Application of Direct Transformation To Manipulate Genetically Staphylococcus aureus and Staphylococcus epidermidis. *Mbio* **3**, (2012).
19. S. Heilbronner, F. Hanses, I. R. Monk, P. Speziale, T. J. Foster, Sortase A promotes virulence in experimental Staphylococcus lugdunensis endocarditis. *Microbiology* **159**, 2141-2152 (2013).
20. T. Bae, E. M. Glass, O. Schneewind, D. Missiakas, Generating a collection of insertion mutations in the Staphylococcus aureus genome using bursa aurealis. *Methods Mol Biol* **416**, 103-116 (2008).
21. L. A. Adolf *et al.*, Functional membrane microdomains and the hydroxamate siderophore transporter ATPase FhuC govern Isd-dependent heme acquisition in Staphylococcus aureus. *Elife* **12**, (2023).
22. Y. Zhao *et al.*, Nasal commensals reduce Staphylococcus aureus proliferation by restricting siderophore availability. *ISME J* **18**, (2024).
23. B. W. Holloway, Genetic recombination in Pseudomonas aeruginosa. *J Gen Microbiol* **13**, 572-581 (1955).
24. D. G. Ha, M. E. Richman, G. A. O'Toole, Deletion mutant library for investigation of functional outputs of cyclic diguanylate metabolism in Pseudomonas aeruginosa PA14. *Appl Environ Microbiol* **80**, 3384-3393 (2014).
25. Y. Kida, J. Taira, K. Kuwano, EprS, an autotransporter serine protease, plays an important role in various pathogenic phenotypes of Pseudomonas aeruginosa. *Microbiology (Reading)* **162**, 318-329 (2016).
26. N. T. Liberati *et al.*, An ordered, nonredundant library of Pseudomonas aeruginosa strain PA14 transposon insertion mutants. *Proc Natl Acad Sci U S A* **103**, 2833-2838 (2006).
27. A. M. Ramirez *et al.*, SarA plays a predominant role in controlling the production of extracellular proteases in the diverse clinical isolates ofStaphylococcus aureusLAC and UAMS-1. *Virulence* **11**, 1738-1762 (2020).
28. Y. Seif *et al.*, A computational knowledge-base elucidates the response of Staphylococcus aureus to different media types. *PLoS Comput Biol* **15**, e1006644 (2019).
29. G. Zampieri, S. Vijayakumar, E. Yaneske, C. Angione, Machine and deep learning meet genome-scale metabolic modeling. *PLoS Comput Biol* **15**, e1007084 (2019).
30. E. J. O'Brien, J. M. Monk, B. O. Palsson, Using Genome-scale Models to Predict Biological Capabilities. *Cell* **161**, 971-987 (2015).
31. A. Kumar, A. Alam, M. Rani, N. Z. Ehtesham, S. E. Hasnain, Biofilms: Survival and defense strategy for pathogens. *Int J Med Microbiol* **307**, 481-489 (2017).
32. L. M. Filkins, G. A. O'Toole, Cystic Fibrosis Lung Infections: Polymicrobial, Complex, and Hard to Treat. *PLoS Pathog* **11**, e1005258 (2015).
33. A. Heinken, A. Basile, J. Hertel, C. Thinnes, I. Thiele, Genome-Scale Metabolic Modeling of the Human Microbiome in the Era of Personalized Medicine. *Annu Rev Microbiol* **75**, 199-222 (2021).
34. S. Rajapitamahuni, E. S. Lyou, B. R. Kang, T. K. Lee, Microbial interaction-induced siderophore dynamics lead to phenotypic differentiation of Staphylococcus aureus. *Front Cell Infect Microbiol* **13**, 1277176 (2023).

Chapter 4

General Discussion

Understanding the metabolic interplay between microbial species within polymicrobial infections is central to deciphering the complexity of chronic and recalcitrant infections. This study has illuminated the nuanced interactions between *Staphylococcus aureus* and *Pseudomonas aeruginosa*, two clinically significant pathogens, as well as provided new insights into the less-characterised but emerging pathogen *Staphylococcus lugdunensis*. These investigations collectively underscore the importance of considering microbial behaviour within ecological contexts, rather than in isolation.

The findings presented here reaffirm the idea that microbial interactions are not purely antagonistic or cooperative, but often involve a spectrum of context-dependent behaviours, including competition, commensalism, and transient mutualism. The use of GEMs has proven useful for predicting basal metabolic capabilities, yet their limitations became apparent in the context of dynamic, adaptive microbial interactions. Despite their capacity to simulate metabolic flux under idealised conditions, GEMs struggle to capture the fluidity of microbial behaviour in response to interspecies pressures and environmental cues.

Toward More Predictive Models of Microbial Interaction

The observed discrepancies between model predictions and experimental results highlight a critical challenge in systems biology: static metabolic reconstructions cannot fully emulate the regulatory complexity of live microbial communities. Adaptive gene expression, regulatory circuit rewiring, post-translational modifications, and quorum sensing all play roles in shaping interspecies interactions, yet these layers are often omitted from computational models.

To address this, future research should prioritise the integration of transcriptomic, proteomic, and metabolomic data into dynamic modelling frameworks. Incorporating

environmental signals (e.g., oxygen levels, iron availability, host immune pressures) and interspecies communication systems (e.g., quorum sensing and small molecule signalling) will enable more realistic simulations of polymicrobial communities. Hybrid modelling platforms—combining constraint-based models with dynamic gene regulatory networks—could represent a next-generation approach to predict microbial behaviour in complex niches such as the cystic fibrosis lung or chronic wound biofilms.

Iron Acquisition as a Central Node of Interaction

A recurring theme across the studied pathogens is the centrality of iron acquisition to survival and interspecies competition. Iron is a limiting nutrient within the host, and as such, microbial success often hinges on the capacity to scavenge iron more effectively than competitors. In this study, *P. aeruginosa* appears to benefit from siderophores produced by *S. aureus*, indicating potential metabolic parasitism or opportunistic resource exploitation. Yet, the inability of *S. aureus* to reciprocally utilise *P. aeruginosa* siderophores suggests a directional relationship, reinforcing a competitive edge for *P. aeruginosa*.

This phenomenon mirrors broader ecological principles of asymmetrical competition and resource monopolisation. Future studies might delve deeper into siderophore biosynthesis and uptake pathways using gene knockout libraries, CRISPRi screening, or siderophore analogue inhibitors. There is also scope for investigating how environmental iron levels or host-derived iron-binding proteins (e.g., transferrin, lactoferrin) modulate these interactions in vivo.

Emerging Pathogens and Novel Virulence Strategies

In addition to characterising classic pathogens, this work draws attention to *S. lugdunensis*, a relatively understudied species with a growing clinical footprint. The identification of SLUSH peptides and their role in hemolysis and iron acquisition points to unique virulence adaptations that could distinguish *S. lugdunensis* from other coagulase-negative staphylococci.

However, the regulatory architecture controlling these peptides remains poorly understood. Follow-up studies using promoter-reporter fusions, global transcriptomic profiling under iron-limited conditions, and comparative genomics may uncover regulatory motifs or transcription factors involved in SLUSH regulation.

There is also significant opportunity to investigate how *S. lugdunensis* interacts with other staphylococci or Gram-negative species. Does it compete for iron in a similar manner to *S. aureus*? Can it exploit the metabolic by-products of more dominant species? These questions will be crucial for understanding its niche specificity and virulence potential in polymicrobial infections.

Therapeutic Implications and Novel Intervention Strategies

One of the most compelling long-term prospects emerging from this work is the potential to target microbial interactions rather than individual pathogens. Disrupting metabolic cooperation, such as siderophore piracy, shared carbon usage, or redox balancing, could undermine the fitness of entire microbial communities. This strategy is particularly attractive in light of the rising challenge of antimicrobial resistance, as it may allow for non-bactericidal interventions that reduce virulence and persistence without driving strong selective pressures.

Future therapies might include- Siderophore antagonists that block uptake pathways and induce metabolic stress. Metabolic decoys or analogues that interfere with cross-feeding. Community re-engineering strategies, where commensal or probiotic strains are introduced to disrupt pathogenic metabolic networks. Targeted gene silencing tools (e.g., CRISPRi) delivered via phage or nanoparticle systems to suppress key metabolic or regulatory genes within polymicrobial consortia.

Broader Applications Beyond Pathogenesis

While the immediate focus is clinical, the implications of this research extend into industrial microbiology and synthetic biology. Understanding microbial metabolic interactions can inform the design of synthetic microbial consortia for biotechnology, such as biofuel production, carbon recycling, and wastewater treatment. Lessons from natural systems—like the ability of *P. aeruginosa* to utilise exogenous siderophores—may be harnessed to engineer more robust and cooperative microbial systems.

In environmental microbiology, insights into iron competition and cross-feeding can shed light on community assembly in soil or aquatic ecosystems.

Conclusion and Future Outlook

This study emphasises that microbial pathogenesis cannot be fully understood without considering the community context. The interactions between *S. aureus* - *P. aeruginosa*, reveal both competitive strategies and unexpected metabolic dependencies that challenge conventional wisdom. As we move forward, the convergence of computational modelling, experimental microbiology, and molecular systems biology will be essential to unravel the complexity of polymicrobial systems.

The future of infection biology lies in capturing the dynamics of microbial behavior in real time, integrating host and environmental variables, and exploiting interspecies relationships for therapeutic gain. This shift from reductionist to ecological thinking could redefine how we diagnose, treat, and ultimately prevent complex infections.

References

1. K. Becker, C. Heilmann, G. Peters, Coagulase-negative staphylococci. *Clin Microbiol Rev* **27**, 870-926 (2014).
2. L. G. Harris, S. J. Foster, R. G. Richards, An introduction to Staphylococcus aureus, and techniques for identifying and quantifying S. aureus adhesins in relation to adhesion to biomaterials: review. *Eur Cell Mater* **4**, 39-60 (2002).
3. J. P. Luyendyk, J. G. Schoenecker, M. J. Flick, The multifaceted role of fibrinogen in tissue injury and inflammation. *Blood* **133**, 511-520 (2019).
4. L. M. Filkins *et al.*, Coculture of Staphylococcus aureus with Pseudomonas aeruginosa Drives S. aureus towards Fermentative Metabolism and Reduced Viability in a Cystic Fibrosis Model. *J Bacteriol* **197**, 2252-2264 (2015).
5. S. Y. Tong, J. S. Davis, E. Eichenberger, T. L. Holland, V. G. Fowler, Jr., Staphylococcus aureus infections: epidemiology, pathophysiology, clinical manifestations, and management. *Clin Microbiol Rev* **28**, 603-661 (2015).
6. F. D. Lowy, Staphylococcus aureus infections. *N Engl J Med* **339**, 520-532 (1998).
7. B. P. Howden *et al.*, Staphylococcus aureus host interactions and adaptation. *Nat Rev Microbiol* **21**, 380-395 (2023).
8. W. C. Noble, H. A. Valkenburg, C. H. Wolters, Carriage of Staphylococcus aureus in random samples of a normal population. *J Hyg (Lond)* **65**, 567-573 (1967).
9. H. F. Wertheim *et al.*, The role of nasal carriage in Staphylococcus aureus infections. *Lancet Infect Dis* **5**, 751-762 (2005).
10. E. J. G. Pollitt, P. T. Szkuta, N. Burns, S. J. Foster, Staphylococcus aureus infection dynamics. *PLoS Pathog* **14**, e1007112 (2018).
11. T. A. Taylor, C. G. Unakal, in *StatPearls*. (Treasure Island (FL), 2024).
12. S. M. Lehar *et al.*, Novel antibody-antibiotic conjugate eliminates intracellular S. aureus. *Nature* **527**, 323-328 (2015).
13. M. Idrees, S. Sawant, N. Karodia, A. Rahman, Staphylococcus aureus Biofilm: Morphology, Genetics, Pathogenesis and Treatment Strategies. *Int J Environ Res Public Health* **18**, (2021).
14. M. Idrees, A. R. Mohammad, N. Karodia, A. Rahman, Multimodal Role of Amino Acids in Microbial Control and Drug Development. *Antibiotics (Basel)* **9**, (2020).
15. R. M. Corrigan, D. Rigby, P. Handley, T. J. Foster, The role of Staphylococcus aureus surface protein SasG in adherence and biofilm formation. *Microbiology (Reading)* **153**, 2435-2446 (2007).
16. A. Dutta, S. Bhattacharyya, A. Kundu, D. Dutta, A. K. Das, Macroscopic amyloid fiber formation by staphylococcal biofilm associated SuhB protein. *Biophys Chem* **217**, 32-41 (2016).
17. K. A. Lacey *et al.*, The Staphylococcus aureus Cell Wall-Anchored Protein Clumping Factor A Is an Important T Cell Antigen. *Infect Immun* **85**, (2017).
18. S. Parthasarathy, S. Shah, A. Raja Sager, A. Rangan, S. Durugu, Staphylococcus lugdunensis: Review of Epidemiology, Complications, and Treatment. *Cureus* **12**, e8801 (2020).
19. L. Bieber, G. Kahlmeter, Staphylococcus lugdunensis in several niches of the normal skin flora. *Clin Microbiol Infect* **16**, 385-388 (2010).

20. S. Heilbronner, T. J. Foster, Staphylococcus lugdunensis: a Skin Commensal with Invasive Pathogenic Potential. *Clin Microbiol Rev* **34**, (2021).
21. N. E. Natsis, P. R. Cohen, Coagulase-Negative Staphylococcus Skin and Soft Tissue Infections. *Am J Clin Dermatol* **19**, 671-677 (2018).
22. T. P. Bowman, A. Deshpande, A. Balfour, K. Harvey-Wood, Staphylococcus lugdunensis in children: A retrospective analysis. *Pediatr Investig* **6**, 163-170 (2022).
23. P. Y. Liu *et al.*, Staphylococcus lugdunensis infective endocarditis: a literature review and analysis of risk factors. *J Microbiol Immunol Infect* **43**, 478-484 (2010).
24. L. R. Non, C. A. Santos, The occurrence of infective endocarditis with Staphylococcus lugdunensis bacteremia: A retrospective cohort study and systematic review. *J Infect* **74**, 179-186 (2017).
25. H. Kyaw *et al.*, Staphylococcus Lugdunensis Endocarditis and Cerebrovascular Accident: A Systemic Review of Risk Factors and Clinical outcome. *Cureus* **10**, e2469 (2018).
26. S. Ravaioli *et al.*, Searching for Virulence Factors among Staphylococcus lugdunensis Isolates from Orthopedic Infections: Correlation of beta-hemolysin, hemolysin III, and slush Genes with Hemolytic Activity and Synergistic Hemolytic Activity. *Int J Mol Sci* **24**, (2023).
27. D. Chin *et al.*, Staphylococcus lugdunensis Uses the Agr Regulatory System to Resist Killing by Host Innate Immune Effectors. *Infect Immun* **90**, e0009922 (2022).
28. M. Nilsson, J. Bjerketorp, B. Guss, L. Frykberg, A fibrinogen-binding protein of Staphylococcus lugdunensis. *FEMS Microbiol Lett* **241**, 87-93 (2004).
29. A. Jochim *et al.*, An ECF-type transporter scavenges heme to overcome iron-limitation in Staphylococcus lugdunensis. *Elife* **9**, (2020).
30. R. S. Flannagan *et al.*, In vivo growth of Staphylococcus lugdunensis is facilitated by the concerted function of heme and non-heme iron acquisition mechanisms. *J Biol Chem* **298**, 101823 (2022).
31. J. Lebeurre *et al.*, Comparative Genome Analysis of Staphylococcus lugdunensis Shows Clonal Complex-Dependent Diversity of the Putative Virulence Factor, ess/Type VII Locus. *Front Microbiol* **10**, 2479 (2019).
32. C. Weidenmaier *et al.*, DltABCD- and MprF-mediated cell envelope modifications of Staphylococcus aureus confer resistance to platelet microbicidal proteins and contribute to virulence in a rabbit endocarditis model. *Infect Immun* **73**, 8033-8038 (2005).
33. J. A. Geoghegan *et al.*, Molecular characterization of the interaction of staphylococcal microbial surface components recognizing adhesive matrix molecules (MSCRAMM) ClfA and Fbl with fibrinogen. *J Biol Chem* **285**, 6208-6216 (2010).
34. F. Szabados *et al.*, Occurrence of genes of putative fibrinogen binding proteins and hemolysins, as well as of their phenotypic correlates in isolates of S. lugdunensis of different origins. *BMC Res Notes* **4**, 113 (2011).
35. S. Heilbronner *et al.*, Genome sequence of Staphylococcus lugdunensis N920143 allows identification of putative colonization and virulence factors. *FEMS Microbiol Lett* **322**, 60-67 (2011).
36. B. Donvito *et al.*, Synergistic hemolytic activity of Staphylococcus lugdunensis is mediated by three peptides encoded by a non-agr genetic locus. *Infect Immun* **65**, 95-100 (1997).

37. G. A. Hebert, Hemolysins and other characteristics that help differentiate and biotype Staphylococcus lugdunensis and Staphylococcus schleiferi. *J Clin Microbiol* **28**, 2425-2431 (1990).

38. G. Sharma *et al.*, Pseudomonas aeruginosa biofilm: potential therapeutic targets. *Biologicals* **42**, 1-7 (2014).

39. S. P. Diggle, M. Whiteley, Microbe Profile: Pseudomonas aeruginosa: opportunistic pathogen and lab rat. *Microbiology (Reading)* **166**, 30-33 (2020).

40. D. Balasubramanian, L. Schneper, H. Kumari, K. Mathee, A dynamic and intricate regulatory network determines Pseudomonas aeruginosa virulence. *Nucleic Acids Res* **41**, 1-20 (2013).

41. A. D. Valderrey *et al.*, Chronic colonization by Pseudomonas aeruginosa of patients with obstructive lung diseases: cystic fibrosis, bronchiectasis, and chronic obstructive pulmonary disease. *Diagn Microbiol Infect Dis* **68**, 20-27 (2010).

42. E. Bouza, A. Burillo, P. Munoz, Catheter-related infections: diagnosis and intravascular treatment. *Clin Microbiol Infect* **8**, 265-274 (2002).

43. N. Sathe *et al.*, Pseudomonas aeruginosa: Infections and novel approaches to treatment "Knowing the enemy" the threat of Pseudomonas aeruginosa and exploring novel approaches to treatment. *Infect Med (Beijing)* **2**, 178-194 (2023).

44. E. Kessler, M. Safrin, J. K. Gustin, D. E. Ohman, Elastase and the LasA protease of Pseudomonas aeruginosa are secreted with their propeptides. *J Biol Chem* **273**, 30225-30231 (1998).

45. J. K. Gustin, E. Kessler, D. E. Ohman, A substitution at His-120 in the LasA protease of Pseudomonas aeruginosa blocks enzymatic activity without affecting propeptide processing or extracellular secretion. *J Bacteriol* **178**, 6608-6617 (1996).

46. A. C. M. Galdino *et al.*, Disarming Pseudomonas aeruginosa Virulence by the Inhibitory Action of 1,10-Phenanthroline-5,6-Dione-Based Compounds: Elastase B (LasB) as a Chemotherapeutic Target. *Front Microbiol* **10**, 1701 (2019).

47. K. K. Grande, J. K. Gustin, E. Kessler, D. E. Ohman, Identification of critical residues in the propeptide of LasA protease of Pseudomonas aeruginosa involved in the formation of a stable mature protease. *J Bacteriol* **189**, 3960-3968 (2007).

48. M. Duplantier, E. Lohou, P. Sonnet, Quorum Sensing Inhibitors to Quench P. aeruginosa Pathogenicity. *Pharmaceuticals (Basel)* **14**, (2021).

49. L. Biswas, F. Gotz, Molecular Mechanisms of Staphylococcus and Pseudomonas Interactions in Cystic Fibrosis. *Front Cell Infect Microbiol* **11**, 824042 (2021).

50. J. P. Pearson, M. Feldman, B. H. Iglewski, A. Prince, Pseudomonas aeruginosa cell-to-cell signaling is required for virulence in a model of acute pulmonary infection. *Infect Immun* **68**, 4331-4334 (2000).

51. A. Hotterbeekx, S. Kumar-Singh, H. Goossens, S. Malhotra-Kumar, In vivo and In vitro Interactions between Pseudomonas aeruginosa and Staphylococcus spp. *Front Cell Infect Microbiol* **7**, 106 (2017).

52. E. J. Murray, J. F. Dubern, W. C. Chan, S. R. Chhabra, P. Williams, A Pseudomonas aeruginosa PQS quorum-sensing system inhibitor with anti-staphylococcal activity sensitizes polymicrobial biofilms to tobramycin. *Cell Chem Biol* **29**, 1187-1199 e1186 (2022).

53. V. T. Anju *et al.*, Polymicrobial Infections and Biofilms: Clinical Significance and Eradication Strategies. *Antibiotics (Basel)* **11**, (2022).

54. M. A. Bachman, J. N. Weiser, in *Trace Metals and Infectious Diseases,* J. O. Nriagu, E. P. Skaar, Eds. (Cambridge (MA), 2015).

55. D. Sharma, L. Misba, A. U. Khan, Antibiotics versus biofilm: an emerging battleground in microbial communities. *Antimicrob Resist Infect Control* **8**, 76 (2019).

56. S. Qin *et al.*, Pseudomonas aeruginosa: pathogenesis, virulence factors, antibiotic resistance, interaction with host, technology advances and emerging therapeutics. *Signal Transduct Target Ther* **7**, 199 (2022).

57. H. W. Boucher *et al.*, Bad bugs, no drugs: no ESKAPE! An update from the Infectious Diseases Society of America. *Clin Infect Dis* **48**, 1-12 (2009).

58. C. Pouget *et al.*, Polymicrobial Biofilm Organization of Staphylococcus aureus and Pseudomonas aeruginosa in a Chronic Wound Environment. *Int J Mol Sci* **23**, (2022).

59. P. M. Alves *et al.*, Interaction between Staphylococcus aureus and Pseudomonas aeruginosa is beneficial for colonisation and pathogenicity in a mixed biofilm. *Pathog Dis* **76**, (2018).

60. M. Fazli *et al.*, Nonrandom distribution of Pseudomonas aeruginosa and Staphylococcus aureus in chronic wounds. *J Clin Microbiol* **47**, 4084-4089 (2009).

61. S. Rajan, L. Saiman, Pulmonary infections in patients with cystic fibrosis. *Semin Respir Infect* **17**, 47-56 (2002).

62. M. P. Anderson *et al.*, Demonstration that CFTR is a chloride channel by alteration of its anion selectivity. *Science* **253**, 202-205 (1991).

63. L. Biswas, R. Biswas, M. Schlag, R. Bertram, F. Gotz, Small-colony variant selection as a survival strategy for Staphylococcus aureus in the presence of Pseudomonas aeruginosa. *Appl Environ Microbiol* **75**, 6910-6912 (2009).

64. L. R. Hoffman *et al.*, Selection for Staphylococcus aureus small-colony variants due to growth in the presence of Pseudomonas aeruginosa. *Proc Natl Acad Sci U S A* **103**, 19890-19895 (2006).

65. E. D. Weinberg, Iron availability and infection. *Biochim Biophys Acta* **1790**, 600-605 (2009).

66. M. I. Hood, E. P. Skaar, Nutritional immunity: transition metals at the pathogen-host interface. *Nat Rev Microbiol* **10**, 525-537 (2012).

67. J. E. Cassat, E. P. Skaar, Iron in infection and immunity. *Cell Host Microbe* **13**, 509-519 (2013).

68. N. D. Hammer, E. P. Skaar, Molecular mechanisms of Staphylococcus aureus iron acquisition. *Annu Rev Microbiol* **65**, 129-147 (2011).

69. J. R. Sheldon, D. E. Heinrichs, Recent developments in understanding the iron acquisition strategies of gram positive pathogens. *FEMS Microbiol Rev* **39**, 592-630 (2015).

70. E. P. Skaar, M. Humayun, T. Bae, K. L. DeBord, O. Schneewind, Iron-source preference of Staphylococcus aureus infections. *Science* **305**, 1626-1628 (2004).

71. S. Heilbronner *et al.*, Competing for Iron: Duplication and Amplification of the isd Locus in Staphylococcus lugdunensis HKU09-01 Provides a Competitive Advantage to Overcome Nutritional Limitation. *PLoS Genet* **12**, e1006246 (2016).

72. C. R. Fontenot, H. Tasnim, K. A. Valdes, C. V. Popescu, H. Ding, Ferric uptake regulator (Fur) reversibly binds a [2Fe-2S] cluster to sense intracellular iron homeostasis in Escherichia coli. *J Biol Chem* **295**, 15454-15463 (2020).

73. B. Troxell, H. M. Hassan, Transcriptional regulation by Ferric Uptake Regulator (Fur) in pathogenic bacteria. *Front Cell Infect Microbiol* **3**, 59 (2013).

74. L. A. Adolf *et al.*, Functional membrane microdomains and the hydroxamate siderophore transporter ATPase FhuC govern Isd-dependent heme acquisition in Staphylococcus aureus. *Elife* **12**, (2023).

75. L. Escolar, J. Perez-Martin, V. de Lorenzo, Opening the iron box: transcriptional metalloregulation by the Fur protein. *J Bacteriol* **181**, 6223-6229 (1999).

76. G. Pishchany *et al.*, IsdB-dependent hemoglobin binding is required for acquisition of heme by Staphylococcus aureus. *J Infect Dis* **209**, 1764-1772 (2014).

77. M. L. Reniere, E. P. Skaar, Staphylococcus aureus haem oxygenases are differentially regulated by iron and haem. *Mol Microbiol* **69**, 1304-1315 (2008).

78. M. Zapotoczna, S. Heilbronner, P. Speziale, T. J. Foster, Iron-regulated surface determinant (Isd) proteins of Staphylococcus lugdunensis. *J Bacteriol* **194**, 6453-6467 (2012).

79. J. R. Brozyna, J. R. Sheldon, D. E. Heinrichs, Growth promotion of the opportunistic human pathogen, Staphylococcus lugdunensis, by heme, hemoglobin, and coculture with Staphylococcus aureus. *Microbiologyopen* **3**, 182-195 (2014).

80. L. Tan, S. R. Li, B. Jiang, X. M. Hu, S. Li, Therapeutic Targeting of the Staphylococcus aureus Accessory Gene Regulator (agr) System. *Front Microbiol* **9**, 55 (2018).

81. C. Jenul, A. R. Horswill, Regulation of Staphylococcus aureus Virulence. *Microbiol Spectr* **7**, (2019).

82. M. Aubourg *et al.*, Inactivation of the Response Regulator AgrA Has a Pleiotropic Effect on Biofilm Formation, Pathogenesis and Stress Response in Staphylococcus lugdunensis. *Microbiol Spectr* **10**, e0159821 (2022).

83. Y. Benito, G. Lina, T. Greenland, J. Etienne, F. Vandenesch, trans-complementation of a Staphylococcus aureus agr mutant by Staphylococcus lugdunensis agr RNAIII. *J Bacteriol* **180**, 5780-5783 (1998).

84. M. Otto, Phenol-soluble modulins. *Int J Med Microbiol* **304**, 164-169 (2014).

85. A. Peschel, M. Otto, Phenol-soluble modulins and staphylococcal infection. *Nat Rev Microbiol* **11**, 667-673 (2013).

86. G. Y. Cheung, H. S. Joo, S. S. Chatterjee, M. Otto, Phenol-soluble modulins--critical determinants of staphylococcal virulence. *FEMS Microbiol Rev* **38**, 698-719 (2014).

87. R. Wang *et al.*, Identification of novel cytolytic peptides as key virulence determinants for community-associated MRSA. *Nat Med* **13**, 1510-1514 (2007).

88. M. Otto, Staphylococcal Biofilms. *Microbiol Spectr* **6**, (2018).

89. G. Y. Liu, Molecular pathogenesis of Staphylococcus aureus infection. *Pediatr Res* **65**, 71R-77R (2009).

90. M. Rautenberg, H. S. Joo, M. Otto, A. Peschel, Neutrophil responses to staphylococcal pathogens and commensals via the formyl peptide receptor 2 relates to phenol-soluble modulin release and virulence. *FASEB J* **25**, 1254-1263 (2011).

91. A. Caminero, M. Guzman, J. Libertucci, A. E. Lomax, The emerging roles of bacterial proteases in intestinal diseases. *Gut Microbes* **15**, 2181922 (2023).

92. M. H. Corre, V. Bachmann, T. Kohn, Bacterial matrix metalloproteases and serine proteases contribute to the extra-host inactivation of enteroviruses in lake water. *ISME J* **16**, 1970-1979 (2022).

93. P. Song *et al.*, Microbial proteases and their applications. *Front Microbiol* **14**, 1236368 (2023).

94. L. Shaw, E. Golonka, J. Potempa, S. J. Foster, The role and regulation of the extracellular proteases of Staphylococcus aureus. *Microbiology (Reading)* **150**, 217-228 (2004).

95. G. R. Drapeau, Role of metalloprotease in activation of the precursor of staphylococcal protease. *J Bacteriol* **136**, 607-613 (1978).

96. G. Dubin, Extracellular proteases of Staphylococcus spp. *Biol Chem* **383**, 1075-1086 (2002).

97. L. S. Engel, J. M. Hill, A. R. Caballero, L. C. Green, R. J. O'Callaghan, Protease IV, a unique extracellular protease and virulence factor from Pseudomonas aeruginosa. *J Biol Chem* **273**, 16792-16797 (1998).

98. A. R. Caballero *et al.*, Pseudomonas aeruginosa protease IV enzyme assays and comparison to other Pseudomonas proteases. *Anal Biochem* **290**, 330-337 (2001).

99. M. Schuster, E. P. Greenberg, A network of networks: quorum-sensing gene regulation in Pseudomonas aeruginosa. *Int J Med Microbiol* **296**, 73-81 (2006).

100. W. Gottstein, B. G. Olivier, F. J. Bruggeman, B. Teusink, Constraint-based stoichiometric modelling from single organisms to microbial communities. *J R Soc Interface* **13**, (2016).

101. X. Fang, C. J. Lloyd, B. O. Palsson, Reconstructing organisms in silico: genome-scale models and their emerging applications. *Nat Rev Microbiol* **18**, 731-743 (2020).

102. S. Dahal, A. Renz, A. Drager, L. Yang, Genome-scale model of Pseudomonas aeruginosa metabolism unveils virulence and drug potentiation. *Commun Biol* **6**, 165 (2023).

103. C. J. Norsigian, X. Fang, Y. Seif, J. M. Monk, B. O. Palsson, A workflow for generating multi-strain genome-scale metabolic models of prokaryotes. *Nat Protoc* **15**, 1-14 (2020).

104. A. Hari, D. Lobo, (2023).

105. F. Bauerle, G. O. Dobel, L. Camus, S. Heilbronner, A. Drager, Genome-scale metabolic models consistently predict in vitro characteristics of Corynebacterium striatum. *Front Bioinform* **3**, 1214074 (2023).

106. J. D. Orth, I. Thiele, B. O. Palsson, What is flux balance analysis? *Nat Biotechnol* **28**, 245-248 (2010).

Contributions to Publications

Chapter 2 - SLUSH peptides of the PSMβ family enable *Staphylococcus lugdunensis* to use erythrocytes as a sole source of nutrient iron

Published in The FASEB Journal, First published: 21 August 2024. DOI:10.1096/fj.202400335R

Sharmila Sekar, Selina Schwarzbach, Dominik Alexander Bloes, and Emanuel Smeds performed experiments. Mulugeta Nega performed HPLC/MS analysis. Dorothee Kretschmer supervised immune stimulation experiments. Timothy J. Foster acquired funding and supervised experiments. Simon Heilbronner designed the study, acquired funding, supervised experiments, and wrote the manuscript.

Chapter 3 - Computer modelling and experimental validation of interactions between *Pseudomonas aeruginosa* and *Staphylococcus aureus*

Manuscript – Draft version

Sharmila Sekar performed wet lab experiments. Nantia Lenidou and Alina Renz assisted with dry lab work and Computational data analysis. Prof. Andreas Dräger contributed to the genome-scale metabolic modelling and supervised the computational aspects. Transcriptomics analysis and interpretation were performed collaboratively with the modelling team. Simon Heilbronner supervised and designed the study.